Prof.Dr. Halil SEZEN
Environmental and Geodetic Engineering, The Ohio State University
USA

Prof.Dr. Huiming TANG
China University of Geoscience..,Faculty ofEngineering,
China

Prof.Dr. Laramie Vance POTTS
New Jersey Institute of Technology,Department of Engineering Technology
USA

Prof.Dr. Lia MATCHAVARIANI
Iv.Javakhishvili Tbilisi State University Faculty of Geography
Georgia

Prof.Dr. Məqsəd Huseyn QOCAMANOV
Baku State University Faculty of Geography
Azerbaijan

Prof.Dr. Muzaffer KAHVECI
Selcuk University Faculty of Engineering
Turkey

Prof.Dr. Nikolai PATYKA
National University of Life and Environmental Sciences of Ukraine
Ukraine

Prof.Dr. Petros PATIAS
The AristotleUniversity of Thessaloniki, Faculty of Rural & Surveying Engineering
Greece

Prof.Dr. Pierre GRUSSENMEYER
National Institute of Applied Science, Department of civilengineering and surveying
France

Prof.Dr. Rey-Jer You
National Cheng Kung University, Tainan · Department of Geomatics
China

Prof.Dr. Xiaoli DING
The Hong Kong Polytechnic University,Faculty of Construction and Environment
Hong Kong

Assoc.Prof.Dr. Elena SUKHACHEVA
Saint Petersburg State University Institute of Earth Sciences
Russia

Assoc.Prof.Dr. Semra ALYILMAZ
Ataturk University Kazim Karabekir Faculty of Education
Turkey

Assoc.Prof.Dr. Fariz MIKAILSOY
Igdir University Faculty of Agriculture
Turkey

Assoc.Prof.Dr. Lena HALOUNOVA
Czech Technical University Faculty of Civil Engineering
Czech Republic

Assoc.Prof.Dr. Medzida MULIC
University of Sarajevo Faculty of Civil Engineering
Bosnia and Herzegovina

Assoc.Prof.Dr. Michael Ajide OYINLOYE
Federal University of Technology, Akure (FUTA)
Nigeria

Assoc.Prof.Dr. Mohd Zulkifli bin MOHD YUNUS
Universiti TeknologiMalaysia, Faculty of Civil Engineering
Malaysia

Assoc.Prof.Dr. Syed Amer MAHMOOD

University of the Punjab, Department of Space Science
Pakistan

Assist. Prof. Dr. Yelda TURKAN
Oregon State University,
USA

Dr. G. Sanka N. PERERA
Sabaragamuwa University Faculty of Geomatics
Sri Lanka

Dr. Hsiu-Wen CHANG
National Cheng Kung University, Department of Geomatics
Taiwan

The International Journal of Engineering and Geosciences (IJEG)

CONTENTS
Volume 4 - Issue 3

ARTICLES

REDUCTION OF MASS APPRAISAL CRITERIA WITH PRINCIPAL COMPONENT ANALYSIS AND INTEGRATION TO GIS

Fatma Bünyan Ünel[1]* and Şükran Yalpir[2]

[1]Mersin University, Engineering Faculty, Department of Geomatics Engineering, Mersin, Turkey.
(fatmabunel@mersin.edu.tr); **ORCID 0000-0002-9949-640X**

[2]Konya Technical University, Engineering Faculty, Department of Geomatics Engineering, Konya, Turkey.
(syalpir@ktun.edu.tr); **; ORCID 0000-0001-9366-5770**

ABSTRACT: In real estate, mass appraisal is a very important subject in the valuation of two and more properties. It can be of benefit in a number of fields including taxation, banking transactions, expropriation, etc. The base problem is which criteria to use for mass appraisal. Because the number of criteria and the criteria themselves vary according to people, regions and countries, they are uncertain. They should be optimum in order to save on time, labour and cost. The aim of this study is to reduce the criteria by determining which ones affect the plot value. A survey which was answered by a total of 2,531 participants was conducted in Turkey. Principal Component Analysis (PCA), one of the criteria analysis methods, was applied to the survey data. The number of criteria was reduced to 14 with separation and to 30 according to the results of PCA. But they decreased in the model verification when criteria data for 558 samples were collected in the Konya study area. An index of the neighbourhood and locational features of these criteria was created by using GIS. Three models were established using Multiple Regression Analysis (MRA) and the performance of the models was examined. The prediction values and the market value were integrated into the GIS to compare the spatial distributions of plot values.

Keywords: Mass Appraisal, Principal Component Analysis (PCA), Geographic Information *Systems (GIS), index.*

1. INTRODUCTION

Real estate valuation is of great significance in many countries, and some of their revenues are acquired through taxes collected from the real estate. The economic value of real estate is also used for taxation, insurance and expropriation as well as for such management of real estate as land management, planning, urban restructuring and zoning. The need for mass valuation emerges in these processes and such traditional methods as comparison, review and cost remain inefficient in this regard, due to the fact that they cannot yield a solution. Relevant criteria should first be identified in order for mass valuation to be carried out. In academic and practice studies, different criteria have been used and universal criteria are not found (Yalpır & Ünel, 2016). There are International Valuation Standards but no standard criteria are globally accepted. However, since the number of criteria is more than necessary this poses a problem. Using all the current criteria is time-consuming, labour-intensive and costly. The optimum criteria to be used for mass appraisal can be determined through research and analysis.

The literature related to the criteria affecting the value of real estate was examined and it was especially seen that criteria studied such as neighbourhood greenspace (Li, 2010), zebra mussels (Henry, 2013), shale gas (Muehlenbachs, Spiller, & Timmins, 2014), or state forests (Smigielski, 2014) had impacts on property values. Zavadskas et al. (2017) mentioned that the sustainability criteria for real estate play a more and more significant role in the different evaluation processes. In a study by Sdino, Rosasco, Torrieri, and Oppio (2018), the real estate characteristics selected to appraise the real estate value in Italy were grouped as extrinsic, intrinsic and technological. The weights of each of the characteristics were calculated with AHP.

Due to the lack of studies on criteria, statistical and advanced real estate valuation methods were taken into consideration and real estate types and their criteria were discussed. In one study, Kauko (2002) applied methods by considering Finland and Helsinki on separate scales through different criteria. He used YSA and the hedonic method for the buildings he chose in the areas by using 16 criteria. In the valuation of buildings, Lynn employed the methods of multiple regression, nonparametric regression, and YSA with a total of 83 criteria, 66 of which were composed of local features. Schulz (2003) compared the success stories by applying linear regression and hedonic regression with the criteria related to buildings after examining German valuation regulations. Modern valuation methods are compared with the regression and hedonic methods, which are usually easy to use and which yield high accuracy in the mass appraisal of real estate. The studies that deal with local criteria at length display an analytic approach based on the development of local features and identified techniques for locational modelling (McCluskey & Borst, 2007). A local weight matrix was used to produce a locational correlation, and locational were analysed through the hedonic method (M. Kryvobokov & Wilhelmsson, 2007); the relationship between the valuation of real estate and green areas, surface water, the effects of noise and view features was researched through correlation analysis (Cellmer, Senetra, & Szczepanska, 2012), and the relationship between the determinants

related to the value of buildings in terms of both the urban environment and the structural features of the building market was analysed in another study (Zoppi, Argiolas, & Lai, 2015).

In the literature review, it was observed that the studies were conducted in a method-based manner first by conducting research concerning the method. It was generally seen that different criteria were used when the applications of the modern valuation methods were developed and compared with regression. However, it was also observed that the criteria affecting the value of real estate were considered on a local basis for these applications, and the criteria research was conducted with all the criteria involved. Rather, the criteria were examined for them to become a basis for the method. In each application, the criteria were observed to be in differing numbers. Because the literature research was conducted on different countries and different areas, it was confirmed that the criteria varied according to these different countries and areas. Besides, studies were generally conducted on buildings in terms of real estate, but there are also studies, although few, in which values related to commercial buildings, were also considered (Bender, Din, Hoesli, & Laakso, 1999; Marko Kryvobokov, 2005, 2006; Son, 2012). It was seen in these applications that the market value, the unit value and the rent value were used as independent variables (El-Gohary, 2004; Son, 2012; Zoppi et al., 2015).

The plot is treated as a form of real estate in this study, and the criteria affecting the plot value are determined from the findings of the literature review. The number of criteria being very high makes the application of mass appraisal very difficult. Also, using all the criteria for mass appraisal does not seem economical and appropriate because collecting, arranging and analysing the data on the criteria takes a long time and requires labour and expense. In addition, the criteria demonstrate significant differences between young and old people (Unel, Yalpir, & Gulnar, 2017).

The purpose of this study is first to determine, at an optimal level, the criteria that can be used for mass appraisal and then to create a geographical data model with neighbourhood and local indices, thus standardizing the criteria. Reduced criteria were obtained by applying Principal Component Analysis (PCA) to the surveys carried out earlier. Since GIS is a powerful tool (Amil, 2018), the neighbourhood and location indices were generated by using ArcGIS software on the data corresponding to the reduced criteria belonging to local and locational features. Three models were obtained in total through the application of Multiple Regression Analysis (MRA) for the verification of the model by using all the criteria and the reduced criteria. Prediction values were calculated from the models and their performance analyses were conducted for a comparison with the market value. The model in which the dependent variable was best explained by independent variables in MRA turned out to be Model 1, which was obtained with a combination of all the criteria. The model closest to Model 1 was seen to be Model 2, which was obtained through local indices from the criteria reduced with PCA.

2. MATERIALS AND METHOD

The outline of this study can be presented as in the following flow chart. First, it defines the problem of

which criteria affect the plot value. It then continues with the criteria and their analysis, model verification, and performance analysis (Fig. 1).
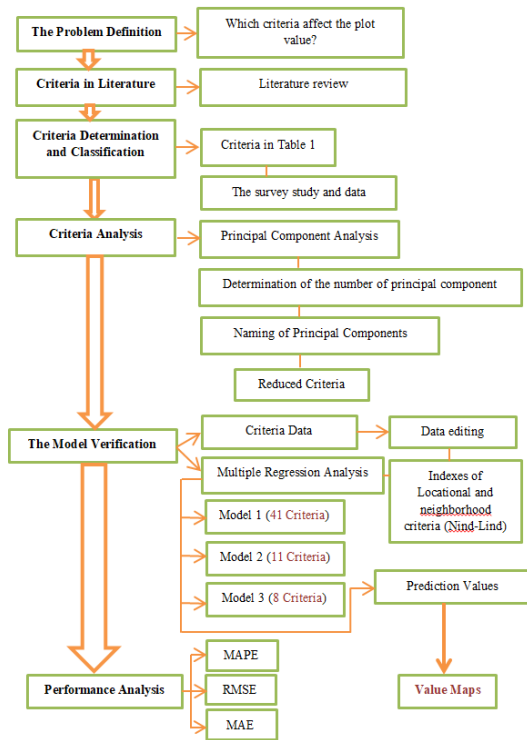

Figure 1 The study diagram

Figure 2 Market Sampling (Ünel, 2017)

2.1 Study Area and Market Sampling

The central neighbourhoods of the city of Konya were identified as the study area, and information regarding local features of the neighbourhoods involved was obtained for each neighbourhood on a small scale. The facilities on the map relating to the criteria under the location features were arranged in ArcGIS software in a plot-based manner, each in different layers, and maps were generated in a vector format. Furthermore, the values of the plots in the central neighbourhoods on which buying and selling transactions were conducted were obtained, and a total of 558 market samplings were collected. Also, data about legal and physical features were collected, and they were arranged in a matrix format. In the verification of the model, the plot values were taken as dependent variables and the other information about the plots was taken as independent variables. Data that could not be accessed were disregarded, and not included in the model.

It should not be expected for the distribution of market samplings on the map to be homogeneous for Konya, as the density of buildings increases towards the city centre and it becomes impossible to find plots for construction. While there are few samplings in the city centre, it is seen that the number of samplings increases with distance from the city (Fig. 2).

2.2 Criteria Affecting the Value of the Plots

In this study, the plots and the criteria that affected their value were identified through the literature review. The criteria were compiled as main, sub and criterion, and they were grouped under the main heading as legal, physical, locational and local features (Table 1). The criteria were arranged in a survey form and the surveys were carried out on 2,531 participants in previous studies (Ünel, 2017). The survey consists of 116 questions related to the criteria. The questions were asked of experts working on real estate valuation, and citizens who played a role in real estate purchases and/or sales in Ankara, Konya, and Kayseri in the Central Anatolia Region. Finally, data collection was conducted in two steps: first the survey data and then the data about the plots were collected. PCA was employed to reduce the criteria for the survey data, while MRA was used to verify the model for the other data.

2.3 Principal Component Analysis

Principal Component Analysis (PCA) is a method of choosing an attribute used to describe the original data with a small cluster of data and with the lowest possible number of samples; it is a statistical analysis with multiple variables (Özdemir, 2010). PCA is a tool that is used in studies carried out in many fields such as psychology, education, quality, agriculture, chemistry, mapping, photographic sciences, market research, economy, anatomy, biology, forest sciences and genetics (M. Çilli & Arıtan, 2010).

PCA converts interrelated variables into a small unrelated theoretical structure called the principal

component (PC). PCA is used to discover and interpret the dependence that exists between variables as well as examining the possible relations between individuals (Timm, 2002). PCA can be used independently; it can also be used as a technique for data collection for other analyses (Sangün, 2007). The mathematical steps of PCA are as follows:

1. The matrix form of the data cluster
2. The mean values of the data cluster
3. Variance covariance matrix
4. The eigenvalue and the eigenvector
5. Determining the number of principal components

Judging from the fact that an x-series is obtained by measuring each of a number of variables such as X_1, X_2,....,X_p on n number of participants, the matrix formed by the raw data is shown on the n × p dimension as an X data matrix in Eq. (1) (Sangün, 2007):

$$X = \begin{bmatrix} x_{11} & x_{12} & x_{13} & \cdots & x_{1p} \\ x_{21} & x_{22} & x_{23} & \cdots & x_{2p} \\ x_{31} & x_{32} & x_{33} & \cdots & x_{3p} \\ \vdots & \vdots & \vdots & \ddots & \vdots \\ x_{n1} & x_{n2} & x_{n3} & \cdots & x_{np} \end{bmatrix} \quad (1)$$

The mean values ($\overline{X}_j$) of the data cluster are obtained by using Eq. (2) for each variable.

$$\overline{X}_j = \frac{\sum_{i=1}^n X_{ij}}{n} \quad (2)$$

i: 1, 2, 3, ….,n (the number of participants),
j: 1, 2, 3, ….,p (the number of variables)

While variance measures the divergence of the points on a variable from the average, covariance measures how much each of them changes from the average in relation to each other (Farag & Elhabian, 2009). The variance–covariance matrix of the data cluster is formed in a p × p dimensional way Eq. (5) by using the variance Eq. (3) and covariance Eq. (4) equalities. One of the most important aspects that differentiate PCA from factor analysis is that PCA is processed through variance–covariance analysis (MathWorks, 2014; Minitab, 2014; Sangün, 2007). The matrixes of variance $var(X)$, covariance $cov(X_1, X_2)$ and variance–covariance cov are shown as

$$var(X) = \frac{\sum_{i=1}^n (X_i - \overline{X})(X_i - \overline{X})}{(n-1)} \quad (3)$$

$$cov(X_1, X_2) = \frac{\sum_{i=1}^n (X_{i1} - \overline{X_1})(X_{i2} - \overline{X_2})}{(n-1)} \quad (4)$$

$$cov = \begin{bmatrix} var(X_1) & cov(X_1,X_2) & cov(X_1,X_3) & \dots & cov(X_1,X_p) \\ cov(X_2,X_1) & var(X_2) & cov(X_2,X_3) & \dots & cov(X_2,X_p) \\ cov(X_3,X_1) & cov(X_3,X_2) & var(X_3) & \dots & cov(X_3,X_p) \\ \vdots & \vdots & \vdots & \ddots & \vdots \\ cov(X_p,X_1) & cov(X_p,X_2) & cov(X_p,X_3) & \cdots & var(X_p) \end{bmatrix} \quad (5)$$

(Farag & Elhabian, 2009; Gaborski, 2010; Polat, 2008; Sangün, 2007).

The eigenvalues and the eigenvectors of the variance–covariance matrix are found; the eigenvectors which have the biggest eigenvalue correspond to the variables that have the strongest relation in the data cluster (Gaborski, 2010). Therefore, the eigenvectors found here are accepted as the new principal components (Orhan, 2013).

Table 1 Criteria affecting the value of the plot (*subheadings are in bold and italic*) (Yalpir & Unel, 2017)**.**

NO	A. LEGAL FEATURES	Q38	*Proximity to Educational Institutions*	Q78	Proximity to underpass/ overpass
Q1	*Property Conditions*	Q39	Proximity to Pre-schools	*Q79*	*Proximity to Unsanitary Areas*
Q2	Full Ownership	Q40	Proximity to High Schools	Q80	Proximity to was disposal areas
Q3	Shared Ownership	Q41	Proximity to Higher Education Institutions	Q81	Proximity to treatment facilities
Q4	*Zoning Status*	Q42	Proximity to courses	Q82	Proximity to natural gas and tube filling facilities
Q5	The Gross Floor Area	*Q43*	*Proximity to Public Institutions*	Q83	Proximity to petrol stations
Q6	Total Construction Area	Q44	Proximity to governorships	Q84	Proximity to base stations
Q7	The number of floors≥10	Q45	Proximity to Municipalities	Q85	Proximity to energy transmission lines
Q8	The number of floors<10	Q46	Proximity to Courthouse	Q86	Proximity to underdeveloped areas
Q9	Detached Building	Q47	Proximity to Jailhouse	Q87	Proximity to marsh areas
Q10	Attached Buildings	*Q48*	*Proximity to Security Units*	Q88	Proximity to natural disaster areas
Q11	*Legal Restraints*	Q49	Proximity to Police Stations	Q89	Proximity to not improved river areas
Q12	Right of Mortgage	Q50	Proximity to Military Zones	*Q90*	*Proximity to Industrial Zones*
Q13	Easement	Q51	Proximity to Fire Departments/ 112 Emergency	*Q91*	*Proximity to Graveyards*
Q14	Annotation of Lease	*Q52*	*Proximity to Attraction Centres*	*Q92*	*Proximity to Worship Places*
Q15	*Plot Area*	*Q53*	*Proximity to Shopping Centres*	*Q93*	*Proximity to Business Centres*
NO	B.PHYSICALFEATURES	Q54	Proximity to Hypermarkets	*Q94*	*Proximity to Parking Areas*
Q16	*The location of the plot*	Q55	Proximity to mini-markets	*Q95*	*The View From The Plot*
Q17	Corner parcel	Q56	Proximity to open/closed bazaars	Q96	Mountain, valley, etc. views
Q18	Intermediate parcel	Q57	Proximity to commercial enterprises	Q97	Lake, river, stream, etc. view
Q19	*Geometric Structure*	*Q58*	*Proximity to Cultural Centres*	Q98	City view
Q20	Length of the Frontage	Q59	Proximity to cinemas/theatres	NO	D.NEIGHBOURHOOD FEATURES
Q21	The number of frontage	Q60	Proximity to historical sites and touristic attractions	*Q99*	*Population density*
Q22	Geometric shape	*Q61*	*Proximity to Entertainment Centres*	Q100	Education Level
Q23	*Technical Infrastructure Services*	Q62	Proximity to fairs, concert areas, etc.	Q101	Level of income
Q24	Water supply	Q63	Proximity to sport facilities	Q102	Immigrant receiving

Q25	Electricity, sewer, natural gas, and telephone	Q64	Proximity to stadium/hippodrome	Q103	Criminal Rate
Q26	Solid waste collection service	Q65	Proximity to entertainment venues	Q104	Neighbourliness Relations
Q27	Storm drainage	Q66	*Proximity to Green Areas*	Q105	Homeowner/tenant
Q28	Unpaved road	Q67	Proximity to forest/copses	Q106	*The Surrounding Environment*
Q29	Asphalt road	Q68	Proximity to recreation areas	Q107	The favourite neighbourhood
Q30	*The Road Condition*	Q69	Proximity to parks	Q108	Residential Density
Q31	The Periphery Road	Q70	Proximity to playgrounds	Q109	Development potential
Q32	Road width≥10	Q71	*Proximity to Public Transportation Points*	Q110	Purchasing and selling mobility of real estate
Q33	Road width<10 metre	Q72	Proximity to airports	Q111	*Underground, soil, and aboveground features*
Q34	*The Slope of The Plot*	Q73	Proximity to railway stations	Q112	Slope of the neighbourhood
NO	C. LOCATIONAL FEATURES	Q74	Proximity to coach station	Q113	Geological condition
Q35	*Proximity to Health Facilities*	Q75	Proximity to tramway, subway and metrobus stations	Q114	Climate Condition
Q36	Proximity to health centre, village clinic, etc.	Q76	Proximity to bus stops	Q115	Air Pollution
Q37	Proximity to State/Private Hospitals	Q77	Proximity to shared taxi routes	Q116	Noise Pollution

The number of components is equal to the number of p variables at the beginning. However, the number of the components chosen must be smaller than p. A curve is drawn to combine the points on which components and the eigenvalues are shown. The breakpoint at which the eigenvalues start to become parallel to the horizontal axis gives the number of components. The number of components can also be identified depending on what percentage of the total variance the first components represent. The acceptance of this percentage ranges in the literature from 70% to 95% (M. Çilli, 2007; Semmlow, 2004).

2.4 Multiple Regression Analysis

In multivariate regression analysis, the independent variables are used to explain the change in the dependent variable simultaneously. The model of the MRA analysis,

$$y_i = \beta_0 + \beta_1 x_{i1} + \beta_2 x_{i2} + \cdots + \beta_k x_{ik} + u_i \qquad (6)$$

y_i : Dependent variable (value of real estate)
$x_{i1}, x_{i2}, \ldots x_{ik}$: Independent variables (share, area, TAKS, KAKS, number of floors, etc.)
u_i : Corruption or error term.
β_0 : Constant
$\beta_1, \beta_2, \ldots \beta_k$: Coefficients of variation

can be demonstrated by a general formula in Eq. (6). The F test in the result of analysis and R^2 are the important concepts to be checked first. The F test is a test with ANOVA to examine whether the regression model is significant. The level of significance corresponding to the value of F resulting from the ANOVA test helps to determine whether the model created is appropriate. When the result of the F test is significant (p<0.05), it is interpreted that the model contributes significantly to explain the dependent variable. The R^2 value indicates what percentage of the variance in the dependent variable is explained by the independent variable (Altunışık, Coşkun, Bayraktaroğlu, & Yıldırım, 2010). The closer this value is to 1, the better the model is explained by the independent variables (Yalpır, 2007).

2.5 Performance Analysis

The results of the mean absolute error (MAPE) Eq. (7), the root mean square error (RMSE) Eq. (8) and the mean absolute error (MAE) Eq. (9) were used in the performance analyses to compare the model values and the market values obtained from the criteria. The performance of the model is investigated with these error rates especially in the studies in which the method is developed for real estate valuation (Fernandez-Martinez, Fernandez-Ceniceros, Sanz-Garcia, Lostado-Lorza, & Martinez-De-Pison-Ascacibar, 2011; Kavas, 2014; Kuşan, Aytekin, & Özdemir, 2010; Lin, 2010; Lughofer, Trawinski, Trawinski, Kempa, & Lasota, 2011; Saraç, 2012).

$$MAPE = \frac{1}{n}\sum_{i=1}^{n}\frac{|y_i - \hat{y}_i|}{y_i} \qquad RMSE = \sqrt{\frac{1}{n}\sum_{i=1}^{n}(y_i - \hat{y}_i)^2}$$

$$(7) \qquad\qquad\qquad (8)$$

$$MAE = \frac{1}{n}\sum_{i=1}^{n}|y_i - \hat{y}_i|$$

y_i : *Market values*,
$\hat{y}_i$: *Model values*,
i : $1, 2, 3, \ldots n$
n : *Number of selected samples*

$$(9)$$

3. RESULTS AND DISCUSSION

3.1 Results of Principal Component Analysis

Principal component analysis is a reduction analysis and is applied to the survey data by using Minitab 17 software. A covariance–variance matrix was preferred because of the fact that raw data were used. The data belonging to legal, physical, location and neighbourhood features were analysed separately in the general sampling group.

Because the principal components were composed of PCA, the main heading and most subheadings were not included in the process of analysis. However, the plot itself was taken as a criterion because there were not any criteria under certain headings such as its size and its slope. A total of 96 criteria were subjected to analysis. The survey data were composed of 96 (p) criteria and they

were measured on 2,474 (n) participants, giving the matrix of the data cluster a size of 96 × 2,474 which consisted of the raw data. Because the legal features had data about 12 sub-criteria, a total of 12 components were calculated. The percentages of the eigenvalues, variance and cumulative variance were given for each component (Table 2). Although the number of components was 12 according to the raw data, it must be lower than 12 according to PCA. Accordingly, the number of components with a significance level of 75 (0.746) % according to the cumulative percentages of variances is 4.

Table 2 Eigenvalue analysis of variance–covariance matrix

Component	The Eigen Value analysis of variance covariance matrix		
	Eigen Value	Rate	Cumulative
PC1	28.068	.407	.407
PC2	9.769	.142	.549
PC3	7.557	.110	.658
PC4	6.048	.088	**.746**
PC5	4.496	.065	.811
PC6	3.371	.049	.860
PC7	3.224	.047	.907
PC8	1.872	.027	.934
PC9	1.517	.022	.956
PC10	1.218	.018	.973
PC11	0.963	.014	.987
PC12	0.870	.013	1.000

Considering that eigenvalues could be 1 and higher than 1, the number of components is 10 (Table 2). The number of components is 2 according to the graphics composed of the numbers of eigenvalues and of components (Fig. 3). This being so, it was concluded that the number of components should be taken as 2 according to the graphics with the lowest number of components.
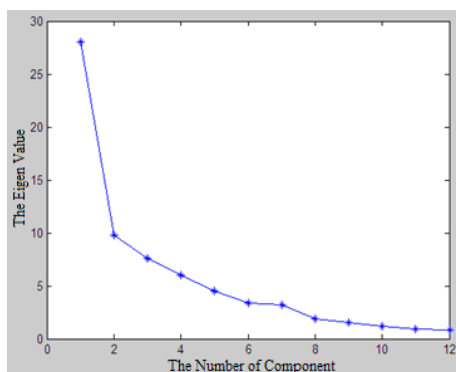

Figure 3 Graphics of eigenvalues–the number of components

PCA was applied to the sub-criteria of the legal features, and the analysis was repeated after removing the criteria that remained below 30% (Q2, Q7, Q8, Q9, and Q10) and those that were composed of a single criterion (Q3). According to the results of the repeated analysis, the cumulative variance percentage of two components was 70 (0.699) % and therefore the analysis was understood to be significant (Table 3).

Table 3 Principal components of the legal features

Component Question No	Mean	Standard Deviation	Legal Restraints	Zoning Status
Q14	-1.64	3.60	.579	
Q13	-2.47	3.34	.575	
Q12	-2.68	3.41	.573	
Q6	3.81	2.04		-.539
Q15	3.83	2.06		-.488
Q5	3.89	1.82		-.466
Eigen Value			26.099	7.048
Cumulative			.550	.699
Reliability			.813	.647
N			3	3

PCA was applied to the sub-criteria of the physical features, and it was seen that Q28 had high loads in two components. The analysis was repeated after leaving Question 28 out. The criteria that remained below 30% (Q17, Q22, Q24, and Q25), a criterion which was discordant with the criteria in the component (Q18) and those which were the only criterion in a component (Q31, Q32, Q33, and Q34) were removed, and then the analysis was repeated. According to the repeated analysis, the cumulative variance percentage of the components was 72 (0.716) %. It was understood that the analysis was significant (Table 4).

Table 4 Principal components of the physical features

Component Question No	Mean	Standard Deviation	Infrastructure Services	Status of Frontage
Q29	3.45	2.14	.463	
Q27	3.54	2.00	.454	
Q26	3.66	1.84	.426	
Q21	3.74	2.12		-.579
Q20	3.75	2.02		-.515
Eigen Value			9.697	5.036
Cumulative			.471	.716
Reliability			.733	.754
N			3	2

PCA was applied to the sub-criteria of the locational features. The criteria that remained below 30% (Q36, Q37, Q39, Q40, Q41, Q42, Q49, Q51, Q52, Q54, Q55, Q56, Q57, Q59, Q60, Q63, Q67, Q68, Q69, Q70, Q74, Q75, Q76, Q77, Q78, Q87, Q88, Q89, and Q98), the criteria that were discordant with the criteria in the component (Q46, Q47, Q50, Q91, Q92, Q93, and Q94), the one which was the only criterion in a component (Q 90) and that with the highest load into components (Q62) were removed, and then the analysis was repeated at least 15 times. The rate of cumulative variance percentage of the five components was 75 (0.748) % in the last analysis. The analysis was understood to be significant (Table 5).

PCA was applied to the sub-criteria of neighbourhood features. The criteria that remained below 30% (Q100, Q103, Q104, Q105, Q107, and Q109) were removed. Then the analysis was repeated. According to the results of the repeated analysis, those discordant with the criteria in the component (Q110, Q113, and Q114), those which were the only criterion in one component (Q101 and Q102) and the one with a high load in two criteria (Q112) were removed. The analysis was repeated. According to the last analysis, the cumulative variance value of the two components was 78 (0.781) %. This showed that the analysis was significant (Table 6).

Table 5 Principal components of the locational features

Component Question No	Mean	Standard Deviation	Unsanitary Areas	Entertainment Areas	Transportation Networks	The View from the Plot	Public Institutions
Q83	-2.90	2.75	-.370				
Q82	-3.58	2.21	-.336				
Q84	-3.44	2.27	-.335				
Q85	-3.37	2.23	-.334				
Q81	-3.56	2.26	-.329				
Q86	-3.32	2.27	-.321				
Q80	-3.70	2.23	-.306				
Q64	1.64	2.92		.408			
Q65	1.77	2.83		.381			
Q72	1.28	3.28			-.704		
Q73	2.43	2.69			-.380		
Q96	3.28	2.26				-.509	
Q97	3.43	2.18				-.495	
Q45	2.88	2.23					.522
Q44	2.81	2.22					.508
Eigen Value			28.010	22.425	9.687	8.079	6.186
Cumulative			.281	.507	.604	.685	.748
Reliability			.925	.683	.672	.843	.879
N			7	2	2	2	2

Table 6 Principal components of neighbourhood features

Component Question No	Mean	Standard Deviation	Population/ Residential Density	Air/Noise Pollution
Q108	0.70	3.61	.727	
Q99	0.90	3.50	.662	
Q116	-3.53	2.37		.676
Q115	-3.53	2.37		.675
Eigen Value			18.346	10.177
Cumulative			.502	.781
Reliability			.599	.910
N			2	2

3.1.1 The Wording of the principal components

A total of 96 criteria were subjected to PCA. As a result of the repeated analysis carried out after removing those that remained below 30%, any which was the only criterion in a component and those that were discordant with the other criteria, 30 criteria remained. These criteria were composed of 11 principal components. A total of 11 principal components, 2 from legal features, 2 from physical features, 5 from locational features and 2 from neighbourhood features, were formed according to PCA (Table 7).

Great attention was paid to the wording of the components in accordance with the criteria in the number of the questions under the components.

Table 7 Principal components at a total of 30 criteria

No of Order	Main Heading	Component No	The Wording of the Main Components	The number of Items	Question No
1	Legal Features	TB1	Legal Restraints	3	Q14, Q13, and Q12.
2		TB2	Zoning Status	3	Q6, Q15, and Q5.
3	Physical Features	TB1	Infrastructure Services	3	Q29, Q27, and Q26.
4		TB2	The Status of the Frontage	2	Q21 and Q20.
5	Locational Features	TB1	Unsanitary Areas	7	Q83, Q82, Q84, Q85, Q81, Q86, and Q80.
6		TB2	Entertainment Areas	2	Q64 and Q65.
7		TB3	Transportation Networks	2	Q72 and Q73.
8		TB4	The View from the Plot	2	Q96 and Q97.
9		TB5	Public Institutions	2	Q45 and Q44.
10	Neighbourhood Features	TB1	Population and Residential Density	2	Q108 and Q99.
11		TB2	Air and Noise Pollution	2	Q116 and Q115.

3.1.2 Separation of the principal components

It is necessary to separate some of the principal components because they involve criteria which require specific information about the plot. The components of zoning and frontage must be separated into sub-criteria. The components of infrastructure services can also be considered separately, depending on whether such services as water, electricity, sewage system, natural gas, telephone, etc. are available. However, because such a separation is impossible due to a lack of data, these criteria were taken as a single criterion and were not separated (Table 8). At the end of this process, a total of 14 reduced criteria were established.

Table 8 Separation of certain components

THE COMPONENTS NOT PUT THROUGH SEPARATION		THE COMPONENTS PUT THROUGH SEPARATION	
No	Factors	No	Zoning Status
1	Legal Restraints	1	The Gross Floor Area
2	Infrastructure Services	2	Total Construction Area
3	Unsanitary Areas	3	The Size of the Plot
4	Entertainment Areas	4	Length of the Frontage
5	Transportation Networks	5	The number of frontage
6	The View from the Plot		
7	Public Institutions		
8	Population and Residential Density		
9	Air and Noise Pollution		**Total=14**

3.2 Formation of the Indexes

Because of the relationship of the criteria about neighbourhood and locational features with the map and because of the difference between evaluation scales, indexes were formed in two basic steps:

- Neighbourhood index (Nind)
- Locational index (Lind)

The formation process is the process of obtaining a separate value for a standard neighbourhood and for the location by combining the value that the criteria of neighbourhood and locational features take on the map and the percentage of the responses from the survey with ArcGIS. The graphical data models were generated with GIS, and index maps were created. These provide that criteria are objectively appraised, standardized, and facilitated in the process of real estate valuation.

The numerical data of the criteria about neighbourhood features and their markings on the map were prepared in a vector environment. Raster format maps with pixel values classified between the standard point ranges are required in order to form an index. The maps of the criteria about neighbourhood features were generated in a standard way in the raster format. The neighbourhood index was obtained by using the weights of the criteria reduced in PCA, combining them and classifying them in a range from 1 to 10 (Fig. 4).

A proximity analysis was conducted by considering accessible distances to facilities of the locational features with the criteria reduced in PCA. The vector format map obtained as a result of this analysis was converted into standard ranges in a raster format. The criteria of locational features reduced with PCA were combined depending on their weight, and a locational index was generated with their classification ranging between 1 and 10 (Fig. 5). Locational and neighbourhood indexes were obtained by applying similar procedures to all the criteria. However, PC4 was not taken into consideration because it contained features such as mountain, lake, river, etc., and these were non-existent in the study area.

3.3 Results of Regression and Performance Analyses

MRA was applied by using market sampling data about a total of 41 criteria composed of legal, physical and neighbourhood features and locational indexes, and Model 1 was formed out of all the criteria. With the application of MRA, Model 2 and Model 3 were obtained by using the criteria reduced from PCA. The data about the gross floor area, total construction area and the size of the plot derived from the legal features, and the data about the infrastructure services, the length of the frontage and the number of the frontage are the same in Model 2 and Model 3.

The neighbourhood index which involved the density of population and of buildings and air and noise pollution were the same in both models and responded to a single value. However, the data about locational features varied. While the indexes of unsanitary areas, entertainment, transportation and public institutions were used to form the locational index in Model 2, the locational index which responded to a single value was used in Model 3. Also, legal restraints about market samplings and the criteria composed of the view status were disregarded and not included in the analysis.
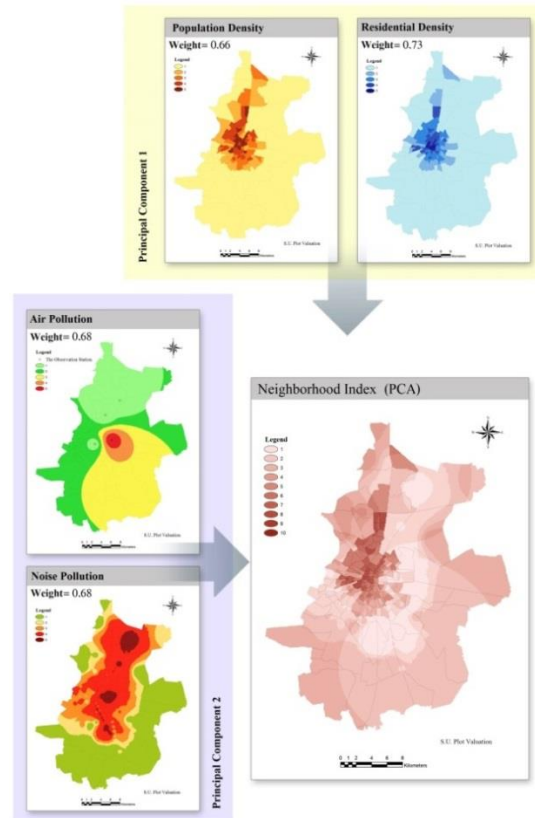

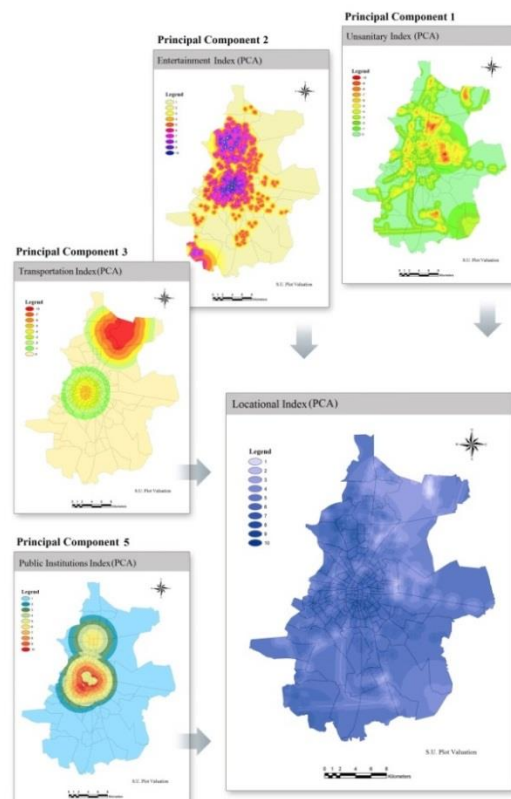Figure 4 Neighbourhood index with the criteria reduced according to PCA

Figure 5 Locational index with the criteria reduced according to PCA

Prediction values were calculated by using mathematical models of Model 1, Model 2 and Model 3. Performance analyses were carried out in order to compare market values with the values obtained from the models, and these were examined (Table 9).

The R^2 value was calculated as 0.815 for Model 1, obtained with all the criteria. Because this was close to 1, it is the best model to explain the dependent variable. The second best model was Model 2 with 11 criteria. It is seen that the R^2 success rate (0.712) of Model 2 is closest to that of Model 1. The MAPE, RMSE and MAE error rates of this model are also closest to those of Model 1. The MAPE and MAE error rates of Model 3 are higher than the others. As the number of criteria decreases, it is observed that error rates increase (Table 9).

3.4 Value Maps

Value maps were produced to see the locational distribution of the values. The market values and the prediction values obtained from Model 1, Model 2 and Model 3 were associated with market samplings in ArcGIS by using GIS. Value maps were generated with the kriging method as the geo-statistical method. Because the value maps were location-based, comparison and analysis were seen to be easier. When the locational distribution of the values was examined, it was established that Model 1 and Model 2 were closest to the market values. Because it contained 11 criteria, Model 2 is more appropriate for mass appraisal. In addition, it was observed that particularly the lowest and the highest values differed from one map to another (Fig. 6).

Table 9 The results of performance

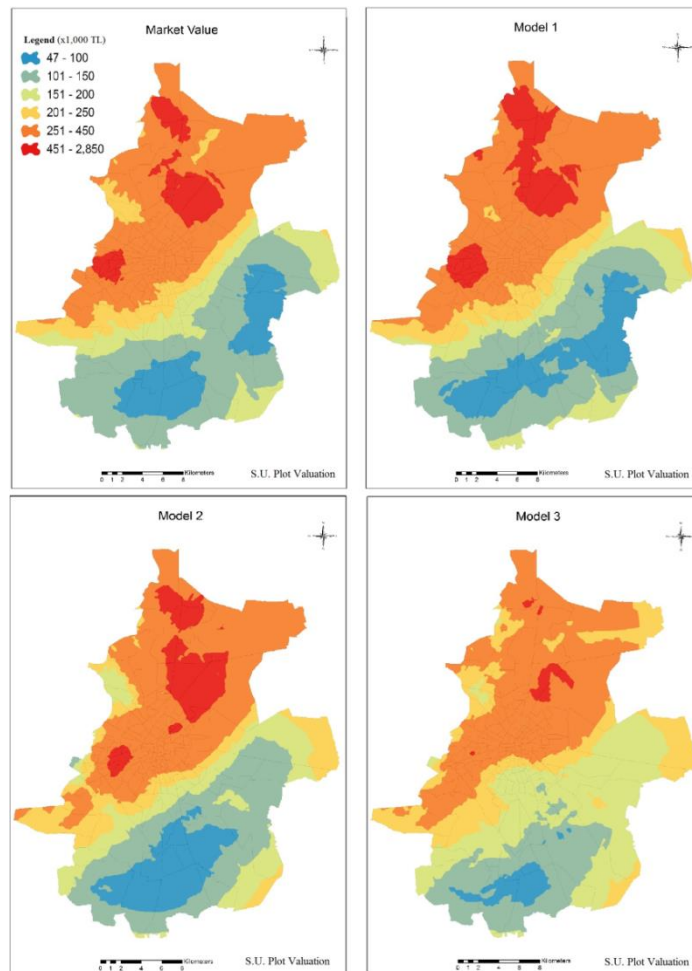| Models	The number of criteria	Standard Deviation	R^2	y=ax	MAPE	RMSE	MAE
Model 1	41	0.030	0.815	y=0.9223x	0.368	0.014	0.009
Model 2	11	0.029	0.712	y=0.8538x	0.389	0.017	0.010
Model 3	8	0.028	0.677	y=0.8397x	0.447	0.017	0.011

Figure 6 Value maps

While the total number of criteria was 116 in the survey, the number of reduced criteria after PCA was 30. The number of criteria used later to generate an index for model verification was 41 in Model 1, 11 in Model 2 and 8 in Model 3. The criteria used in Model 2 were the reduced criteria as a result of PCA. Locational and neighbourhood criteria were obtained in the form of an index and were turned into an objective form (Fig. 7).
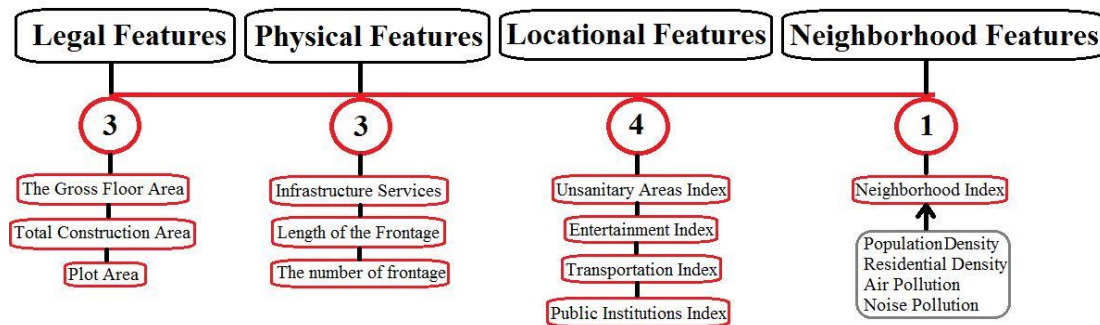
THE REDUCED CRITERIA IN MODEL 2

Figure 7 Reduced criteria used in model 2

4. CONCLUSION

It is observed that criteria change according to the study area concerned in the literature. When they are listed as a table, there are a large number of criteria that affect the plot value. Using all of them for mass appraisal is not considered to be economical. The optimum criteria and the number of criteria should be determined by taking into consideration the structural characteristics of the real estate in the country of interest. In addition, they should be obtained as independent from dependent variables such as price, letting value.

The criteria were reduced by using PCA and the results of criteria analysis were objectively evaluated. Neighbourhood and locational indexes were created by generating a geographical data model on ArcGIS with criteria for neighbourhood and locational features. Model verification was conducted by applying MRA to the data of the criteria of the plots. When the performances of Model 1 (all criteria), Model 2 (11 criteria) and Model 3 (8 criteria) were examined, Model 2 is closer to the market value than Model 3. In addition, it was concluded that the inexplicable part of Model 2 (nearly 29 %) resulted from the unstable economy, annuity, political situations and unavailable data.

Collecting, editing, and getting ready for the analysis of data relating to criteria are difficult and time-consuming processes. The reduced criteria save time, labour and expense in the processes. They will be a basis for mass appraisal and a system of real estate valuation. The application will be facilitated by standardizing real estate valuation in Turkey. In future, criteria will be separately defined according to all real estate types. Analyses should be carried out in critical regions where the criteria have changed, such as whether a property has sea view or not.

REFERENCES

Altunışık, R., Coşkun, R., Bayraktaroğlu, S., & Yıldırım, E. (2010). Sosyal Bilimlerde Araştırma Yöntemleri SPSS Uygulamalı (6. ed.). Sakarya: Sakarya Yayıncılık.

Amil, T. A. (2018). Determining Of Different Inundated Land Use in Salyan Plain During 2010 The Kura River Flood Through GIS and Remote Sensing Tools. International Journal of Engineering and Geosciences (IJEG), 3(3), 80-86. doi:10.26833/ijeg.412348

Bender, A., Din, A., Hoesli, M., & Laakso, J. (1999). Environmental quality perceptions of urban commercial real estate. Journal of Property Investment & Finance, 17(3), 280 - 296.

Cellmer, R., Senetra, A., & Szczepanska, A. (2012). The effect of environmental factors on real estate value. Paper presented at the FIG Working Week 2012, Rome, Italy.

Çilli, M. (2007). İnsan hareketinin modellenmesi ve benzeşiminde Temel Bileşenler Analizi yönteminin kullanılması. Hacettepe Üniversitesi, Sağlık Bilimleri Enstitüsü, Doktora Tezi, Ankara.

Çilli, M., & Arıtan, S. (2010). Temel Bileşenler Analizi yardımı ile elde edilen daha az sayıda değişken kullanılarak farklı hızlarda insan koşusunun fourier tabanlı modelinin oluşturulması. Hacettepe J. of Sport Sciences, 21(1), 1-12.

El-Gohary, M. (2004). Property valuation model effect of traffic noise on property value. Retrieved from

Farag, A. A., & Elhabian, S. (2009). A Tutorial on Principal Component Analysis. Retrieved from http://dai.fmph.uniba.sk/courses/ml/sl/PCA.pdf

Fernandez-Martinez, R., Fernandez-Ceniceros, J., Sanz-Garcia, A., Lostado-Lorza, R., & Martinez-De-Pison-Ascacibar, F. J. (2011). Dimensionality reduction in a database related with viticulture crops using wrapper techniques. International Journal of Mathematical Models And Methods In Applied Sciences, 5(5), 866-873.

Gaborski, R. S. (2010). Principal Components Analysis. Retrieved from http://www.cse.psu.edu/~rcollins/CSE586Spring2010/lectures/pcaLectureShort_6pp.pdf

Henry, E. N. N. (2013). From turtle populations to property values: The effects of lakeshore residential development and The Invasive Zebra Mussel. Michigan State University, PhD, Michigan.

Kauko, T. J. (2002). Modelling the locational determinants of house prices: neural network and value tree approaches. Utrecht University, PhD, Netherlands.

Kavas, S. (2014). Konut fiyatlarının çok kriterli bir karar destek modeli ile tahmin edilmesi İstanbul Teknik Üniversitesi, Fen Bilimleri Enstitüsü, Yüksek Lisans Tezi, İstanbul.

Kryvobokov, M. (2005). Estimating the weights of location attributes with the Analytic Hierarchy Process in Donetsk, Ukraine. Nordic Journal of Surveying and Real Estate Research, 2(2), 5-29.

Kryvobokov, M. (2006). Mass valuation of urban land in Ukraine: From normative to a market-based approach. Real Estate and Construction Management School of Architecture and The Built Environment Royal Institute of Technology, PhD, Stockholm.

Kryvobokov, M., & Wilhelmsson, M. (2007). Analysing location attributes with a hedonic model for apartment prices in Donetsk, Ukraine. International Journal of Strategic Property Management, 11, 157-178.

Kuşan, H., Aytekin, O., & Özdemir, İ. (2010). The use of fuzzy logic in predicting house selling price. Expert Systems with Applications, 37, 1808–1813. doi:10.1016/j.eswa.2009.07.031

Li, Q. C. (2010). Neighborhood greenspace's impact on residential property values: understanding the role of spatial effects. Faculty of the USC Graduate School University of Southern California, PhD, California.

Lin, C. C. (2010). Critical analysis and effectiveness of key parameters in residential property valuations. State University of New York, The Faculty of The Graduate School of The University at Buffalo, PhD, New York.

Lughofer, E., Trawinski, B., Trawinski, K., Kempa, O., & Lasota, T. (2011). On employing fuzzy modeling algorithms for the valuation of residential premises. Information Sciences, 181, 5123–5142. doi:10.1016/j.ins.2011.07.012

MathWorks. (2014). İstatistik, Faktör Analizi. Retrieved from http://www.mathworks.com/products/demos/statistics/factorandemo.html

McCluskey, W. J., & Borst, R. A. (2007). Specifying the effect of location in multivariate valuation models for residential properties: A critical evaluation from the mass appraisal perspective. Property Management, 25(4), 312-343. doi:10.1108/02637470710775185

Minitab. (2014). What are the differences between principal components analysis and factor analysis? Retrieved from http://support.minitab.com/en-us/minitab/17/topic-library/modeling-statistics/multivariate/principal-components-and-factor-analysis/differences-between-pca-and-factor-analysis/

Muehlenbachs, L., Spiller, E., & Timmins, C. (2014). The housing market impacts of shale gas development. Retrieved from Washington, New York:

Orhan, U. (2013). Makine öğrenmesi. Retrieved from http://bmb.cu.edu.tr/uorhan/DersNotu/Ders11.pdf

Özdemir, A. T. (2010). Erken ventriküler kasılmalarda YSA tabanlı bir sınıflandırıcının FPGA ile gerçekleştirilmesi. Erciyes Üniversitesi, Fen Bilimleri Enstitüsü, Doktora tezi, Kayseri.

Polat, K. (2008). Biyomedikal sinyallerde veri ön-işleme tekniklerinin medikal teşhiste sınıflama doğruluğuna etkisinin incelenmesi. Selçuk Üniversitesi, Fen Bilimleri Enstitüsü, Doktora Tezi, Konya.

Sangün, L. (2007). Temel bileşenler analizi, ayırma analizi, kümeleme analizleri ve ekolojik verilere uygulanması üzerine bir araştırma. Çukurova Üniversitesi, Fen Bilimleri Enstitüsü, Doktora tezi, Adana.

Saraç, E. (2012). Yapay sinir ağları metodu ile gayrimenkul değerleme. İstanbul Kültür Üniversitesi, Fen Bilimleri Enstitüsü, Yüksek Lisans Tezi, İstanbul.

Schulz, M. A. R. (2003). Valuation of properties and economic models of real estate markets. Humboldt-University, Wirtschaftswissenschaftlichen Fakultat, PhD, Berlin.

Sdino, L., Rosasco, P., Torrieri, F., & Oppio, A. (2018). A Mass Appraisal Model Based on Multi-Criteria Evaluation: an Application to the Property Portfolio of the Bank of Italy. NMP2018, 128 (7), 1-10.

Semmlow, J. L. (2004). Biosignal and biomedical image processing, MATLAB-Based applications

Smigielski, E. (2014). Effect of New York State Forests on residential property values. State University of New York, MSc, Syracuse, New York.

Son, K. (2012). Regression model predicting appraised unit value of land in San Francisco county from number of and distance to public transit stops using GIS. Texas A&M University, PhD, Texas.

Timm, N. H. (2002). Applied multivariate analysis Retrieved from http://hbanaszak.mjr.uw.edu.pl/TempTxt/Shorts/_XeL3 THpJaw.pdf

Unel, F. B., Yalpir, S., & Gulnar, B. (2017). Preference Changes Depending on Age Groups of Criteria Affecting the Real Estate Value. International Journal of Engineering and Geosciences (IJEG), 2(2), 41-51.

Ünel, F. B. (2017). Taşınmaz Değerleme Kriterlerine Yönelik Coğrafi Veri Modelinin Geliştirilmesi. Selçuk Üniversitesi, Fen Bilimleri Enstitüsü, Doktora Tezi, Konya.

Yalpir, S., & Unel, F. B. (2017). Use of Spatial Analysis Methods in Land Appraisal; Konya Example. Paper presented at the 5th International Symposium on Innovative Technologies in Engineering and Science (ISITES2017), Baku, Azerbaijan.

Yalpır, Ş. (2007). Bulanık mantık metodolojisi ile taşınmaz değerleme modelinin geliştirilmesi ve uygulaması: Konya örneği. Selçuk Üniversitesi, Fen Bilimleri Enstitüsü, Doktora Tezi, Konya.

Yalpır, Ş., & Ünel, F. B. (2016). Türkiye 'de ve Uluslararası çalışmalarda arsa değerlemede kullanılan kriterlerin irdelenmesi ve Faktör Analizi ile azaltımı. Afyon Kocatepe Üniversitesi Fen ve Mühendislik Bilimleri Dergisi, 16(025502), 303-322. doi:10.5578/fmbd.28134

Zavadskas, E. K., Bausys, R., Kaklauskas, A., Ubarte, I., Kuzminske, A., & Gudiene, N. (2017). Sustainable market valuation of buildings by the single-valued neutrosophic MAMVA method. Applied Soft Computing, 57, 74–87.

Zoppi, C., Argiolas, M., & Lai, S. (2015). Factors influencing the value of houses: Estimates for the city of Cagliari, Italy. Land Use Policy, 42, 367–380.

PERFORMANCE OF NETWORK RTK CORRECTION TECHNIQUES (FKP, MAC and VRS) UNDER LIMITED SKY VIEW CONDITION

Hüseyin Pehlivan[1], Mert Bezcioğlu [1] and Yılmaz Muhammet[2]

[1] Gebze Technical University, Engineering Faculty, Department of Geomatics Engineering, Gebze-Kocaeli, Turkey
(hpehlivan@gtu.edu.tr, mbezcioglu@gtu.edu.tr)**; ORCID 0000-0002-0018-6912 ; ORCID 0000-0001-7179-8361**

[2] Division of Geodetic and Geographical Information Technologies, Graduate School of Natural and Applied Sciences, Gebze Technical University, Gebze-Kocaeli, Turkey
(muhammet@geomatikhizmetler.com.tr); **ORCID 0000-0002-2265-035X**

ABSTRACT: In recent years, the continuously operating reference station – Turkey (CORS-TR) system has been widely used in engineering and cadastral work in Turkey due to ease of use, low cost, and national legislative requirements. In this study, long-term Network RTK (Real-time Kinematic) data were collected under 10°, 20°, 30° and 40° satellite views using a different approach from previous work. In order to evaluate the positioning performance of the system, the measurements were undertaken at different elevation angles (open, partially blocked and extremely blocked) and by considering three different correction techniques (FKP, VRS and MAC), and the results were evaluated in terms of repeatability. From the analysis of the data, it was understood that the performances of the three correction techniques were generally similar, and even in the case of a limited satellite view, the errors remained below 7 cm in all three techniques. However, when the 2D and 3D components were analyzed together, VRS technique showed better results than the other two techniques.

Keywords: CORS-TR, FKP, MAC, VRS, Network RTK.

1. INTRODUCTION

The global positioning system (GPS) provides precision at cm level when the position is determined by a relative method (Seeber, 2003). However, requiring at least two receivers, precise trajectory information, and software knowledge, the relative method is not efficient in performing positioning in terms of the time and effort (Gumus et al., 2012; Tusat and Ozyuksel, 2018). Today, developments in GPS/GNSS technology have enabled real-time determination of point locations. First, the classical RTK (Real Time Kinematic) method, which determines point positions in real time at cm level, was developed. However, in this method, the distance between the reference station and the user is limited to about 10 km to prevent atmospheric, orbit error, and system-related effects. Therefore, to overcome the limitations in the classical RTK method, a new idea was proposed to set up multiple fixed stations (Raquet, 1998). Since the 1990s, continuously operating reference stations (CORS) are used for the geodetic measurements requiring high accuracy and provide real-time location information at cm level based on GPS systems (Rizos, 2002; Sunantyo, 2009; Aykut et al., 2015; Bülbül et al., 2017; Bascifci et al., 2018). As a result of the implementation of this idea and the experiences acquired, fixed GNSS networks (RTK network) emerged. GNSS technology (Network-RTK) is now widely used to obtain instantaneous location data with high accuracy. In Turkey, as of May 2009, there are 146 stations the CORS-TR (TUSAGA Active) network, four located in the Turkish Republic of Northern Cyprus. This system eliminated dependence on a single reference station and allowed the use of atmospheric modeling of a particular region by utilizing data from a large number of reference stations.

CORS systems provided by the U.S. National Geodetic Survey (NGS) offer three-dimensional position information by evaluating GNSS data, such as carrier phase and pseudo-range observations (https://www.ngs.noaa.gov/CORS/). The CORS Networks consists of fully operational and continuously running stations, which are available to users who wish to correct parameters, such as ionosphere, troposphere and time (Öcalan & Tunalıoğlu, 2010). The following three methods are used to calculate the correction parameters in CORS systems: virtual reference station (VRS) (Wanninger, 2003), linear area corrections (Flächen-Korrektur-Parameter; FKP) (Wübbena & Bagge, 1998), and master auxiliary concept (MAC) (Brown et al., 2005). A few studies have investigated which correction method works better for the CORS-TR system. (Gumus et al., 2012), Forty-nine different coordinates obtained from RTK, CORS-TR and IskiCors were corrected using FKP and MAC and the results were compared with the classical local method of total station measurements. The authors reported that the performance of the correction methods for the CORS-TR system was superior. (Bütün and Baybura, 2010), in another study, point coordinates from the CORS-TR stations and static measurement results were compared, and it was determined that the coordinate differences decreased as the measurement period increased. (Gumus et al., 2016), the contribution of the VRS, FKP and MAC to the height data was investigated and VRS was found to provide the most consistent results. (Pırtı, 2016), in a forest area, the performance of VRS and FKP techniques in the CORS-TR system was compared with total station measurement and the sensitivity was calculated as 1-3 cm horizontal and 2-4 cm vertical. (Öğütcü et al., 2016), in an urban area, a few observations were undertaken under the same conditions to analyze the performance of the three different correction techniques, and it was concluded that there was no significant difference between them. (Yıldırım et al., 2013), in another study, the authors suggested that the CORS-TR system was suitable for obtaining tectonic movements. (Eren et al., 2009), the performance of the CORS system in three different networks with three different GNSS receivers was analyzed both in real time and in postprocess using FKP, VRS, PRS, and MAC correction techniques, and it was concluded that even in the case of increased base length, these correction techniques yielded successful results.

There are different studies on the precise of CORS-TR in the literature. However, to date, no researcher in the national or international arena has clearly explained the contribution of this system to determination of location in case of limited satellite vision through an assessment of long-term CORS measurements using these correction techniques and repeatability of the coordinates. This study adopted a different approach from the literature in that long term CORS-TR data was collected and evaluated based on positional performance, open, partially closed, closed, restricted of satellite visibility, and three different correction techniques.

1.1 CORS-TR

The CORS-TR Project, officially started on May 1, 2006 with the support of TUBITAK, was carried out jointly by Istanbul Kültür University (IKU), General Directorate of Mapping (HGM), General Directorate of Land Registry and Cadastre (TKGM) and completed in December 2008 (Eren et al., 2009). The main purpose of this project was to establish CORS-TR stations that work continuously based on the principles of RTK, contribute weather forecasts, create an atmospheric model via Turkey (Musa et al., 2005), follow tectonic movements, determine crustal deformations, provide positions with the accuracy of mm level, contribute to earthquake prediction and early warning systems (Brownjohn et al., 2004), and determine the conversion parameters between ED50 and ITRFxx datum (Kempe et al., 2006).

The CORS-TR system consists of 146 stations located in Turkey and the Turkish Republic of Northern Cyprus (Yıldırım et al., 2013). The system has three control centers, two of which are in Ankara and one in Istanbul. The coordinates of the control centers are in the ITRF96 datum. The distribution of the CORS-TR stations is shown in Figure 1. When the stations were planned, the most optimal data were taken into consideration to observe the movements of the plate (Mekik et al., 2011; Uzel et al., 2011). These control centers send correction data to the user using FKP, MAC and VRS techniques

(Gumus et al., 2012).

Figure.1 CORS-TR Stations (Yıldırım et al., 2013)

1.2 Network RTK correction Techniques

1.2.1 FKP

The FKP technique, also known as the field correction parameter, is one of the first Network-RTK corrections developed by the German SAPOS group (Satellitenpositionierungsdienst der deutschen Landesvermessung) (Kahveci, 2009). The content of FKP corrections is linear ionospheric and geometric correction parameters around the reference station. These linear corrections refer to the changes in east-west and north-south directions and are used for the exact calculation of the receiver's actual position by interpolation (Pırtı, 2016). The FKP method creates a different FKP plane for each reference surface (Figure 2) (Kahveci, 2009).
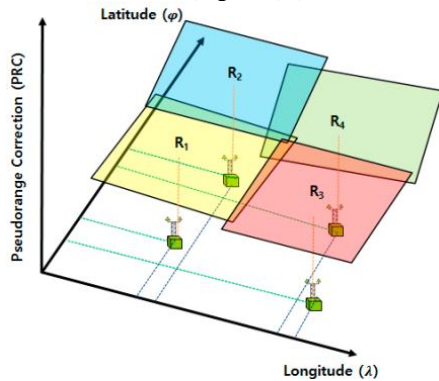

Figure 2: FKP Method for Four Reference Stations (Kim et al., 2017)

1.2.2 VRS

VRS is the most widely used augmentation technique worldwide. It provides accurate and precise services for static users. VRS can be used for all GNSS receivers using the RTCM message. VRS also has better performance than other correction techniques. However, corrections are only transmitted after the exact location of the mobile GNSS receiver has been determined (Park, B. et al., 2010). Therefore, if the mobile GNSS receiver has traveled a significant distance within the same campaign period, corrections will not be available for the new recipient location (Landau et al., 2003).

1.2.3 MAC

The MAC technique improves the VRS technique and eliminates the disadvantages of FKP, and thus obtains more accurate position information than the other two methods. MAC consists of one master and several subsidiary reference points. Each subsidiary reference point sends measurements to the main control center and an inter-station correction difference is used to estimate the required correction. This correction can also be divided into ionospheric and geometric corrections (Park, B. et al., 2010).

2. TEST MEASUREMENTS AND METHODOLOGY

The test was carried out at a selected point from Istanbul (Turkey) and the study area is shown in Figure 3. To assess the performance of correction methods of CORS-TR (Network-RTK), a GEOMAX ZENITH25 GNSS receiver was used. And the coordinates of fixed point were determined as a result of precise static measurements (Figure 4). Test measurements were performed at the same point (28º.86382 E - 41º.06595 N) on different days. The data of different measurement techniques were collected on different days (between 25.03.2017 and 04.04.2017 dates). In test, different elevation angles and three different correction techniques, namely FKP, MAC and VRS, were used in an open area with no obstacles. For each combination, the observations were performed for 12 to 51 hours with an epoch interval of 1 second. In the test, the data were obtained as north and east coordinates and height, and the analysis of the collected data was conducted with the help of MATLAB software.

Table 1: Duration of Test and Epochs Used

Cut-Off Angle	Correction Technique	Duration	Epoch Number	Used Epoch Number
10°	FKP	36h 4m 4s	130494	109865
	MAC	44h15m46s	159346	103364
	VRS	51h29m24s	185364	123883
20°	FKP	11h52m41s	42761	42395
	MAC	11h54m45s	42885	42321
	VRS	20h17m48s	73068	68583
30°	FKP	23h43m58s	85438	75535
	MAC	16h09m38s	58178	44418
	VRS	19h36m31s	70591	36644
40°	FKP	20h59m17s	75557	51940
	MAC	-	-	-
	VRS	15h01m20s	54080	25447

Figure 3. Study area.

Figure 4. A view from test measurement.

3. RESULTS AND DISCUSSION

Histograms of the differences show that the observations collected in the 11 different combinations given in Table 1 and the distribution of differences from the mean value of these observations. The histograms of the differences are given from Figure 5 to Figure 8. While the time series were obtained based on time, the analysis was performed as epoch-epoch. In the figures, blue, red and green represent the X, Y and h components, respectively. Although the time series collected at an elevation angle of 10° and 20° were partially discontinued, they appeared to be more consistent than the data collected at an elevation angle of 30° and 40°. When the histograms of the data collected in the open, partially closed and extremely closed environments of the satellite view were analyzed, it was seen that the errors in the X and Y direction were generally ± 2 cm, and those in the H direction were ± 5 cm. The MAC correction technique provided no data under the 40° satellite view. When the degree of the satellite view decreased, the differences in the time series became clearer. Furthermore, when the histograms data were analyzed under the 40° satellite view, the Gaussian error distribution was removed and the errors in the X, Y direction were ± 4 cm while those in the h component were ± 10 cm.
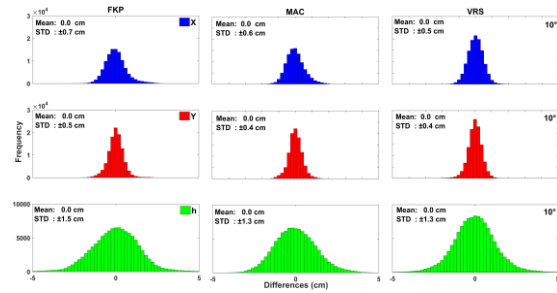

Figure 5. Histograms of differences in measurements of 28-10 hour, using the FKP-MAC-VRS correction techniques (elevation cut-off angle: 10 degree).
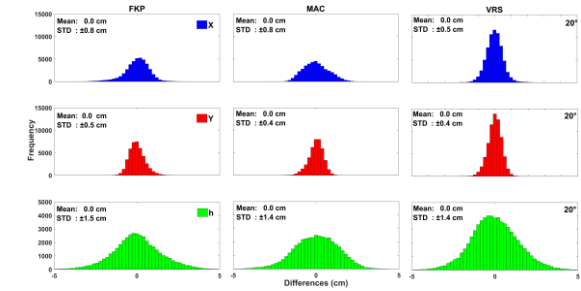

Figure 6. Histograms of differences in measurements of 12-19 hour, using the FKP-MAC-VRS correction techniques (elevation cut-off angle: 20 degree).
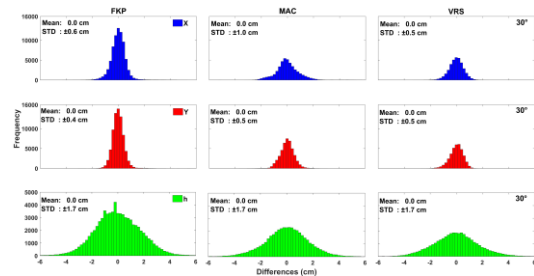

Figure 7. Histograms of differences in measurements of 10-21 hour, using the FKP-MAC-VRS correction techniques (elevation cut-off angle: 30 degree).
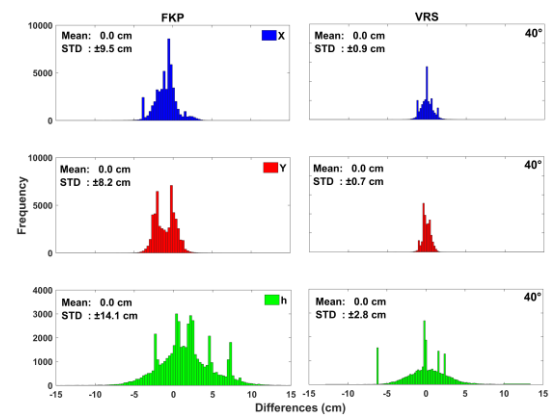

Figure 8. Histograms of differences in measurements of 7-14 hour, using the FKP-MAC-VRS correction techniques (elevation cut-off angle: 40 degree).

The exact coordinates of the point where the measurements were performed were determined using the Leica Geo Office program based on the CORS-TR network. The coordinates were accepted as exact value and the differences of the mean value of each observation from the exact value were taken. Table 2 presents the differences of the mean values of observations with 11 different combinations. As can be seen from Table 2, the horizontal components are consistent at all levels of correction techniques and at a sub-cm level at all elevation cut-off angle. But in the elevation component, it is seen that as the elevation cut-off angle increases, the differences increase.

Table 2. Differences of the mean values of observations with 11 different combinations from the exact value

		Differences (cm)		
		X	Y	h
10°	FKP	0,0	0,6	-2,5
	MAC	0,3	0,8	-0,8
	VRS	-0,6	0,2	-2,7
20°	FKP	-0,3	0,8	-2,1
	MAC	0,8	0,9	-2,1
	VRS	-0,5	0,2	-2,7
30°	FKP	-0,2	0,6	-3,1
	MAC	0,9	0,8	-3,5
	VRS	-0,4	0,2	-4,1
40°	FKP	0,6	1,2	-6,0
	MAC	-	-	-
	VRS	-0,6	0,0	-5,3

Table 3 contains the results of the statistical analysis of the differences obtained from 11 different combinations. According to the results obtained from the environment where the satellite view was open, all three methods provided similar results concerning the standard deviations of position and height components. When the minimum and maximum values were analyzed, the VRS technique produced better results compared to the MAC method for the X and Y components, while MAC performed better for the height component (Kahveci, 2009). The results related to the partially closed environment revealed that the standard deviation results of the X, Y and h components were similar to the values obtained under the 10° elevation angle for all three methods. Concerning the minimum and maximum values, MAC had better performance than the VRS method for the X, Y and h components. Lastly, when the satellite view was limited, the standard deviation performance of the X, Y and h components were similar for the three methods. However, according to the minimum and maximum values, the highest performance belonged to the VRS technique. As mentioned before, in cases where the satellite view is limited, MAC does not provide any data.

Table 4 contains the percentage distribution of error amounts which the three components (X, Y, h) and positioning (P) parameters obtained from 11 different data sets. We can explain that the concept of error used in here. The error values ($\pm \sigma$) found for each element of the X, Y and h time series is the error found by subtracting each measure from the mean value of the corresponding time series. The error amount of the position parameter refers to the square root value of the sum of the squares of X and Y values.

Table 3. Statistical Analysis of Data.

Cut-Off Angle	Correction Technique	Std. (cm)			Min. (cm)			Max. (cm)		
		X	Y	h	X	Y	h	X	Y	h
10°	FKP	0,7	0,5	1,5	-2,9	-3,1	-6,6	3,3	2,4	13,9
	MAC	0,6	0,4	1,3	-2,2	-1,6	-5,2	2,3	2,1	5,5
	VRS	0,5	0,4	1,3	-2,0	-2,3	-6,2	2,2	1,9	9,3
20°	FKP	0,8	0,5	1,5	-3,8	-1,7	-6,7	2,9	2,1	8,2
	MAC	0,8	0,4	1,4	-2,9	-2,9	-2,1	-6,0	1,4	4,7
	VRS	0,5	0,4	1,4	-2,4	-1,9	-6,4	8,2	3,3	6,0
30°	FKP	0,6	0,4	1,7	-4,2	-2,9	-10,0	5,2	5,5	12,5
	MAC	1,0	0,5	1,7	-4,8	-3,5	-9,8	7,5	2,9	8,7
	VRS	0,5	0,5	1,7	-3,2	-2,8	-7,6	2,3	1,9	9,9
40°	FKP	9,5	8,2	14,1	-44,6	-44,3	-176,1	-127,5	72,3	15,9
	MAC	-	-	-	-	-	-	-	-	-
	VRS	0,9	0,7	2,8	-48,8	-4,0	-13,9	5,5	56,3	12,6

In Table 4, the error amounts for each time series (X, Y, P, h) were expressed in the percentage and the comparison was intended to be simplified. The expression "100" indicates that all error values remain within the range of the given error. This analysis includes that the inspection up to 7 cm of errors in accordance with applicable regulations in Turkey.

Using different correction techniques under the 10º satellite view, the X, Y and P components were below 4 cm, whereas the "h" component reached 5 cm for MAC, 6 cm for VRS, and 7 cm for FKP. It was observed that 90% of the X, Y and P component results obtained using the VRS technique were between 0 and 1 cm.

Furthermore, for the height measurement, VRS provided the most accurate results.

The results obtained from the 20º satellite view showed that the Y component was below 3 cm for all three corrective techniques, the X component was below 3 cm for MAC and VRS and below 4 cm for FKP. Similar to the 10º, the height component was below 5 cm for MAC, and below 6 and 7 cm for VRS and FKP, respectively. It is suggested that the VRS technique is more efficient in measuring X, Y and P, whereas all three techniques have similar performance for height measurements.

Table 4. Error distribution of differences in percentages.

Diff. (cm)	Data	10 °			20 °			30 °			40 °		
		FKP	MAC	VRS	FKP	MAC	VRS	FKP	MAC	VRS	FKP	MAC	VRS
0-1	X	89,2	92,9	96,9	85,7	79,8	95,3	93,9	70,8	93,6	51,1	-	78,2
	Y	95,5	97,1	97,8	96,7	97,5	98,2	97,5	93,4	93,7	55,0	-	92,0
	P	82,6	87,3	92,2	79,7	73,3	90,7	88,7	60,7	84,1	23,7	-	66,6
	h	53,7	58,3	59,6	54,3	55,6	53,5	44,2	47,9	46,9	17,7	-	39,0
< 2	X	98,8	99,9	100,0	97,3	99,5	99,9	99,3	97,2	99,9	87,7	-	98,8
	Y	99,9	100,0	100,0	100,0	100,0	100,0	99,7	99,7	99,9	96,3	-	100,0
	P	98,1	99,7	99,9	96,5	99,3	99,8	98,8	95,9	99,4	68,9	-	98,4
	h	85,3	89,1	88,7	83,0	87,1	84,6	75,7	78,5	76,9	43,9	-	63,0
< 3	X	100,0	100,0	100,0	99,8	100,0	100,0	99,8	99,5	100,0	97,5	-	99,8
	Y	100,0	100,0	100,0	100,0	100,0	100,0	100,0	100,0	100,0	98,2	-	100,0
	P	99,9	100,0	100,0	99,6	100,0	100,0	99,7	99,4	100,0	96,5	-	99,8
	h	95,7	97,7	97,1	94,8	96,7	95,9	91,8	92,5	91,7	63,4	-	79,6
< 4	X	100,0	100,0	100,0	100,0	100,0	100,0	100,0	99,7	100,0	98,2	-	100,0
	Y	100,0	100,0	100,0	100,0	100,0	100,0	100,0	100,0	100,0	98,4	-	100,0
	P	100,0	100,0	100,0	100,0	100,0	100,0	99,9	99,6	100,0	98,0	-	100,0
	h	98,3	99,6	99,2	98,9	99,4	99,2	97,7	97,7	97,7	76,8	-	87,3
< 5	X	100,0	100,0	100,0	100,0	100,0	100,0	100,0	100,0	99,8	98,3	-	100,0
	Y	100,0	100,0	100,0	100,0	100,0	100,0	100,0	100,0	100,0	98,4	-	100,0
	P	100,0	100,0	100,0	100,0	100,0	100,0	100,0	99,8	100,0	98,3	-	100,0
	h	99,4	100,0	99,7	99,8	100,0	99,9	99,3	99,2	99,3	84,5	-	90,8
< 6	X	100,0	100,0	100,0	100,0	100,0	100,0	100,0	100,0	100,0	98,4	-	100,0
	Y	100,0	100,0	100,0	100,0	100,0	100,0	100,0	100,0	100,0	98,4	-	100,0
	P	100,0	100,0	100,0	100,0	100,0	100,0	100,0	99,9	100,0	98,4	-	100,0
	h	99,8	100,0	99,9	100,0	100,0	100,0	99,8	99,6	99,8	87,9	-	92,5
< 7	X	100,0	100,0	100,0	100,0	100,0	100,0	100,0	100,0	100,0	98,4	-	100,0
	Y	100,0	100,0	100,0	100,0	100,0	100,0	100,0	100,0	100,0	98,4	-	100,0
	P	100,0	100,0	100,0	100,0	100,0	100,0	100,0	100,0	100,0	98,4	-	100,0
	h	99,9	100,0	100,0	100,0	100,0	100,0	99,9	99,8	100,0	89,3	-	93,2

Under the 30º satellite view, the results obtained using the VRS technique showed that the X, Y, P and h components were all below 4 cm whereas the FKP and MAC technique revealed that the position components were close to 6 cm and the height component reached 7 cm. The FKP technique despite its performance where satellite view was clear (10º satellite view) or partially blocked (20º satellite view), appeared to be more effective than the other two techniques. As mentioned earlier in this paper, under the 40º satellite view, no data was obtained from the MAC technique. In the same view, it was observed that VRS was superior to the FKP technique.
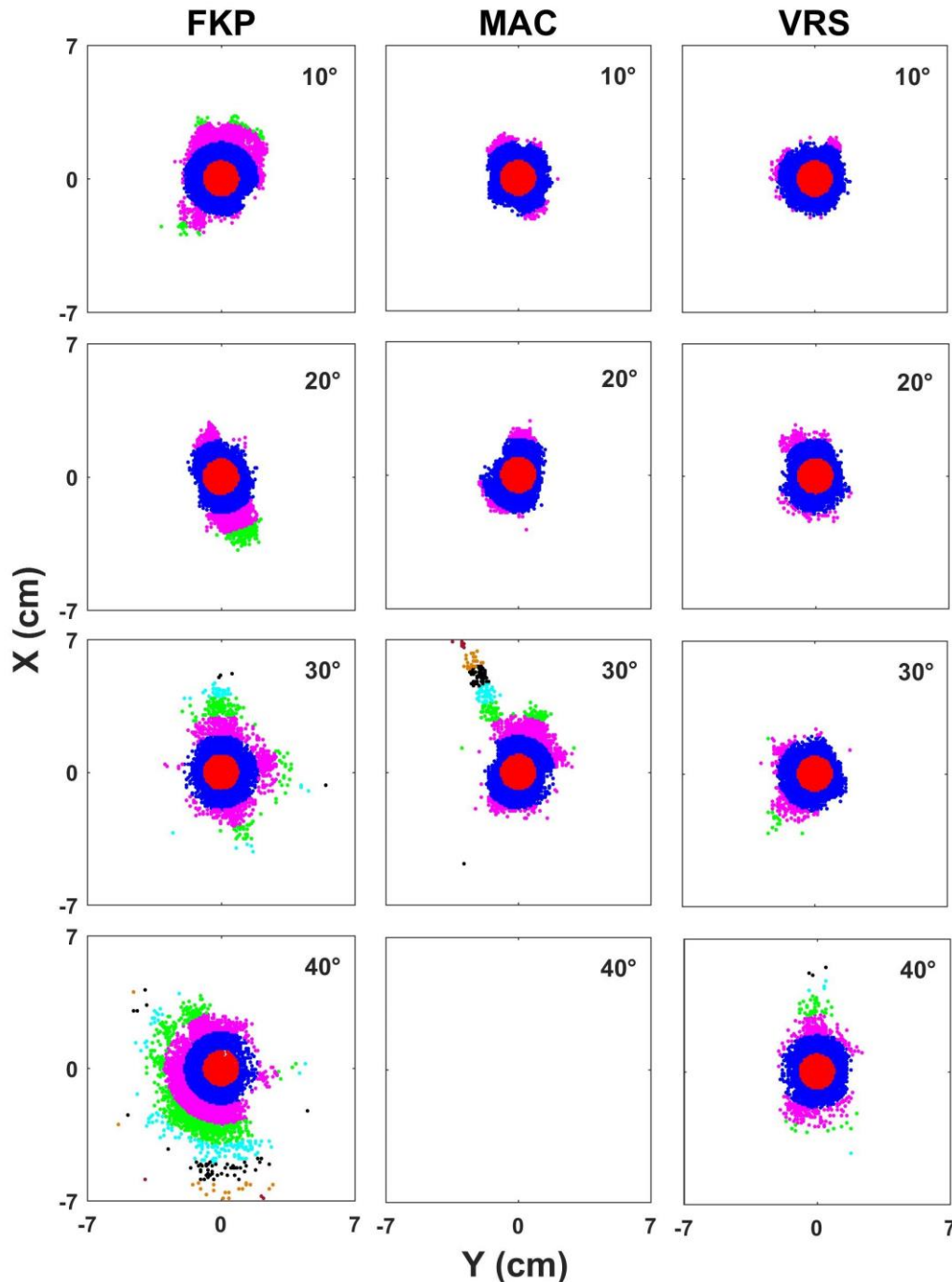
Figure 9. Error Distribution of the Horizontal Position Coordinates.

Figure 9 shows the distribution of the positioning analysis errors obtained from four different satellite angles using three different correction techniques. The colors in this figure represent the error distribution according to the order in Table 4. As a result of the evaluations based on all satellite views and correction techniques, approximately 85% of the measurements were within 0 to 1 cm and approximately 12% were within 1 to 2 cm.

Table 5 shows that the percentage distribution of the errors reached 7 cm. When the data obtained by the FKP, MAC and VRS correction techniques under the 10° satellite view were analyzed, it was determined that the VRS technique gave better results than the FKP for X and Y and MAC for X, Y, and h analyses. Among the three correction techniques, FKP provided the worst results. For the 20° satellite view, the errors in the X and Y analyses were smaller than 4 cm and those in the X, Y and h analyses were less than 5 cm when the MAC technique was applied. However, when the percentage of errors were analyzed, it was seen that the technique with the best result was VRS, whereas MAC performed the worst. For the 30° satellite view, the FKP technique was partially better or similar compared to VRS. Similar to 20°, MAC gave the worst results in all three methods. In the analyses of 40° satellite view, VRS achieved better results than FKP for all components. The errors of VRS concerning the X, Y, and h components were less than 4 cm, and this method performed well even under very limited satellite view. In the analysis of the combination of the three position components, the FKP method showed poor performance.

Table 5: Cumulative Errors of 2D and 3D Analysis of Data Obtained from Test measurements.

Diff. (cm)	Data	10 °			20 °			30 °			40 °		
		FKP	MAC	VRS	FKP	MAC	VRS	FKP	MAC	VRS	FKP	MAC	VRS
0-1	X, Y	85,9	90,6	94,9	84,3	78,3	93,8	91,9	67,3	88,5	32,1	-	71,5
	X, Y, h	48,3	53,6	56,7	46,1	44,3	50,1	41,5	33,4	42,4	6,3	-	33,8
< 2	X, Y	98,7	99,9	100,0	93,8	99,5	99,9	99,0	97,1	99,8	86,0	-	98,8
	X, Y, h	84,8	89,0	88,6	50,1	86,8	84,5	75,2	76,7	76,7	40,9	-	62,7
< 3	X, Y	100,0	100,0	100,0	99,8	100,0	100,0	99,8	99,5	100,0	97,3	-	99,8
	X, Y, h	95,7	97,7	97,1	94,6	96,7	95,9	91,6	92,4	91,7	63,0	-	79,5
< 4	X, Y	100,0	100	100,0	100,0	100,0	100,0	99,9	99,7	100,0	98,1	-	100,0
	X, Y, h	98,3	99,6	99,2	98,9	99,4	99,2	97,6	97,6	97,7	76,7	-	87,3
< 5	X, Y	100,0	100,0	100,0	100,0	100,0	100	100,0	99,8	100	98,3	-	100,0
	X, Y, h	99,4	100,0	99,7	99,8	100,0	99,9	99,3	99,2	99,3	84,5	-	90,8
< 6	X, Y	100	100,0	100,0	100,0	100,0	100,0	100,0	100,0	100,0	98,4	-	100,0
	X, Y, h	99,8	100,0	99,9	100,0	100,0	100,0	99,8	99,6	99,8	87,8	-	92,5
< 7	X, Y	100,0	100,0	100,0	100,0	100,0	100,0	100,0	100,0	100,0	98,4	-	100,0
	X, Y, h	99,9	100,0	100,0	100,0	100,0	100,0	99,9	99,8	100,0	89,3	-	93,2

4. CONCLUSION

In order to test the repeatability of the network of RTK measurements, at previously known fixed coordinates and different elevation cut-off angle, long-term data were collected using three different correction techniques (FKP, MAC and VRS) with a one-second epoch interval. In this study, the repeatability of the horizontal and vertical coordinate from each combination was analyzed. When the standard deviation and minimum-maximum values were examined, three correction techniques had similar performance for 10° and 20° elevation cut-off angle, and after increasing the elevation cut-off angle, there was an increase in the standard deviation of the h component. In the analysis of X, Y, P and h components, it was seen that the performance of the three correction techniques was generally similar, but the VRS technique yielded slightly better results. However, when 2D and 3D coordinate components were analyzed together, it was clear that the VRS technique gave better results compared to the other two techniques. Furthermore, even in the case of limited satellite vision, errors in all three techniques remained below 7 cm. This 7 cm error value in the study, according to the relevant current regulations in Turkey (Large Scale Map and Map Information Production Regulation - 2018) is an appropriate result. In the current conditions, considering both time and cost, static CORS-TR measurements make a great contribution to the users in terms of the accuracy provided.

REFERENCES

Seeber, G. (2003). Setallite Geodesy, Foundations, Methods and Applications, second edition , de Gruyer.

Gumus, K., Celik, C., Erkaya H. (2012). Investıgatıon Of Accurate Method In 3-D Posıtıon Usıng Cors-Net In Istanbul.

Sunantyo, T. Aris. (2009). GNSS CORS Infrastructure and Standard in Indonesia. 7th FIG Regional Conference, Spatial Data Serving People: Land Governance and the Environment – Building the Capacity, Hanoi, Vietnam, 19-22 October.

Öcalan, T., Tunalıoğlu, N. (2010). Data communication for real-time positioning and navigation in global navigation satellite systems (GNSS)/continuously operating reference stations (CORS) Networks. Sci. Res. Essays,Vol. 5(18), pp. 2630-2639.

Wanninger L., (2003). Virtual reference stations (VRS). GPS Solutions 7:143–144.

Wübena G., Bagge A. (1998). GNSS multi-station adjustment for permanent deformation analysis networks, Symp. on Geodesy for Geotechnical & Structural Engineering of the IAG Special Commission 4, Eisenstadt, Austria, 20-22 April, 139-144.

Brown N., Keenan R., Richter B., Troyer L. (2005). Advances in ambiguity resolution for RTK applications using the new RTCM V3.0 Master-Auxiliary messages. In: Proc ION GNSS 2005, Long Beach, California, September 13-16.

Eren K., Uzel T., Gülal E., Yıldırım O., Cingöz A. (2009). Results from a Comprehensive Global Navigation Satellite System Test in the CORS-TR Network: Case Study.

Bütün O. F., Baybura T. (2010). Tusaga Aktif (Cors-TR) Istayonlarınıdan Elde edilen Nokta Koordinat Dogrulugunun Incelenmesi, 5. Ulusal Muhendislik Olcmeleri Semposyumu, 20-22 Ekim 2010, Zonguldak, Turkiye.

Bulbul S., Inal C., Yildirim O. and Basciftci F. (2017). Velocity Estimation of Turkish National Permanent GNSS Network- Active Points Located at Central Anatolia Region. Bilge International Journal of Science and Technology Research, 1(Special Issue), 18-25, 2017

Pırtı A. (2016). The Seasonal Effects Of Decıduous Tree Folıage In Cors-Gnss Measurements (Vrs/Fkp).

Gümüş K., Selbesoğu M., Celik C. (2016). Accuracy investigation of height obtained from Classical and Network RTK with ANOVA Test.

Öğütücü S., Kalaycı I. (2016). Investigation of network-based RTK techniques: a case study in urban area.

Musa T., A., Lim S., Rizos C. (2005). Low latitude troposphere: A preliminary study using GPS CORS data in South East Asia. U.S. Institute of Navigation National Tech. Meeting, San Diego, California, January 24-26, pp. 685-693.

Brownjohn J. M., Rizos C, Tan G. H., Pan T. C. (2004). Real-time long-term monitoring and static and dynamic displacements of an office tower, combining RTK GPS and accelerometer data. 1st FIG Int. Symp. On Engineering Surveys for Construction Works & Structural Engineering.

Kempe C., Alfredsson A., Engberg L. E., Lilje M. (2006). Correction model to rectify distorted co-ordinate system. XXIII FIG Congress.

Yıldırım O., Yaprak S., Inal C. (2013). Determination of 2011 Van/Turkey earthquake (M= 7.2) effects from measurements of CORS-TR network.

Mekik C., Yildirim O., Bakici S. (2011). The Turkish real time kinematic GPS network (TUSAGA-Active) infrastructure. Sci Res Essays. 6(19):3986–3999.

Aykut N. O., Gülal E., Akpınar B. (2015). Performance of Single Base RTK GNSS Method versus Network RTK, Earth Sci. Res. J. Vol. 19, No. 2 (December, 2015): 135 – 139.

Uzel T., Eren K., Gulal E., Dindar A., Tiryakioglu I., Yilmaz H. (2011). Tectonic plate displacement monitoring with TUSAGA - Active (CORS-TR) data. Paper presented at: 13th Turkey Map Scientific and Technical Conference; Ankara, Turkey (In Turkish).

Kahveci M. (2009). Kinematik GNSS ve RTK CORS Ağları.

Park, B. and Kee, C. (2010). The Compact Network RTK Method: An Effective Solution to Reduce GNSS Temporal and Spatial Decorrelation Error. J. Navig., 63, 343–362.

Landau H. Vollath U. Chen X. (2003). Virtual Reference Stations, Journal of Global Positioning System, (2): 137-143.

Raquet, J. (1998). Development of a Method for Kinematic GPS Carrier-Phase Ambiguity Resolution Using Multiple Reference Receivers. PhD Thesis, University of Calgary.

Rizos, C. (2002). Network RTK Research and Implementation –A GeodeticPerspective, Journal of Global PositioningSystems, Vol.1, No.2:144- 150.

Kim, J., Song, J., No, H., Han, D., Kim, D., Park, B., Kee, C. (2017). Accuracy Improvement of DGPS for Low-Cost Single-Frequency Receiver Using Modified Flächen Korrektur Parameter Correction, ISPRS International Journal of Geo-Information 6 (7) : 222.

Bascifci, F., Inal, C., Yildirim, O., Bülbül, S. (2018). Comparison Of Regional And Global Tec Values: Turkey Model, International Journal of Engineering And Geosciences, 3(2), 61-72.

Tusat, E., Ozyuksel, F. (2018). Comparison of GPS Satellite Coordinates Computed From Broadcast and IGS Final Ephemeridides, International Journal of Engineering and Geosciences (IJEG),3 (1), 012-019.

USER-CENTRED DESIGN AND EVALUATION OF MULTIMODAL TOURIST MAPS

Emre Mulazimoglu[1]* and Melih Basaraner[2]

[1]Yildiz Technical University, Graduate School of Science and Engineering, Division of Geomatic Engineering, Remote Sensing and GIS Programme, Istanbul, Turkey
(emremulazimoglu7@gmail.com); **ORCID ID 0000-0002-9117-1950**

[2] Yildiz Technical University, Department of Geomatic Engineering,
Division of Cartography, Istanbul, Turkey
(mbasaran@yildiz.edu.tr); **ORCID ID 0000-0002-4619-7801**

ABSTRACT: User-centred maps are designed to provide users with the geospatial information they need primarily by their interests and thus more powerful support for their geospatial decision-making. In many cases, creating this kind of maps involves designing maps at multiple modes. Tourism is one of the areas that various kinds of maps both analogue and digital are widely used. Well-designed tourist maps can contribute to increasing the attractiveness of a region and the satisfaction of the visitors. Although some applications are available on user-centred multimodal tourist maps for web and mobile environments, there is no comprehensive study dealing with the paper maps. Therefore, this article focuses on the design and production as well as the evaluation of user-centred multimodal tourist maps for the analogue environment in the case of Kyrenia (Girne) district of the Turkish Republic of Northern Cyprus. The study consists of three main phases. In the first phase, a tourist geospatial database was constructed for the district of Kyrenia. In the second phase, user-centred multimodal tourist maps were designed and produced for three types of tourism, considering the prominent characteristics of the district in this respect. In the third phase, user evaluations were carried out for the existing and produced tourist maps. For this purpose, newly designed maps (as a group) and an existing tourist map of the district were evaluated individually and comparatively by potential users of different gender, age and education characteristics by face-to-face survey method. The survey results showed that the user-centred multimodal maps are more preferable than the general tourist map.

Keywords: Map Design, Multimodal Tourist Map, User-Centred Design, Kyrenia (Girne)

1. INTRODUCTION

Tourism is the name given to trips to the unknown (Brown, 2007). Tourist maps are the most important documents that help tourists and should be able to answer all questions about the destination that the user visited (Yan et al., 2014). In this respect, well-designed maps have an utmost importance. However, most GIS applications do not consider cartographic design principles sufficiently. This also stems from the poor capabilities of GIS software packages that are often used for making maps. This has started to change along with new cartographic tools incorporated in GIS. People demand high-quality maps, and GIS analysts have a responsibility to ensure that they communicate their work effectively using the tools available. Maps may be produced for a general-purpose audience, or to be used by a very specific user group, and so the maps should fit for purpose (Hardy and Field, 2012). In this context, user-centred map design has gained more importance recently. Today, this can be carried out more easily through GIS capabilities (Ulugtekin et al., 2013).

Five basic design principles, well known in cartography, can be mentioned for efficient maps. These principles are shape and ground relationship, hierarchy, contrast, balance and readability. The main reason for the application of these principles is to ensure that the information on the map is delivered to the user effectively (Buckley, 2012).

Nowadays, due to its socio-economic advantages, the interest of the countries in tourism is increasing. So, it is important to make improvements to the existing tourist maps in order to better respond to the growing tourism potential.

1.1 Related Works

There are many studies focusing on tourist map design and tourist GIS creation. Clarke (1989) uses a symbol comprehension method to evaluate the efficiency of symbols in the legends of two comparable published tourist maps. Filippakopoulou and Nakos (1995) present one of the first tourist GIS implementations that can allow performing tourism-specific spatial analysis with a map-based interface. Basaraner (1997) and Basaraner and Selcuk (1999) present one of the first examples of tourist GIS applications in Turkey in the case of Antalya city centre based on a large-scale map dataset. Comert and Bostancı (1999) present a tourist GIS application based on 1:10000 scale tourist map of Trabzon province (Turkey). Brown et al. (2001) summarize the common errors confronted in tourist web map design and provides suggestions on good design practice. Erdogan and Tiryakioglu (2004) develop a tourist GIS for the province of Afyonkarahisar

(Turkey), aiming to use in tourism promotion activities. Xinwei and Wangfusheng (2005) propose a tourism information system for the city of Beijing (China) through the integration of geospatial information with tourism data. Almer et al. (2006) provide a multi-platform solution for the geographic-based tourism information system. The study covers two-dimensional and three-dimensional visualization of tourism elements with geospatial knowledge and provides an interface to platforms such as Google Earth and Google Maps. Kariotis et al (2007) create a digital, interactive tourist map, which can be transformed according to users' needs. Yin et al. (2008) design a tourism GIS that can be used by tourists who travel independently of any tour program. Then, an online questionnaire was conducted to test the adequacy of the system and the deficiencies of the system were determined according to the results of the survey. Demirci and Kavzoglu (2010) present a tourism GIS application for Kocaeli province (Turkey). Ceylan et al. (2011) present a GIS-based tourist map design for Istanbul historical peninsula (Turkey). Yan and Wang (2012) present a web-based tourist GIS application including virtual reality technology. Alamaki and Dirin (2014) adapt the user-centred tourist map for mobile devices. Pucihar et al. (2014) establish an internet-based user-centred tourism GIS, designed to ensure the sustainability of tourism in the city of Gorenjska (Slovenia). Mutlu et al. (2017) develop a web-based tourist GIS for Bodrum district (Turkey).

1.2 Motivation and Aim of the Study

This study focuses on the design and production of user-centred multimodal tourist maps. Tourist maps that are produced for general purposes may be insufficient to meet the information requirements of the specific user groups. Tourism is divided into different sub-types. These sub-types have emerged from some specific needs or preferences of tourists. Therefore, designing user-centred multimodal tourist maps that support different types of tourism in addition to general-purpose tourist maps can provide an additional contribution not only to meeting the specific geospatial information needs of tourists but also the promotion and marketing of tourism potential of a region. Although the design of user-centred maps has been dealt with for web and mobile devices in the literature, making such a design for paper maps, having a wide use, will be a logical approach considering the possible benefits mentioned above. There is no comprehensive study about paper maps within this scope. Therefore, this study aims to create user-centred tourist map designs produced in three different modes (i.e., multimodal) for Kyrenia district of the Turkish Republic of Northern Cyprus (TRNC). These modes correspond to the different tourism types determined by

considering the tourism characteristics of the district. In addition, these maps (as a group) are evaluated individually and in comparison, to the current tourist map of the district through user surveys.

2. GENERAL CHARACTERISTICS OF TOURIST MAPS

Tourist maps are cartographic products designed to provide information on various topics to the tourists visiting an area. These maps play an important role in the promotion of tourism areas (Medynska-Gulij, 2003). Oliveira (2005) mentions the necessity of maps for introducing a city in a touristic sense. With the help of tourist maps:

- User/tourist can access quality information about tourism resources.
- Travel agencies can provide more active guidance for tourists and create alternative routes.
- Managers may obtain a detailed analysis of the geographic distribution of tourism demand and supply in deciding on the regional planning of tourism.

Tourist maps, like other thematic maps, should employ visual hierarchy when they are designed. Applying visual levels in map design allows significant map elements to be emphasized over the others and thus provides effective communication of geospatial information specific to the purpose of the map. Table 1 shows the visual levels for thematic maps (Dent et al., 2009; Wesson, 2018).

Table 1. Basic visual hierarchy of any map, from Visual Level 1 as the highest, most prominent elements, through to Visual Level 5, as the least prominent (adapted from Wesson, 2018).

Visual level	Map elements
1	Thematic overlay (titles, symbols, legend, key information)
2	Other (base) map symbols and labels
3	Base map (topography and other features of map body)
4	Annotation, locator maps, figures
5	Other useful elements (scalebar, grid, graticules, frame, tool tips, credits and acknowledgements)

On a single tourist map, it is often not possible to clearly show all the attractions and resources that a city offers its visitors. In such cases, it may be necessary to produce more than one type of map. In this context, producing tourist maps by considering the prominent tourism types of the region and by putting the user in the centre of the design will increase the interest of the tourist on the map (Yan and Lee, 2014).

3. USER-CENTRED MAP DESIGN

The basic philosophy of user-centred design is to put the human factor at the centre of the development process. When designing or developing a product, the designer should focus on what people will use and what to do with it, because a usefully designed product will assist people in decision-making process (Haklay and Nivala, 2010).

It has become easier for people to access geospatial information through developing and changing technological elements, the increasing number of internet-based geospatial data services and free software. However, data and easy access to mapping tools are not a guarantee of an optimized map. The power of the map is related to the ability of the cartographer to convey the information to the user in an accurate way (Shneiderman and Plaisant, 2005).
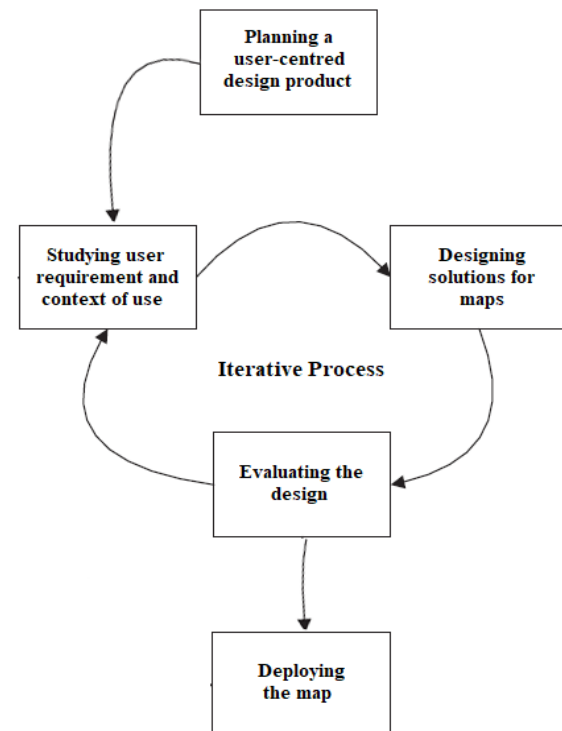

Figure 1. User-centred map design process (adapted from Haklay and Nivala, 2010).

User-centred design can be seen as an iterative process that starts by recognizing the potential user, purpose and tasks. The design process then continues

to use this information to check the availability of the product. The process continues iteratively until it meets all specified requirements. When the system determines that the user-centred design needs are met, it stops and the result is obtained (Haklay, 2010).

The personalization of tourist maps with user feedback considers user needs in the identification of city symbols, information layers and symbols on the map. In his study, Reichenbacher (2001) argues that minor changes in map symbolization can have a large impact on the user. In addition, Nivala and Sarjakoski (2005) analysed the effects of changes in map characteristics on human and determined that emphasizing colours, increasing contrast and adjusting symbol dimensions for the specific purpose give positive results in user feedback.

4. METHODOLOGY AND EXPERIMENTAL STUDY

This study, which deals with the user-centred design and evaluation of multimodal tourist maps, consists of the steps given in Figure 2.
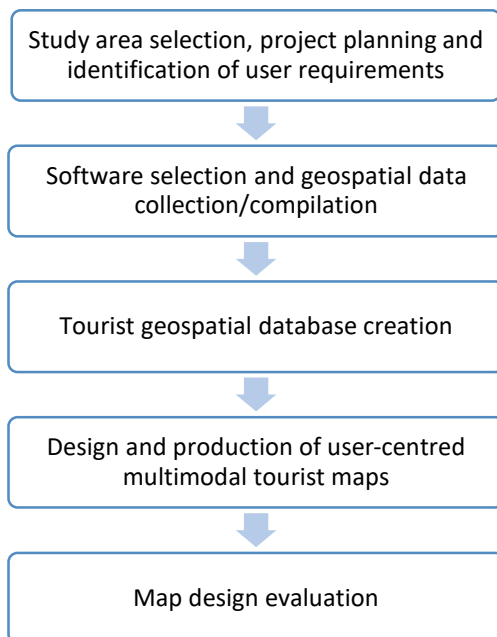
Figure 2. Workflow of the study.

4.1 Study Area Selection, Project Planning and Identification of User Requirements

Kyrenia district of the Turkish Republic of Northern Cyprus was chosen as the study area (Figure 3). The geographic location, climate, historical and cultural values and the growing tourism potential have been influential in this decision.

After the study area was selected, it was investigated which tourism types of the district came to the fore and it has been understood that the district offers good opportunities with respect to cultural, gastronomy and entertainment tourisms. Accordingly, it is found appropriate to design different user-centred tourist maps for these types of tourism.

Figure 3. Location of the study area.

Afterwards, the appropriate map scales were decided by taking into account the geographic extent of Kyrenia district as well as the density and distribution of the tourist features in the district. For the maps to be produced, the largest possible scales were selected to be able to present the information that the visitors may need as comprehensive as possible. The distribution of features about historical buildings and cultural heritage in the district was examined and it was decided that 1:3 000 scale was suitable for the cultural tourism map. The same scale was found suitable for gastronomy tourism map. For the entertainment tourism map, 1:3 600 scale was found to be appropriate, being different from the other two maps. Since the important entertainment places in the district are in relatively scattered locations, this scale has been selected in to be able to show all of them.

4.2 Software Selection and Geospatial Data Collection/Compilation

Three software packages were used in the study. Among them, ArcGIS 10.5 software was used in the creation of a tourist geospatial database and the design of user-centred tourist maps. The models of buildings or structures to be shown in three dimensions were created in SketchUp 2018 software. In addition, Adobe Photoshop CS6 software was used for filtering photographs and designing some point symbols and legends.

OpenStreetMap (OSM) data became the primary data for the creation of the Kyrenia district tourist geospatial database and the design of the user-centred multimodal tourist maps. However, the

amount of detail of this data was not enough. For this reason, additional data were collected from the field with the hand-held GPS device as well as captured from the satellite image of 2015 by connecting to the Web Coverage Service (WCS) of the DigitalGlobe in the GIS software. Thus, it became possible to remove incorrect data and add missing data. Furthermore, existing paper maps, web maps as well as the websites of Kyrenia Municipality and TRNC Ministry of Culture and Tourism were used as additional data sources. In the cultural tourism map, it was decided to show the significant features of the cultural heritage with photographs. The photographs required for this purpose were obtained through field studies.

Geographic (WGS 84) / EPSG: 4326, being the original coordinate system of OSM data, was used in the study.

4.3 Tourist Geospatial Database Creation

The literature (Gerber et al., 1990, Filippakopoulou and Nakos, 1995, Basaraner, 1997, Basaraner and Selcuk, 1999) and various tourist maps were examined to determine the content of the tourist geospatial database on which user-centred multimodal maps rely. For a study wider in scope, a multi-representation spatial database approach may be followed (Memduhoglu and Basaraner, 2018).

Table 2 shows the content of the database. Buildings and structures were represented with points in this database. When they also needed to be shown as polygons in terms of maps, they were externally obtained from the OSM data.

4.4 Design and Production of User-Centred Multimodal Tourist Maps

Three user-centred multimodal tourist maps were designed and produced for three types of tourism (cultural tourism, gastronomy tourism and entertainment tourism) in this phase. Thanks to the multimodal maps, tourists visiting the district will be able to use the appropriate tourist map according to their interests. Thus, tourists will be able to reach more specific geospatial information for their purpose(s) of the visit and make their decisions easily and quickly.

This phase includes generalization and symbolization operations applied to the geospatial data.

4.4.1 *Generalization*

In this phase, some generalization operations were performed on the base map (i.e. OSM data) in order to remove unnecessary detail, prevent the graphic conflicts and ensure an aesthetic appearance in the maps. Various generalization operations were applied interactively and thus the appearance of the features was modified. Since the contents of the maps were partly different, the generalization differed slightly depending on the map type.

The general steps of the generalization were as follows:

- Buildings were selected/eliminated depending on their necessity for target map.
- Buildings (area) were collapsed to point.
- Buildings with detailed geometry were simplified.
- Parking lots, recreation areas and cemetery were simplified and smoothed.
- Most of the roads were enlarged.
- In most cases, texts and in some cases, point symbols were displaced slightly when required.

4.4.2 *Symbolization*

In this phase, convenient symbols were determined for each feature to be shown on the map. For this purpose, many local and foreign tourist city maps, as well as common web maps such as Google Maps, Yandex Maps and Bing Maps were examined. In the first stage, the symbols used in the library of GIS software were used. In cases where this is not sufficient, the symbols taken from the existing digital maps were used after being rearranged in the image editing and graphic design software and added in the map through the GIS software.

For the maps, light and pastel colours were preferred for the background features such as blocks and recreation areas (Figure 4), and more vivid colours were used for the significant features. The roads in the tourist geospatial database are represented with line geometry as in the OSM data. However, at large scale maps, roads are represented as areas (polygons). So, areal road representation (i.e. areal symbols) were obtained with buffering in the GIS software. Three different symbol widths were determined for three different types of roads within the geographic extent of the study area (Table 3). Since the roads are significant for tourist maps, their symbol sizes (i.e., width) were usually set larger than the corresponding road widths in reality. Afterwards, the roads were appropriately coloured by considering their hierarchy. Border lines were also added to the road symbols for emphasizing their representation.
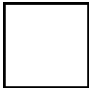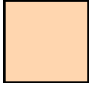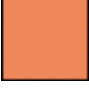
Table 2. The content of the tourist geospatial database.

CATEGORY	FEATURE CLASS	GEOMETRY	ATTRIBUTES
Accommodation	Hotel Hostel Holiday Village Pension Guesthouse	Point	Feature_name, Feature_subclass, Number_of_stars, Address
Transportation	Road Airport Port Bus Station Taxi Stops Parking Lot	Line Point Point Point Point Point	Feature_name, Feature_subclass
Cultural Heritage	Historical Building Museum Monument Ancient Harbour Ancient Lighthouse Library School Cemetery	Point	Feature_name, Purpose_of_use, Definition
Entertainment	Bar Disco Theatre Cinema Scuba Diving Paragliding Shore Fishing Casino	Point	Feature_name
Service	Bank Exchange Office ATM Post Office Prayer Room Information Office Public Toilet Court Gas Station Car Rental	Point	Feature_name
Emergency	Police Station Fire Department Hospital Cottage Hospital Pharmacy	Point	Feature_name
Recreation	Green Area Park Playground Sports Field	Polygon	Feature_name
Facility	Restaurant Cafe Market Shopping Centre	Point	Feature_name, Feature_subclass

Figure 4. Colour selection for the base map.

Table 3. Properties of roads shown on the map.

Colour	Colour Code	Feature Subclass	Road Symbol Width (m)*
	R:255 G:255 B:255	Street	10
	R:255 G:214 B:175	Avenue	17
	R:238 G:135 B:89	Main Avenue	20

* in reality

Kyrenia Castle, being the most salient landmark in the district, was shown with a 3D symbol (Figure 5). To this end, its 3D model was created in the 3D modelling software. Today, 3D models of cultural heritage collected with photogrammetric techniques are more accessible (Yakar and Dogan, 2018).

The modelling process was carried out in four stages. In the first stage, the footprint of Kyrenia Castle, digitized from satellite imagery, was extruded to its real dimensions. In addition, an enlargement process was applied to the Shipwreck Museum building within the castle so as to make it more distinguishable on the map. After this process, the photographic texture of the castle was applied to its wall. In the third phase, some landscape features around the castle (i.e., tree, bench, lighting lamp) were added in the model. In the last stage, the model was rendered by applying a suitable daylight setting.
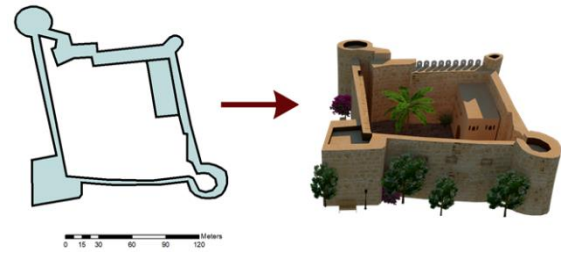
Figure 5. Digitized footprint (left) and 3D model (right) of Kyrenia Castle.

In the multimodal maps, those features were shown as common but sometimes with different symbology (Figure 6): Tourism Information Offices, Museums, Historical buildings and structures, Monuments, Harbour, Lighthouses, Theatres, Library, Schools, Playgrounds, Accommodation facilities, Banks, ATMs, Hospitals, Pharmacies, Parking lots, Bus stations, Taxi stops, Airport service stops, Gas stations, Roads, Administrative buildings, Post offices, Courts, Fire departments.
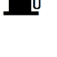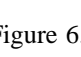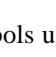
Figure 6. Common map symbols used for all of the maps.

In the cultural tourism map, for historical and cultural landmark features, photographs are used to represent them more saliently after applying visual filters (e.g., dynamic lighting, watercolour effect, etc.) (Figure 7).

Figure 7. Photograph of a landmark after visual filtering.

In the gastronomy tourism map, the restaurants and other gastronomy related features were shown using appropriate point symbols (Figure 8). All symbols in this map were designed in the image editing and graphic design software.

	Mediterranean Restaurant
	Seafood Restaurant
	Turkish Restaurant
	Local Food Restaurant
	European Restaurant
	Kebab Restaurant
	Italian Restaurant
	Café-Patisserie
	Bar

Figure 8. Map symbols specifically used for different restaurant types and other gastronomy related features.

In the entertainment tourism map, those features were shown, unlike other tourist maps (Figure 9):

Boat tour offices, Extreme sports centres, Football fields, Casinos, Bars/Discotheques (Bars were shown also in the gastronomy tourism map), Rent a yacht services, Car rental companies.

	Boat Tour Office
	Rent a Yacht Service
	Paragliding
	Casino
	Football Field
	Car Rental Company
	Bar/Discotheque

Figure 9. Map symbols specifically used in the entertainment tourism map.

4.4.3 Other elements

In this phase, some other elements were added to the map designs. Those were as follows:

- Title
- Scale bar (both linear and ratio scale).
- Grid references
- Index
- Inset map
- North arrow

4.5 Map Design Evaluation

A survey was conducted to test to evaluate the design and the usability of user-centred multimodal tourist maps against the general tourist map of the district. The number of participants in the survey was 60. The survey questions were prepared in two different languages (Turkish/English) considering domestic and foreign tourists. The data were collected by face-to-face survey method with the support of a local tourism agency. The questionnaires were completed under the supervision of the first author.

Figure 10. General tourist map of Kyrenia (not to scale) (URL 1).

The survey consists of four main parts. In the first part, individuals were asked about some types of personal information such as age, gender and educational status, as well as what kind of media (digital or paper) they used during their tourism activities. In the second part, nine questions were asked to evaluate the general tourist map of Kyrenia (Figure 10), produced by TRNC Tourism and Promotion Office, and the user-centred multimodal tourist maps (as a group), produced in this study. The participants were expected to score 1 to 5 in these questions. These scores mean: 1: very bad, 2: bad, 3: enough, 4: good, 5: very good. In the third part of the survey, six questions were asked to compare user-centred multimodal tourist maps with the general tourist map of Kyrenia. In the last part of the survey,

the questionnaire was completed by asking which of the maps (general purpose or user-centred multimodal) they prefer to use during their visits when all the factors were considered.

5. RESULTS AND DISCUSSION

Three user-centred multimodal tourist maps of Kyrenia were designed and produced by considering the specific information needs of different visitors, as mentioned above. Figures 11, 12 and 13 show these maps created for cultural tourism, gastronomy tourism and entertainment tourism, respectively. The maps are shown smaller than the actual size and scale in these figures.
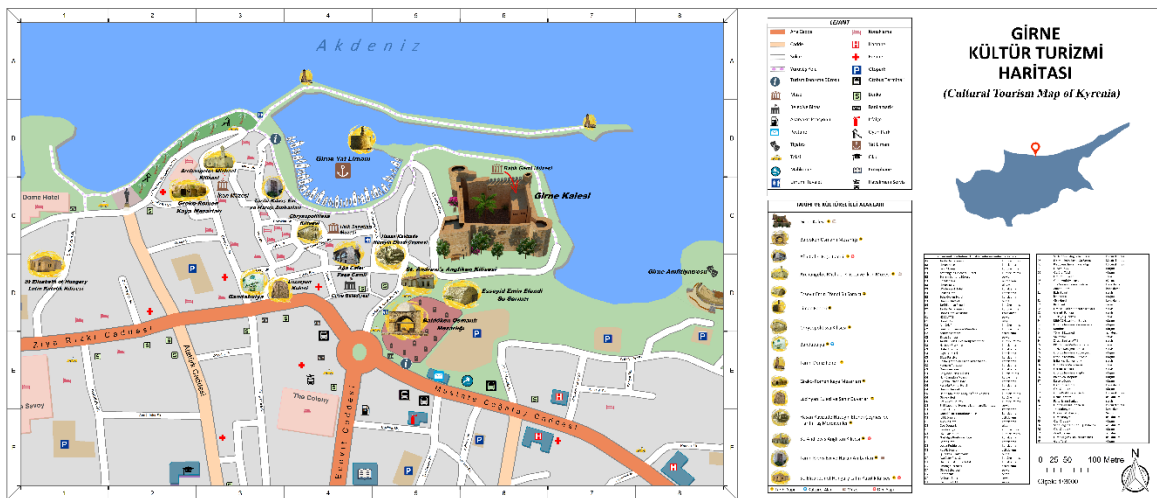
Figure 11. Cultural tourism map of Kyrenia (not to scale).
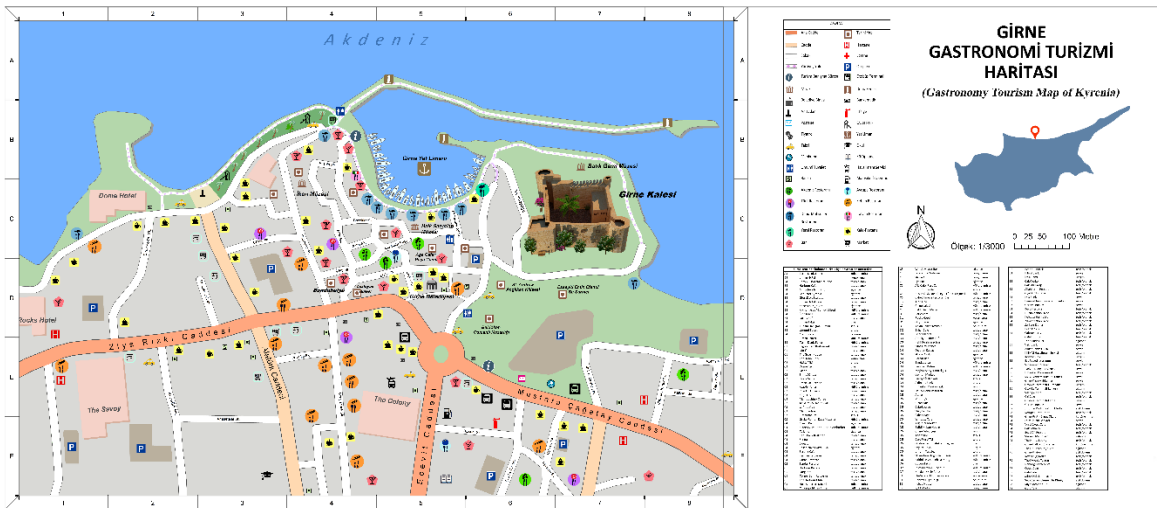

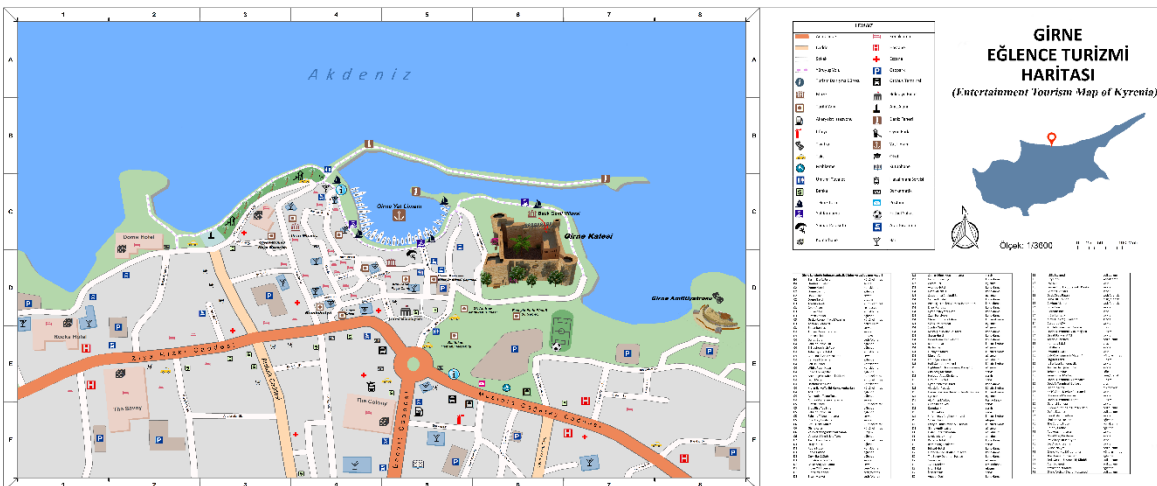Figure 12. Gastronomy tourism map of Kyrenia (not to scale).

Figure 13. Entertainment tourism map of Kyrenia (not to scale).

The evaluation of maps was performed by user surveys. The profile of the participants in terms of gender, age and educational status was given in Table 4.

Table 4. Demographic profile of the survey participants (N: 60).

Variable	Category	%
Gender	Female	46.7
	Male	53.3
Age	18-35	28.3
	36-55	36.7
	56 or above	35
Educational Status	Primary/Secondary School	6.7
	High School	30
	University	63.3

The survey findings show that paper maps are still used commonly (Figure 14). The majority of the participants said that they use paper and digital maps together during their visits.

The findings show that the general tourist map of Kyrenia is insufficient in some aspects. The user-centred multimodal tourist maps were found more preferable and useful. The average score (out of 5)

Table 5. Average scores of the variables of maps.

for the variables of the maps given by participants is shown in Table 5.
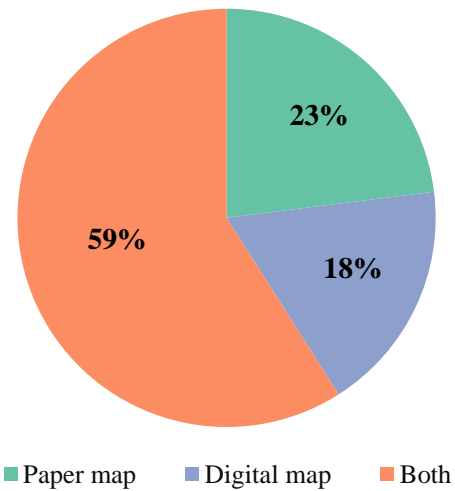
Figure 14. Map type preference of the participants.

Another remarkable result of the survey was in the field of map aesthetics and visual quality. In this respect, the average score of the general tourist map of Kyrenia was 2.15 out of 5. The user-centred multimodal maps got 4.32 out of 5. This shows that they are more attractive in view of the visitors.

Variable	Average Score	
	General Tourist Map	User-Centred Multimodal Tourist Maps
Scale (level of detail)	3.50	4.12
Map size	4.08	3.92
Aesthetic quality	2.15	4.32
Map legend	3.32	4.35
Easiness for reading and understanding	2.77	4.00
Scope of information provided	2.58	4.07
Placement (Existence) of landmarks for wayfinding	3.17	4.23
Sufficiently comprehensive information for touristic places	2.77	4.13
Covering all street names of interest	3.62	4.25

Table 6. The map preference made by the participants according to some technical specifications.

Variable	The Choice of the Participants (N:60)	
	General Tourist Map %	User-Centred Multimodal Tourist Maps %
Map size and scale	38.33	61.67
Ability to respond to specific user requirements	3.33	96.67
Ease of use	35	65
Map language (legibility and clarity)	30	70
Map aesthetics/visual quality (colours, symbols, legends etc.)	8.33	91.67
Ease of wayfinding (accurate and complete representation of landmarks and points of interest)	18.33	81.67

Another investigation was made on how the demographic profile of the participants affected their map preferences. Accordingly, as the education level of the participants increases, the interest to the general tourist map decreases, and the interest to the user-centred multimodal tourist maps increases (Figure 15). In terms of age and gender, no significant difference was observed in the preferences.
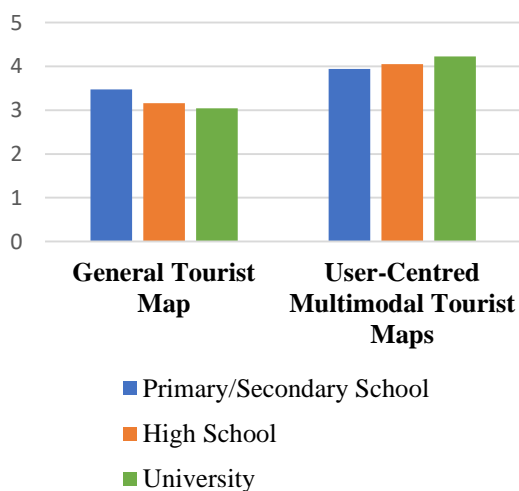
Figure 15. The score averages given by the participants to the tourist maps according to the educational status.

6. CONCLUSIONS

Tourist maps are cartographic products that provide geospatial information for tourists visiting a place. These maps are important for the visitors to percept and explore a region that they visited or planned to visit. Therefore, tourist maps not only affect the satisfaction of the tourists during the visit but also may impact their decision for destination choice.

This study presented the design and production as well as the evaluation of user-centred multimodal tourist maps, which communicate more specific information to the tourists in comparison to general tourist maps. In this context, the map designs for the Kyrenia district of TRNC were developed for three particular types of tourism (cultural, gastronomy and entertainment), based on the tourist geospatial database constructed in the earlier phase of the study. According to the map evaluation study based on user surveys, it was observed that user-centred multimodal tourist maps created in this study were more preferred by the participants. Besides, it is observed that it is important to show the information on the tourist maps correctly, specifically and attractively as much as possible.

Future works may focus on other kinds of tourism maps. In addition, a web map interface allowing user interaction and supporting multiple map modes may be developed for this purpose. Furthermore, user studies may be done with a larger number of participants.

REFERENCES

Alamaki, A. and Dirin, A. (2014). Designing mobile guide service for small tourism companies using user centered design principle, International Conference on Computer Science, Computer Engineering, and Social Media, 12-14 December 2014, Thessaloniki, Greece.

Almer, A., Schnabel, T., Stezl, H., Stieg, J. and Luley, P. (2006). A tourism information system for rural areas based on a multi-platform concept. In: J.D. Carswell and T. Tezuka (eds.) Web and Wireless Geographical Information Systems - Proceedings of the 6th International Symposium (W2GIS'06), LNCS vol. 4295, 31-41.

Basaraner, M. (1997). Turistik Amaçlı Coğrafi Bilgi Sistemi Oluşturulması, Master of Science Thesis, YTU, Istanbul, Turkey.

Basaraner, M. and Selcuk, M. (1999). From tourist map to tourist GIS, Third Turkish-German Joint Geodetic Days, 23-26 September 1999, Istanbul, Turkey.

Brown, A., Emmer, N. and Worm, J. (2001). Cartographic design and production in the internet era: the example of tourist web maps. The Cartographic Journal 38(1), 61-72.

Brown, B. (2007). Working the problems of tourism. Annals of Tourism Research 34(2), 364-383.

Buckley, A. (2012). Make maps people want to look at: five primary design principles for cartography. ArcUser Winter 2012, 46-51.

Cartwright, W., Peterson, M.P. and Gartner, G. (2007). Multimedia Cartography, Second Edition. ISBN: 978-3-540-36650-8., Springer, Heidelberg.

Ceylan, M., Sarici, H. and Basaraner, M. (2011). İstanbul tarihi yarımada için coğrafi bilgi sistemi tabanlı turistik harita tasarımı, TMMOB Coğrafi Bilgi Sistemleri Kongresi 31 Ekim-4 Kasım 2011, Antalya, Turkey.

Clarke, L.M. (1989). An experimental investigation of the communicative efficiency of point symbols on tourist maps. The Cartographic Journal 26(2), 105-110.

Comert, C. and Bostanci, T. (1999). Turist bilgi sistemleri ve Trabzon örneği, Yerel Yönetimlerde Kent Bilgi Sistemi Uygulamaları Sempozyumu, 13-15 Ekim 1999, Trabzon, Turkey.

Demirci, Y.Z. and Kavzoglu T. (2010). Kocaeli turizm bilgi sisteminin tasarlanması, III. Uzaktan Algılama ve Coğrafi Bilgi Sistemleri Sempozyumu, 11-13 October 2010, Kocaeli, Turkey.

Dent, B., Torguson, J. and Hodler, T. (2009). Cartography: Thematic Map Design, Sixth Edition. ISBN: 978-0-072-94382-5, McGraw-Hill, Boston.

Erdogan, S. and Tiryakioglu, I. (2004). Turizm-tanıtım faaliyetlerinde coğrafi bilgi sistemlerinin kullanımı: Afyon örneği, 3rd GIS Days in Turkey, 6-9 October 2004, Istanbul, Turkey.

Filippakopoulou, V. and Nakos, B. (1995). Is GIS technology the present solution for creating tourist maps?. Cartographica: The International Journal for Geographic Information and Geovisualization 32(1), 51-62.

Gerber, R., Burden, P. and Stanton, G. (1990). Development of public information symbols for tourism and recreational mapping. The Cartographic Journal 27(2), 92-103.

Haklay, M. and Nivala, A. (2010). User-centred design. In: M. Haklay (ed.) Interacting with Geospatial Technologies, ISBN: 978-0-470-99824-3, Wiley, Sussex.

Hardy, P., and Field, K. (2012). Portrayal and cartography. In: W. Kresse and D.M. Danko (eds.) Springer Handbook of Geographic Information, ISBN: 978-3-540-72680-7, Springer, Heidelberg.

Kariotis, G., Panagiotopoulos, E., Karitou, G. and Karanikolas, N. (2007). Creation of a digital interactive tourist map with the contribution of GPS and GIS technology to visualization of the information, XXIII International Cartographic Conference, 4-10 August 2007, Russia.

Medynska-Gulij, B. (2003). The effect of cartographic content on tourist map users. Cartography 32(2), 49-54.

Memduhoglu, A. and Basaraner, M. (2018). Possible contributions of spatial semantic methods and technologies to multi-representation spatial database paradigm. International Journal of Engineering and Geosciences 3(3), 108-118.

Mutlu, A., Vural G., Aydin, O., Guney, B., Hamamci S. F., Aya, A., Sur, N., Ulugtekin, N. and Bektas Balcik, F. (2017). Bodrum turistik bilgi sistemi web ve mobil uygulamaları, 16. Türkiye Harita Bilimsel ve Teknik Kurultayı, 3-6 May 2017, Ankara, Turkey.

Nivala, A.M. and Sarjakoski, L.T. (2005). Adapting map symbols for mobile users, 22th International Cartographic Conference Mapping Approaches into a Changing World, 9-16 July 2005, A Coruna, Spain.

Oliveira, I.J. (2005). Cartografia aplicada ao planejamento do turismo. Boletim Goiano de Geografia 25(1), 29-46.

Pucihar, A., Malesic, A., Lenart, G. and Borstnar, M.K. (2014). User-centered design of a web-based platform for the sustainable development of tourism services in a living lab context. In: B. Auilani, T. Abbate and A.M. Braccini (eds.) Smart Organizations and Smart Artifacts, Springer, Cham.

Reichenbacher, T. (2001). Adaptive concepts for a mobile cartography. Journal of Geographical Sciences, 11(1), 43-53.

Sneiderman, B. and Plaisant, C. (2005). Designing the User Interface: Strategies for Effective Human-Computer Interaction, Fourth Edition. ISBN: 0-321-19786-0, Pearson, Boston.

Ulugtekin, N.N., Dogru, A.O. and Bildirici, I.O. (2013). CBS haritalarının tasarımı, TMMOB Coğrafi Bilgi Sistemleri Kongresi, 11-13 November 2013, Ankara, Turkey.

Wesson, C. (2018). Layout, balance, and visual hierarchy in map design. In: A.J. Kent and P. Vujakovic (eds.) The Routledge Handbook of Mapping and Cartography, Routledge, Abingdon, Oxon.

Xinwei, Z. and Wangfusheng, W. (2005). The design and development of Beijing tourism information system based on GIS. Geomatics & Spatial Information Technology 28(4),33-35.

Yakar, M. and Dogan, Y. (2018). GIS and three-dimensional modeling for cultural heritages. International Journal of Engineering and Geosciences 3(2), 50-55.

Yan, L. and Lee, Y. (2014). Are tourists satisfied with the map at hand?. Current Issues in Tourism 18(1), 1048-1058.

Yan, X. and Wang, Y. (2012). Development of Zaozhuang tourism information system based on WebGIS. International Journal of Computer Science Issues 9(6), 249-252.

Yin, P., Jiang, X. and Ma, Y. (2008). Research on tourism information systems for self-drive tourists, IEEE International Conference on Service Operations, Logistics and Informatics, 2, 1915-1921.

URL 1, KKTC Turizm Tanıtma ve Pazarlama Dairesi, http://turizmtanitma.gov.ct.tr/Tanıtım-Broşürleri/Bölgeler/Girne, accessed on 1 March 2019.

POSITIONING BUILDINGS ON A ZONING ISLAND TO PROVIDE MAXIMUM SHADING: A CASE STUDY

Hüseyin İnce[1] and Nuri Erdem[2*]

[1]Vocational School of Higher Education for Mapping and Land Survey, Hitit University, Çorum, Turkey, (huseyinince@hitit.edu.tr); **ORCID 0000 0001 6118 5502**

[2*]Engineering Faculty, Department of Geomatics Engineering, Osmaniye Korkut Ata University, Osmaniye, Turkey (nurierdem@osmaniye.edu.tr); **ORCID 0000-0002-1850-4616**

ABSTRACT: Because summer days are long, and the weather is too hot, people desire shady spaces to escape the overwhelming effect of the sun. To keep buildings and open-air environments in the shade, a suitable building location design may be created at the planning stage. Positioning of buildings and recreation areas in the maximum amount of shade is closely dependent on the location of the buildings to be built, the distance between the buildings, the time of the day and the sun angles at a particular hour. It was found necessary to carry out this study, since no study was found to be carried out regarding the positioning of buildings in the maximum amount of shade. For buildings to be built in residential areas, separate or block arrangements are applied. This study discusses a building to be built on a reconstruction island in Adana in the Eastern Mediterranean Region of Turkey. First of all, the shading effects of the buildings adjacent to the building in a parcel were examined in detail based on various positions of the façades of the building and different values of the solar azimuth. As a result of the study, the positioning of the buildings for providing the maximum shading was investigated. If the front and rear façades of the buildings were located in the west-east direction, according to the positioning of the buildings in the north-south direction, the front and rear façades would be exposed to less sunlight and more shade. In h = ± 6 sun hours, the façades of buildings in the parcels facing the north were under the influence of the sun rays coming from the side, and the rear façades of the buildings were in the shade.

Keywords: Sun Angles, Shading, Building Shading Positions, Energy Efficiency

1. INTRODUCTION

In Turkey, because summer days are long and the weather is too hot, shady places are desired for getting rid of the sun's overwhelming effect. In order to ensure that buildings or open-air rest areas are kept in the shade, they can be designed with buildings or recreation areas at the planning stage (Kuşak and Küçükali, 2019; Ekercin et al., 2019). Positioning the specified spaces in the maximum amount of shade is closely related to the location of the buildings, the distance between the buildings, the sun's azimuth angle and the solar zenith angle, as well as the time of the day and the sun declination angle at that time.

The locations of the buildings or recreational areas to be built on parcels in a reconstruction island are designed in a parceling plan. In studies on the subject in practice (Yüceer, 2010; Yüceer, 2011; Selim and Demir, 2019), external shade element designs were suggested, and the shape and yield of external shade elements in Adana in the Eastern Mediterranean Region of Turkey were investigated with shade line charts. The shape and size of the shading elements required for the four main directions of a P window sample of 120/140 size as the shading element were specified.

This study was based on the height of five-story buildings as a shading element in a reconstruction island in Adana. In the parcel where five-story buildings are located in the neighboring garden, in the side garden, in the back garden and in the front garden, the warmest days of the year, from May 1st to October 1st, were taken into consideration for the period from local lunch time to ± 6 solar hours. The locations where the structures to be constructed in a discrete structure order to be kept in the shade were investigated by considering the average latitude of the region and the hour angles of sunrise and sunset in the specified period. It was found necessary to carry out this study because previous studies (Yeang, 1995; Oktay, 2004; Farr, 2008) did not report on this particular topic.

2. GARDEN DISTANCES AND ROAD WIDTHS ACCORDING TO THE TYPE RECONSTRUCTION REGULATION

For buildings to be built in the settlement areas, a separate order or block order is applied. For a building to be built in a parcel, according to the Planned Areas Type Reconstruction Regulation in force, garden distances are accounted for. In the Implemented Planned Areas according to the provisions of the Type Reconstruction Regulation, front garden distance, side garden distance, neighboring garden distance and back garden distance are indicated as follows:

- In buildings with up to 4 floors (including 4 floors); front garden distance = 5 m., side garden distance = 5 m., neighboring garden distance = 3 m.
- In buildings with up to 5 floors (including 5 floors); front garden distance = 5 m., side garden distance = 5 m., neighboring garden distance = 0.50 m for each floor. After 4 floors, the distance is increased.
- While examining the shading effect of buildings in for building on a reconstruction island opposite another building, there is a need for road width between buildings.

On the subject of the Type Reconstruction Regulation;
- Width of road in 3-storey buildings (excluding basement): 7.00 - 10.00 m
- Width of road in 4-storey buildings (excluding basement): 10.00 - 12.00 m.
- Width of road in 5-storey buildings (excluding basement): 12.00 - 15.00 m, this cannot be less, and provisions are included.

3. SOLAR ANGLES

While positioning structures to benefit from sunlight, incidence direction angles of sun rays (azimuth angles) are utilized. The azimuth angle of the sun consist of the latitude of the construction site (φ), the declination angle of the sun for a particular day of the year (δ) and the angle of sunrise and sunset according to the local noon. These angles are called azimuth (Olgyay, 1957; Soler and Oteıza, 1997; Abood, 2015; Som and Pathak; 2015).

Latitude (angle) φ: It is the angle of the line which combines the aboveground N point to the centrosphere, with the equatorial plane. It is marked with a (+) from the Equator to the north and with a (-) to the south.

Hour Angle (h): It is the angle between the line which combines the longitude of the considered point on earth with the centrosphere and the longitude indicated by sun rays. The hour angle is calculated from the "solar noon", when the longitude of the sun and the longitude of the point which is being considered are the same. The difference is marked with a (–) for before the local noon and with a (+) for after the local noon. Every one-hour time difference is considered as an hour angle of 15°.

Declination Angle (δ): It is the angle of sun rays to the equatorial plane (Figure 1). This angle results from the 23° 27' degrees of difference between the rotational axis of the world and the normal of the orbital plane. The absolute value in the solstices is maximum (June 21 summer solstice = +23°.45, December 22 winter solstice = -23°.45). The declination angle is obtained from the equation:

$$\delta = 23°.45 \sin\left(360\left(\frac{n+284}{365}\right)\right) \qquad (1)$$
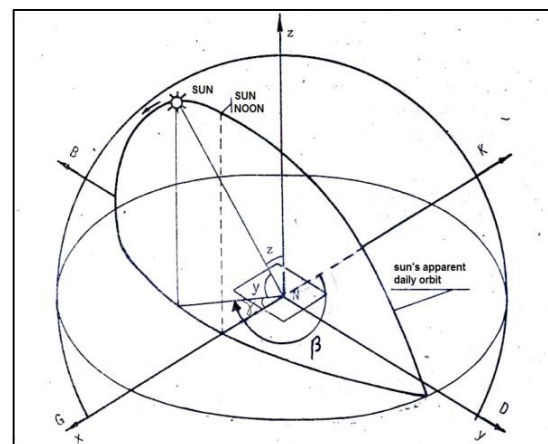
Here, n is the number of days.

Figure 1. Schematic of the Solar Zenith Angle, Elevation and Azimuth Angle, at the Spherical Triangle from a Point on Earth of N (Abood, 2015)

Zenith angle (z): It is the angle between direct sun rays and the normal of the horizontal plane (Figure 1). At sunrise and sunset, z=90º. The zenith angle is obtained with the formula below.

$$\text{Cos } z = \cos \delta \cos \varphi \cos h + \sin \delta \sin \varphi \qquad (2)$$

Solar elevation angle (y): It is the angle of the horizontal rays of the sun. As seen in Figure 1, z+y =90º. The solar elevation angle is obtained with the formula: y=90 - z.

Solar azimuth angle (β): This angle represents the deviation of sun rays' rotation in reference to the clockwise direction of north (Figure 1). β as follows;

Before the local noon (in degrees), β=180º-γº (or in grade β=200 -γ^G) $\qquad (3)$

After the local noon (in degrees), β=180º +γº (or in grade β=200+γ^G) $\qquad (4)$

$$\text{Cos } \gamma = \frac{\cos \delta \cos \varphi \cos h - \sin \delta \cos \varphi}{\cos y} \qquad (5)$$

4. CALCULATION OF SUN ANGLES AND SHADING LENGTHS FOR THE EASTERN MEDITERRANEAN REGION

In order to determine the shading position of a building in sunny weather in the Eastern Mediterranean region, there is a need for sunrise and sunset angles, solar declination angle, solar zenith angle and solar azimuth angle at a specified time interval.

In the calculation of the solar zenith angle, the solar elevation angle and the solar azimuth angle, the following elements were firstly calculated:

- The values of 1, 15 and 22 of each month from 1 May to 1 October were calculated by using correlation (1) for solar declination.
- The Eastern Mediterranean Region is located between 32º 56 ' and 36º 42' in longitudes and 35º 52 ' and 38º 00' in latitudes. The value φ = 37º for Adana was used as the average value representing the region.
- The hour angles of sunrise and sunset were obtained from the information on calendars showing the specified time in Adana, Hatay, Osmaniye and Mersin. In the examination of the four aforementioned provinces, it was seen that there was a difference of 5-6 minutes between their times of sunrise, sunset and midday time on 21 June. Therefore, from 1 May to 1 October, the clock angles of sunrise and sunset were used for Adana, and the results are shown in Table 1.

Table 1. Time in Adana, watch angels of Sunrise and Sunset

Days of Year	n	Solar Times			Sun Watch Angle	
		Sunrise	Noon	Sunset	Sunrise (h)	Sunset (h)
1 May	121	5:37	12:43	19:36	12:43-5:37=7:06	19:36-12:43=6:53
15 May	135	5:24	12:42	19:48	12:42-5:24=7:18	19:48-12:42=7:06
1 Jun	152	5:14	12:43	19:59	12:43-5:14=7:29	19:59-12:43=7:16
22 Jun	172	5:12	12:48	20:11	12:48-5:12=7:36	20:11-12:48=7:23
1 July	182	5:16	12:49	20:09	12:49-5:16=7:33	20:09-12:49=7:60
15 July	196	5:24	12:52	20:07	12:52- 5:24=7:28	20:07-12:52=7:15
1 Aug	213	5:37	12:51	19:54	12:51-5:37=7:1	19:54-12:51=7:03
15 Aug	227	5:49	12:50	19:40	12:50-5:49=7:01	19:40-12:50=6:50
1 Sept	244	6:03	12:46	19:17	12:46-6:03=6:43	19:17-12:46=6:31
15 Sept	258	6:14	12:41	18:56	12:41-6:14=6:27	18:56-12:41=6:15
1 Oct	273	6:27	12:36	18:32	12:36-6:27=6:09	18:32-12:36=5:56

When Table 1 is examined, it is seen that the sun hour angles of sunrise and sunset in Adana, determined on the selected days of the year, changed between 5.56 and 7.60 hours, and the value h = ± 6 was considered in the study. For the times indicated in Table 1, the solar declination angles, solar zenith angles and solar elevation angles corresponding to the solar hour angles from h = 0 to h = ± 6.0 were calculated by the aforementioned correlations and are shown in Table 2. The γ angles required for the

calculation of the azimuth angle of the sun were calculated by considering the angles in Table 2 and are shown in Table 3.

A mathematical error (cos h> 1.0) was generated in the calculation of for h = ± 1 in Table 3. For the calculation of the solar azimuth angles for h = ± 1, half of the calculated in the interval of h = ± 2 were taken.

Table 2. Solar zenith angles and sun height angles from 1 May to 1 October in Adana (in grad units) (italic figures are solar height angle values)

Days of Year	Declinations Angle δ°	Hour Angels						
		0	1	2	3	4	5	6
1 May	14.9009	24.5546	28.6786	38.4445	50.5934	63.6360	76.9298	90.1082
		75.4554	*71.3214*	*61.5555*	*49.4066*	*36.3640*	*23.0702*	*9.8918*
15 May	18.7919	20.2312	24.9527	35.4850	49.0452	61.2416	74.5263	87.5796
		79.7688	*75.0477*	*64.5150*	*50.9548*	*38.7584*	*25.4737*	*12.4204*
1 Jun	22.0396	16.6226	22.0001	33.2184	46.0796	59.3538	72.5864	85.4982
		83.3774	*77.9999*	*66.7816*	*53.9204*	*40.6462*	*27.4136*	*14.5018*
21 Jun	23.4498	15.0558	20.7799	32.3028	45.2774	58.5684	71.7648	84.6040
		84.9442	*79.2201*	*67.6972*	*54.7226*	*41.4316*	*28.2352*	*15.3960*
1 July	23.1205	15.4217	21.0609	32.5126	45.4618	58.7499	71.9554	84.8122
		84.5783	*78.9391*	*67.4874*	*54.5382*	*41.2501*	*28.0446*	*15.1878*
15 July	21.5173	17.2030	22.4625	33.5687	46.3850	59.6501	72.8940	85.8309
		82.7970	*77.5375*	*66.4313*	*53.6150*	*40.3499*	*27.1060*	*14.1691*
1 Aug	17.9132	21.2076	25.7785	36.1321	48.6033	61.7703	75.0618	88.1436
		78.7924	*74.2215*	*63.8679*	*51.3967*	*38.2297*	*24.9382*	*11.8524*
15 Aug	13.7836	25.7960	29.7767	39.3356	51.3597	64.3479	77.6344	90.8402
		74.2040	*70.2233*	*60.6644*	*48.6403*	*35.6521*	*22.3656*	*9.1598*
1 Sept	7.7246	32.5282	35.8827	44.4237	55.7465	68.3748	81.5536	94.8447
		67.4718	*64.1173*	*55.5763*	*44.2535*	*31.6252*	*18.4464*	*5.1553*
15 Sept	2.2169	38.6479	41.5859	49.3399	60.0163	72.2447	85.2368	98.5178
		61.3521	*58.4141*	*50.6601*	*39.9837*	*27.7553*	*14.7632*	*1.4822*
1 Oct	-4.2155	45.7950	48.3589	55.3274	65.2643	76.9643	89.6472	
		54.2050	*51.6411*	*44.6726*	*34.7357*	*23.0357*	*10.3528*	

In obtaining the azimuth angles of the sun, calculation was made by using the formulae (3) and (4) based on the values in Table 3.

Table 3- The γ angles used for calculating solar azimuth angles for Adana (in grad units)

Days of Year	Hour Angles						
	h=0	h=1	h=2	h=3	h=4	h=5	h=6
1 May	0ᵍ.00	14.2030	28ᵍ.0464	63.0901	82.2809	96.9353	110.0134
15 May	0.00	16.3265	32.6536	67.4510	85.5846	99.8742	112.6638
1 Jun	0.00	18.6540	37.3080	70.3266	88.4969	102.3988	114.8935
22 Jun	0.00	19.7860	39.5719	71.9288	89.8064	103.5159	115.8671
1 July	0.00	19.5150	39.0299	71.5494	89.4981	103.2539	115.6395
15 July	0.00	18.2538	36.5076	69.7481	88.0188	101.9883	114.5337
1 Aug	0.00	15.7620	31.5238	65.9703	84.8211	99.2025	112.0634
15 Aug	0.00	13.4532	26.9063	62.0829	81.3685	96.1081	109.2561
1 Sept	0.00	11.0117	22.0234	57.1551	76.6859	91.7437	105.1723
15 Sept	0.00	9.6478	19.2956	53.3778	72.7903	87.9399	101.4826
1 Oct	0.00	8.9107	17.8214	49.6840	69.6261	83.6685	

4.1. Calculation of Shading Lengths According to Zenith Angles in the Azimuth Angle Direction

4.1.1. Calculation of distance between neighboring buildings in the direction of the solar azimuth angle

The sun's rays reach a certain location on earth in the direction of the solar azimuth angle. The shading of a building occurs in the direction of the sun's azimuth angle (Mcmullan, 1990; Ok, 1992; Atabek, 1996; Capeluto et al., 2003).

According to the Planned Areas Type Reconstruction Regulation for 5-storey buildings, the specified neighboring garden distance is 3.5 m, back garden distance is 7.75 m, side garden distance is 5 m, and front garden distance is 5 m.

The horizontal distance between the directions perpendicular to the surfaces of two neighboring buildings;

Neighboring garden distance = 7.00 m, back garden distance = 15.50 m, side garden distance + road width = 17.00 m, and front garden distances + road width = 22.50 m.

The symbols X_K, X_A, $X_Ö$, X_Y in the Figures were defined as follows in the direction of the solar azimuth angle.

X_K: the horizontal distance between buildings in the neighboring garden,

X_A: the horizontal distance between buildings in the back garden,

$X_Ö$: the horizontal distance between buildings in the front garden,

X_Y: the horizontal distance between buildings in the side garden.

The horizontal distance in the garden, considering the sum of the aforementioned distances and angles) (Fig. 2 (a), (b)) is calculated with the following relations:
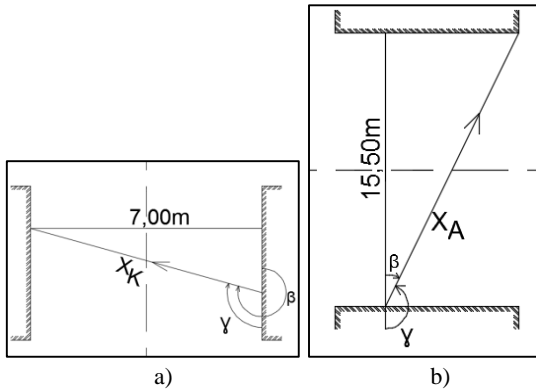

Figure 2- Horizontal distance between neighboring buildings in the direction of the solar azimuth angle.

$X_K = 7.00 / \sin \gamma$ for buildings in neighboring gardens (7)

$X_A = 15.50 / \sin \gamma$ for buildings in back gardens (8)

$X_Ö = 22.50 / \sin \gamma$ for buildings in front gardens (9)

For buildings in side gardens, $X_Y = 17.00/\sin \gamma$ (10)

4.1.2. Calculation of Shading Length According to Solar Zenith Angles

When the sun's rays of z_1 and z_2 at sunny times at different times (or at elevation angles of y_1 and y_2) (Figure 3) pass through the point A of a building at height AB, the BC and FB shading lengths of the rays are obtained with the following relations (Anderson and Mikhail, 1998; Bannister et al., 1998).

$BC = AB/\tan y_1 = AB*\tan z_1$ (11)
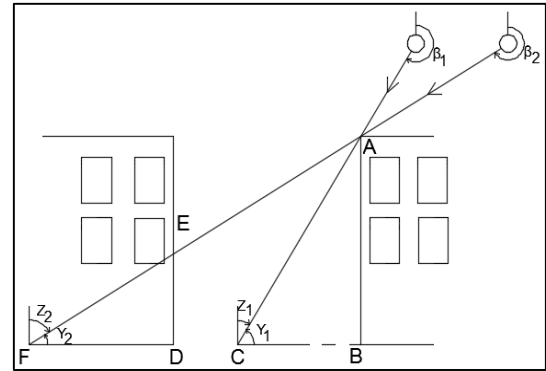$FB = AB/\tan y_2 = AB*\tan z_2$ (12)

Figure 3 - Shading lengths of the sun's rays that come at different times in sunny weather on the ground and neighboring building surfaces

Here,
FB: The length of the shade on the floor in line with

FA (in the direction of the $\beta2$ solar azimuth angle)

DB: horizontal length between neighboring buildings calculated by correlation (7) or (8) or (9) or (10)

FD: Shading length at the base of the neighboring building in the shading direction

ED: In the case of FB>DB, the height of the shading of the AB wall on the surface of the neighboring building.

FD and ED are obtained with the following relations:

$FD = AB*\tan z_2-$ (The length obtained by the relationship between (7) or (8) or (9) or (10)) (13)

$ED = FD*\tan y_2$ (14)

The building wall in a parcel must be FB> DB to form a shading on the surface of the building in the neighboring parcel.

If FB <DB, then the shading of the building exposed to the sun is formed in the neighboring garden area or the back-garden area between the neighboring buildings (Arumi-Noe, 1996; Data, 2001; (Kuşak and Küçükali, 2019)).

For h = 0, the shadings of the objects are not formed since the sun's rays come in a direction perpendicular to the earth, so the sun angles between h = ± 1 and h = ± 6 were used in the calculations.

According to the issues described above; The length of the shading formed in a 5-storey building structure, area of neighboring gardens, area of back gardens and area of front gardens (or side gardens) in a zoning parcel, as well as the height of the shade on the neighboring building surface, are shown in Figures 4 through 11.
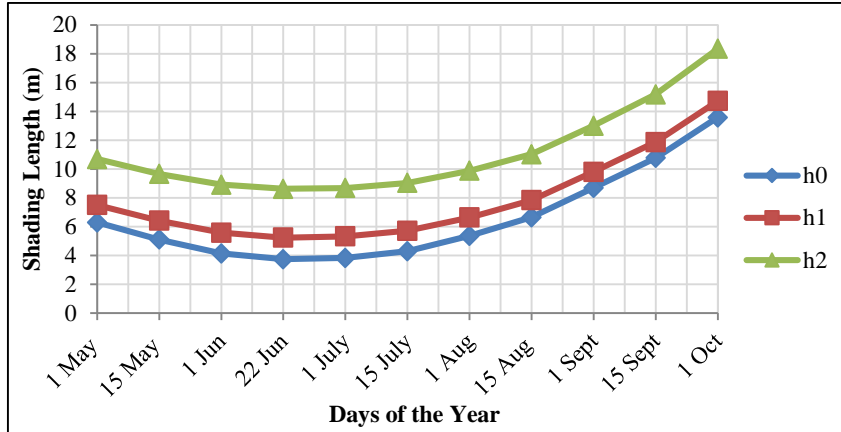
Figure 4- Length of Shading in Neighborhood Garden Areas According to the Months and Sun Hours (in m units).
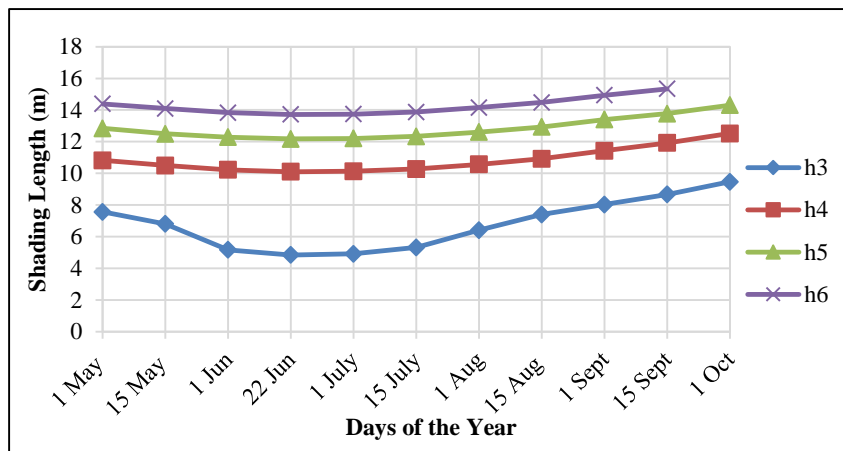
Figure 5- Shade Length According to Sun Hours and the Months on the Building Surface in the Neighborhood Garden (in m units)
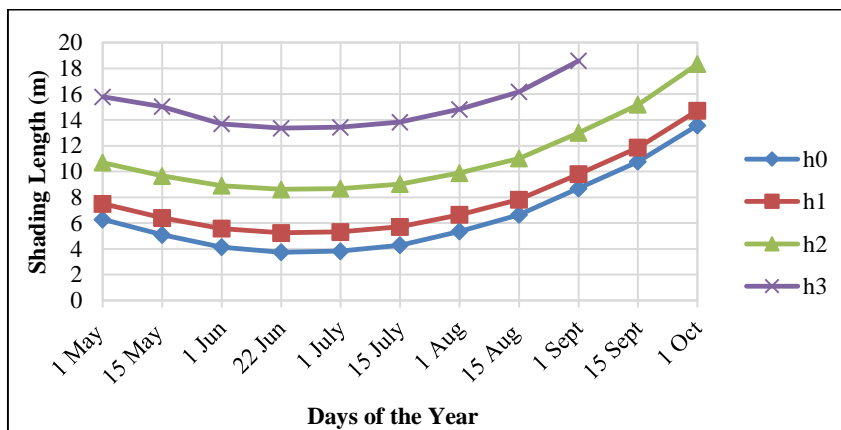
Figure 6- Shade Length in the back garden area according to Sun Hours and the Months (in m units)
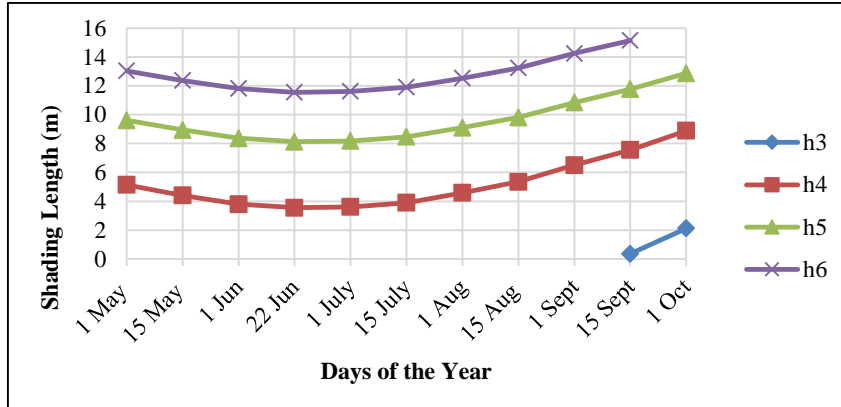
Figure 7- Shading Length in the neighboring building surface in the back garden according to Sun Hours and the Months (in m units)

Figure 8- Shading Length in the front garden areas according to Sun Hours and the Months (in m units)

Figure 9- Shading Length in the building surface of the front neighboring garden according to Sun Hours and the Months (in m units)

Figure 10-Shade Length in the field of side gardens according to Sun Hours and the Months (in m units)

Figure 11- Shading length in the building surface in the side garden according to Sun hours and the Months (in m units).

5. INVESTIGATION OF BUILDING POSITION IN ADJACENT ISLAND AND PARCEL SUITABLE FOR SHADING

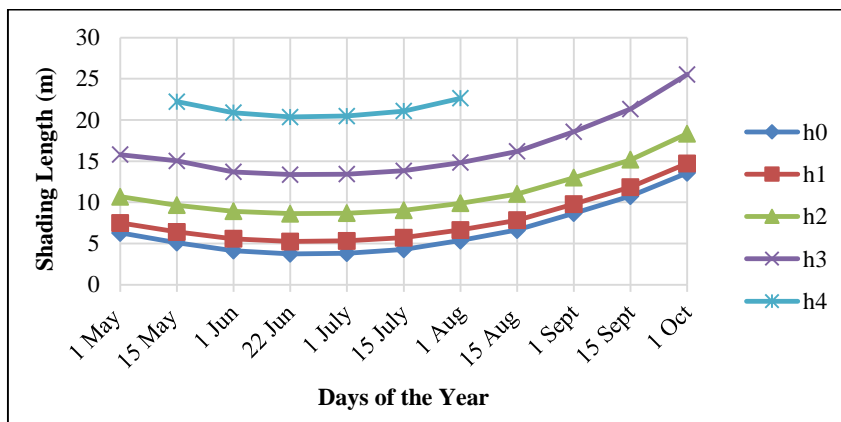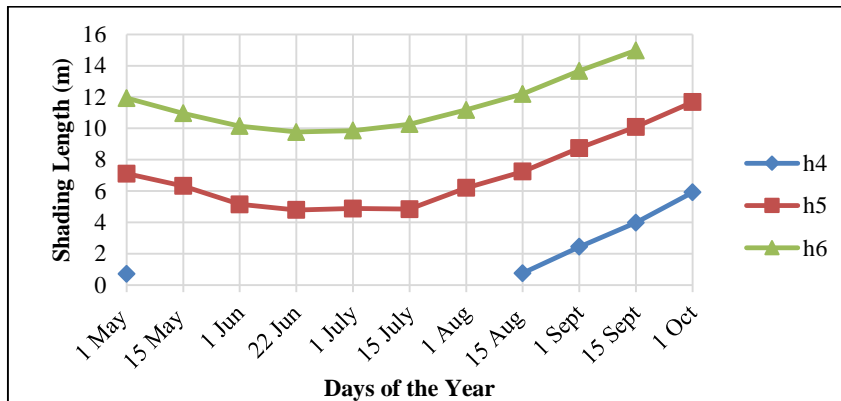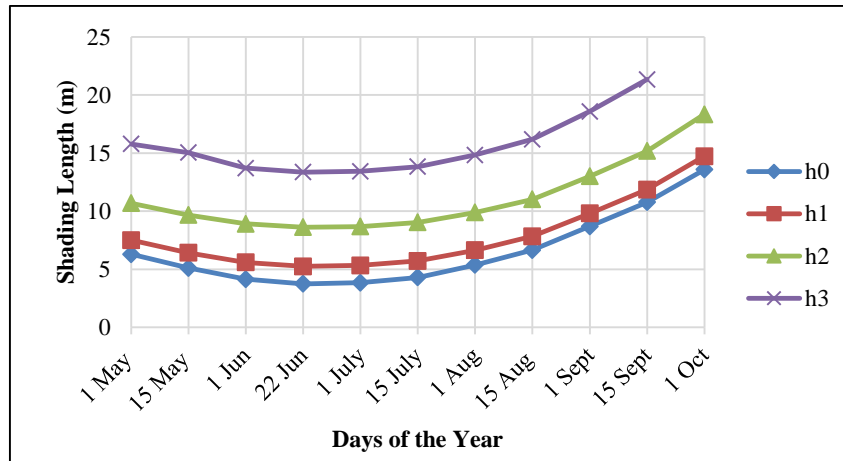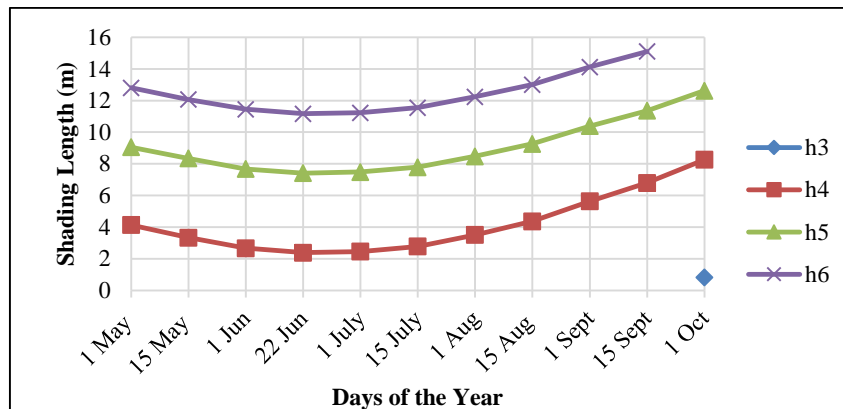For construction in a settlement area, the azimuth angles of the district lines of the reconstruction island may have various values (Szokolay, 1980; Al-Sareef et al., 2001; Tavares and Martins, 2007; Selim and Demir, 2019; Ekercin et al., 2019). The values of this specified angle may be in practice 0g (or 200), 50g (or 250g), 100g (or 300g), 150g (or 350g) or fractional values.

If the façade of a building and the zoning parcel, the island where the sun will be used during the day is positioned according to 50^g to 250^g of the solar azimuth angles.

- The parcel area to be calculated according to the building façade, the building depth and the garden distance given in the project are at minimum values.

- In terms of space saving, for the parcel or island façade to be created, where the solar azimuth angles 50g-150g or 150g-250g should be positioned according to a research on the subject requires information (İnce & Erdem, 2018).

In order not to sunbathe during a day in a building on a zoning island, it must be closely examined whether the azimuth angle of the reconstruction island façade is 0g or 100g, that is, in the north-south direction or west-east direction of the zoning island front line (Fig. 12 and Fig. 13).

When the situation before the local afternoon in Figure 12 is examined between May 1 and October 1 of the year, the following issues may be mentioned:

- Between the hours h = 0 and h = -5, the façades of all buildings in the parcels facing north and west remain in the shade, and the façades of the buildings facing east are under the influence of the sun.

- Between the hours h = -3 and h = -5, the southern façades of the buildings on the zoning island are under the influence of the sun.

When the situation after the local afternoon in Figure 12 is examined between May 1 and October 1 of the year, the following may be mentioned:

- The façades of the west-facing buildings of the zoning islands are exposed to the sun between h = 0 and h = 5, and the eastern and northern façades of the buildings are over-shaded.

The shade lengths on the east side façades and adjacent garden areas of the buildings located from the right to the left after the buildings to the east of the reconstruction island between the morning and the local noon are shown in Figure 4.

The shading lengths on the west side façades and adjacent garden areas of the buildings located from the left to the right after the buildings to the west of the reconstruction island are shown in Figure 5.

The h = ± 4 shade length is 10.82 m on 1 May, while it decreases to 10.10 m on June 21 and increases to 12.52 m on 1 October.

The shade length at h = ± 5 is 12.84 m on May 1 and 12.17 m on 21 June, and it rises to 14.31 m on 1 October.

The shade length at h = ± 6 decreases to 13.72 m on June 21, 14.39 m on 1 May and 15.34 m on 15 September.

The shadings formed between h = 0 and h = ± 2 are located in the neighboring garden areas between the buildings. Between h = 0 and h = ± 3, the shadings remain

in the backyard areas (Figures 4-6). Shading length generated: 7.74 m to 18.34 m in the neighboring garden areas and 6.29 m to 18.58 m in the backyard areas (Figures 4-6).

- At h = ± 6 solar hour, the north facing façades of all buildings in the plots are under the influence of the sun rays coming from the side.

- Between the hours of h = 0 and h = ± 5, the façades of the buildings facing north, where the southern façades of the buildings on the zoning island are under the influence of the sun, are over-shaded.

The shadings between h = ± 3 and h = ± 6 create shading lengths of 4.84 m to 15.53 m on the building surface of the neighboring garden and 3.55 m to 15.15 m on the building surface in the backyard (Figures 5-7).

When Figure 13 is examined, it may be observed that the issues mentioned in Figure 12 apply here.
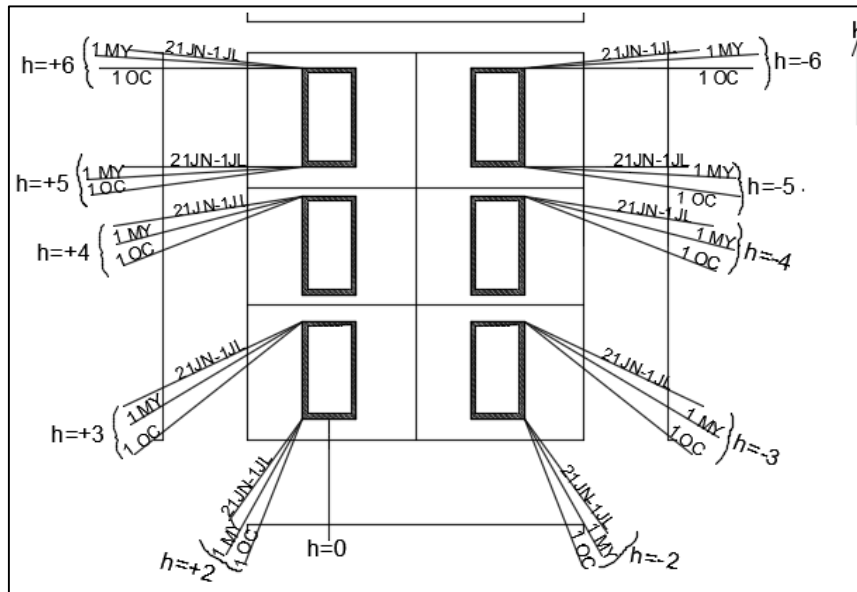

Figure 12-Shading-brightness effects of sun rays in buildings at various values of the solar azimuth angle when the façade of the reconstruction island is in the north-south direction (JN: June, JY: July, MY: May, OC: October).
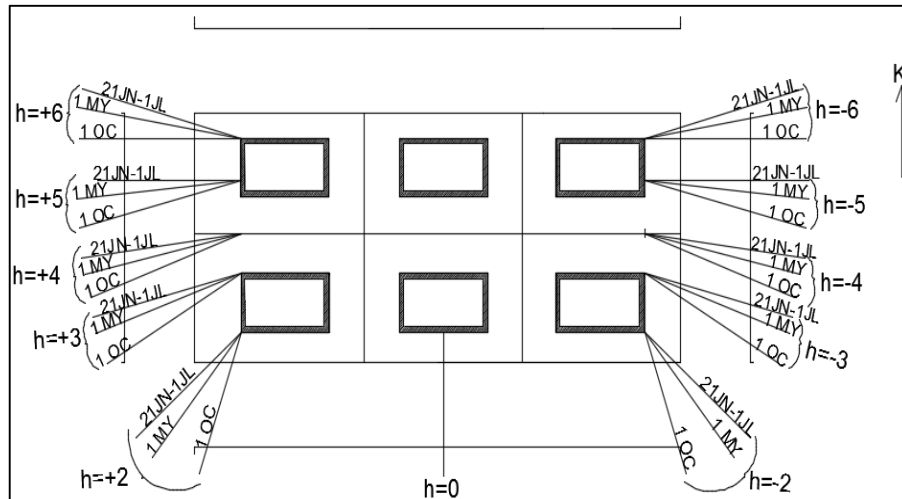
Figure 13-Shading- brightness effects of solar rays on buildings at various values of the solar azimuth angle when the façade of the reconstruction island is in the west-east direction.

6. DISCUSSION

If the front and rear façades of buildings are positioned in the west-east direction between May 1 and October 1, the following situations may be considered:

- At h = ± 6, the façades of the buildings facing north in the parcels are under the influence of the sun rays coming from the side, and the rear façades of the buildings are in the shade.

- Between h = ± 3 and h = ± 5, the side façades of the buildings in the parcels, which are generally closed, and the south facing façades of the buildings are exposed to sunlight. The façades of the buildings facing north (the façades of the buildings located in the north of the zoning island and the façades of the buildings in the south of the zoning island) remain in the shade.

- Between the h = 0 and h = ± 2, the south facing façades of the buildings in the zoning island are exposed to sun rays. The north-facing façades of the buildings remain in the shade.

Between 1 May and 1 October, when the front and rear façades of the buildings are positioned in the north-south direction, the following conditions occur:

- At h = ± 6, the north side of the buildings in the parcels and the generally closed side façades are under the influence of the sun rays coming from the side. The façades of the buildings and the south-facing façades are in the shade.

- Between h = ± 3 and h = ± 5, the façades of the buildings in the parcels and the south-facing side façades are exposed to sunlight, and the back façades of the buildings are in the shade.

- Between h = 0 and h = ± 2, the south-facing façades of the buildings in the parcels, i.e. the buildings in the south of the island, are exposed to sunlight. The north-facing façades of the buildings are in the shade.

If the front and back façades of the buildings are located in the west-east direction, according to the positioning of the buildings in the north-south direction, the front and back façades are exposed to less sun hours and more shade (Van Moeseke et. al., 2007).

7. CONCLUSIONS

1-From 1 May to 1 October in sunny weather, depending on the solar azimuth angle and the solar height of the sun, the lengths of the shadings formed by the buildings in the discrete structure of a zoning island in Adana are described below:

a-The shadings are formed between the h = 0 and h = ± 2 sun hours in the neighboring garden areas and between the h = ± 3 and h = ± 6 sun hours on the surfaces of the neighboring parcel.

b-The shadings are formed between the h = 0 and h = ± 3 sun hours in the backyard areas and the h = ± 4 and h = ± 6 sun hours on the building surfaces in the rear parcel.

c-The shadings are formed between h = 0 and h = ± 3 in the front yard areas and h = ± 4 and h = ± 6 sun hours on the building surfaces in the rear parcel.

d- The shadings are formed precisely between h = 0 and h = ± 3 in the front yard areas and partly at h = ± 4 h (between May 15 and August 1) between h = ± 5 and h = ± 6 and at h = ± 4 hours (May 1, August 15 to October 1).

2-The shading length changes in the sun hours mentioned above are described below:

a-The length of the shading formed in the neighboring garden areas is between 3.74 m and 18.34 m. The length of the shading formed on the adjacent building surfaces is 4.91 m to 15.34 m from the ground.

b-The length of the shading formed in the backyard areas is between 3.83 m and 18.58 m. The length of the shading formed on the rear building surfaces is 3.55 m to 15.14 m from the ground.

c-The length of the shading formed in the front yard areas is between 3.74 m and 25.33 m. The length of the shading formed on the rear building surfaces is 0.71 m to 14.98 m from the ground.

d-The length of the shading formed in the side garden areas is between 3.83 m and 18.58 m. The height of the shading formed on the rear building surfaces is 2.67 m to 15.10 m.

3-If the front and rear façades of the buildings are located in the west-east direction, according to the positioning of the buildings in the north-south direction, the front and rear façades are exposed to less sun hours and more shade.

4-If the front and rear façades of the buildings are located in the west-east direction, the following points arise:

a- At h = ± 6, the façades of the buildings in the parcels facing north are under the influence of the sun rays coming from the side, and the rear façades of the buildings are in the shade.

b-Between h = ± 3 and h = ± 5, the façades of the buildings, which are generally without windows, and the south facing façades are exposed to sunlight. The façades of the buildings facing north (the façades of the buildings located in the north of the zoning island, the façades of the buildings in the south of the zoning island) remain in the shade.

c- Between h = 0 and h = ± 2, the south-facing façades of the buildings in the parcels, i.e. the buildings in the south of the island, are exposed to sunlight. The north-facing façades of the buildings are in the shade.

REFERENCES

Abood, A. A. (2015), "A Comprehensive solar angles simulation and calculation using Matlab", International Journal of Energy and Environment (IJEE), Volume 6, Issue 4, pp. 367-376.

Al-Sareef, F. M., Oldham, D. J., Carter, D. J. (2001), "A computer model for predicting the daylight performance of complex paralel shading systems," Building and Environment, n: 36; 605-18.

Anderson, J.M. and Mikhail, E.M. (1998), "Surveying theory and practice", 7th ed. Boston, MA: Mc Graw Hill.

Arumı-Noe, F. (1996), "Algorithm for geometric contruction of an optimum shading", Automation in Construction, n: 5; 211-7.

Atabek, E. (1996), "Computer aided shadowing effect analysis of buildings", Yüksek Lisans Tezi, Mimarlık Bölümü, ODTÜ, Ankara.

Bannister, A., Raymond, S. and Baker, R. (1998), "Surveying". 7th ed. Harlow, UK: Addison Wesley Longman Limited Edinburg Gate, 81–82.

Capeluto, G.I., Yezioro, A., Shaviv, E. (2003), "Climatic Aspects in Urban Design: A Case Study", Building and Environment, Vol.38, Issue 6, pp.827-83.

Data G. (2001), "Effect of fixed horizontal louver shading devices on thermal performance of building by TRNSYS simulation", Renewable Energy, n: 23; 497-507.

Erdem, N., and İnce, H. (2016), "The Proposal Of The Building Application For More Benefiting From Solar Light", International Journal of Engineering and Geosciences, 1 (1), 7-14. DOI: 10.26833/ijeg.285215

Ekercin, S, Orhan, O, Dadaser-Celik, F. (2019), "Investigating Land Surface Temperature Changes Using Landsat-5 Data And Real-Time Infrared Thermometer Measurements at Konya Closed Basin in Turkey", International Journal of Engineering and Geosciences, 4 (1), 16-27. DOI: 10.26833/ijeg.417151

Farr, D. (2008), "Sustainable Urbanism: Urban Design with Nature", Wiley, New Jersey.

Kuşak, L, Küçükali, U. (2019), "Outlier Detection of Land Surface Temperature: Küçükçekmece Region", International Journal of Engineering and Geosciences, 4 (1), 1-7. DOI: 10.26833/ijeg.404426

İnce, H., and Erdem, N. (2018), "Gün Işığından Azami Yararlanacak Şekilde Yapılacak Binalar İçin Alan Tasarrufu Bakımından Parsel Konumunun Araştırılması", Mühendislik Alanında Akademik Araştırmalar, ISBN.978-605-288-390-7, www.gecekitapligi.com, s.143-161, Ankara.

Mcmullan, R. (1990), "Environmental Science in Building", Macmillan, Hong Kong.

Ok, V. (1992), "A procedure for calculation cooling load due to solar radiation: the shading effects from adjacent or nearby buildings", Energy and Buildings, Vol.19, 11 – 20.

Oktay, D. (2004), "Urban Design for Sustainability: A Study on the Turkish City", International Journal of Sustainable Development and World Ecology, 11/1, March, 24-35.

Olgyay, V. (1957), "Solar Control and Shading Devices", Princeton University Press, Princeton.

Selim, S, Demir, N. (2019), "Detection of Ecological Networks and Connectivity With Analyzing Their Effects on Sustainable Urban Development", International Journal of Engineering and Geosciences, 4 (2), 63-70. DOI: 10.26833/ijeg.443114

Soler, A., Oteiza, P. (1997), "Light self-performance in Madrid, Spain", Building and Environment, (32:2) 87-93.

Som, T. and Pathak, R. (2015), "Maximum Solar Power Generation through Optimization of Tilt Solar Angles of Solar Panels by Heuristic Technique", International Journal of Innovative Research in Electrıcal, Electronics,

Instrumentation and Control Engineering, DOI 10.17148/IJIREEICE.2015.3409, Vol. 3, Issue 4, April.

Szokolay, S.V. (1980), "World Solar Architecture", John Wiley and Sons Inc, New York.

Tavares, P.F.A.F. and Martins, A.M.O.G. (2007), "Energy Efficient Building Design Using Sensitivity Analysis: A Case Study", Energy and Buildings, Vol.39, pp.23-31.

Van Moeseke, G., Bruyère I., De Herde, A. (2007), "Impact of control rules on the efficiency of shading devices and free cooling for office buildings", Building and Environment (42:2) 784-93.

Yeang, K. (1995), "Design with Nature: The Ecological Basis for Architectural Design", McGraw-Hill, New York.

Yüceer, N. S. (2010), "Gölge Elemanı Tasarımına Bir Yaklaşım Ve Adana Örneği", METU JFA 201/2, 27:2 1-3, DOI:10.4305/METU.JFA.2010.2.1, s.1-12,

Yüceer, N. S. (2011), "Gölgelenme Elemanlarının Önemi ve Adana Üzerine Bir Deneme", Ekoloji Mimarlık, Güney Mimarlık, TMMOB Mimarlar Odası Adana Şubesi Yayını, sayı 6, s. 54-56, Adana

COMPLEXITY MEASURES OF SPORTS FACILITIES ALLOCATION IN URBAN AREA BY METRIC ENTROPY AND PUBLIC DEMAND COMPATIBILITY

Serdar Bilgi [1]*, Ayse Giz Gulnerman [1], Birgul Arslanoglu[2], Himmet Karaman[1], Ozge Ozturk[3]

[1] Istanbul Technical University, Civil Engineering Faculty, Department of Geomatics Engineering, Istanbul, Turkey
(bilgi/gulnerman/karamanhi@itu.edu.tr); **ORCID 0000-0002-8396-3202, ORCID 0000-0002-9163-6068,
ORCID 0000-0003-0507-6920,**

[2] Istanbul Technical University, Department of Physical Education, Istanbul, Turkey
(demirkolb@itu.edu.tr); **ORCID 0000-0003-4923-3561,**

[3] Yildiz Technical University, Civil Engineering Faculty, Department of Geomatics Engineering, Istanbul, Turkey
(ozgeo@yildiz.edu.tr); **ORCID 0000-0002-9017-9651**

ABSTRACT: Sports has an important role for the health of present societies and the next generations as an element of urban design. Sports facilities have strong effects on the social life in urban areas. The facilities supply the communication between the dynamics of the cities and generate synergy in the city life of people interacting with each other for improvement in their lives. Before the construction of the sports facilities, the planners must evaluate the type and size of them in terms of the population of the whole city and, the population of neighboring settlement areas, which use the facility. Entropy can be used as a criterion for the quantitative measure of spatial information on maps. In the study, the location of the sports facilities in Istanbul are compared by using the entropy as a quantitative criterion. As a result, the success of the location selection for the sports facilities in urban areas are estimated by using the entropy as a component. Metric entropy method and applications were carried out by a case study in the city of Istanbul for defining the spatial distribution of sports facility locations with the posts of people including "sports" and sports-related keywords on social media.

Keywords: Metric entropy, Urban complexity and spatial distribution, Social media data, Volunteered geographic information (VGI)

1. INTRODUCTION

In the "The Culture of the Cities" by Lewis Mumford, the city is defined as; the space where diverse behaviors and expectations on the perspectives of life infiltrate into the same point, with advantages of both social efficacy and relevance as well as where personal practice reformed with symbols, terms of conducts and legal regulations (Mumford, 1938). Adams (1935), states city and town planning as "a science, an art, and a movement of policy concerned with the shaping and guiding of the physical growth and arrangement of towns in harmony with their social and economic needs''.

Cities with a population over 10 million are generally called as megacities. According to the United Nations (UN) data, there were 45 cities with populations between 5 and 10 million and 31 megacities worldwide in 2016. In the UN report, the number of megacities is extrapolated to increase up to 41 until 2030. Whereas 23% of all population of the world lived in urban areas in 2016, extrapolated results indicate that 27% of global population will center in cities with at least 1 million population (United Nations, 2016).

Urban areas should be designed aesthetically, sustainably, interactively and sufficiently to advance the public life standards. The rapid growth of the urban population increases the pressure on human life, living in the urban since this population flow has triggered the needs of housing with no previous expectation. This kind of growth has made urban areas full of buildings without planning and infrastructure. While population has grown in the urban areas, public life standards and health have been an outstanding issue in local, national and global levels. People living in the city tend to get away from the city and integrate with nature as they find the opportunity to keep away from stress in terms of current living conditions and their effects (Kuşçu et al., 2018). However, sports facilities have substantial positive impacts on the social life of public in urban areas, supplying the communication, in addition to generating synergy in the city life by establishing better, healthier community in which people are socializing with each other. Technological developments increase every day. Especially communication technologies have developed extraordinarily for last 30 years and still developing making it easy to access worldwide information and sources of information (Iscan and Ilgaz, 2017).

Land-use is one of the essential issues in the human impact on the environment. Land-use planning is the design of valuation assets over potentials of land and water, the considerations of replacements in order to choose and implement socioeconomically best options (Food and Agriculture Organization of the UN, 2016). The function of land-use planning by assessing and overviewing all potentials is to ensure supplying the needs of public and preserving resources for future (De Wrachien, 2003). Elements of urban design including "Land-use," "Community design," and "Transportation design" noticeably affect the local quality of air and water supply as well as traffic safety and physical activity. The industrial revolution fostered rapid population growth in cities thanks to a ubiquitously increasing number of manufacturing industries in the 19th century. These cities with unrestrainedly growing population required sanitary infrastructures to overcome the inextricable masses. Therefore; land-use planning management became important (Schilling, and Linton, 2005).

Planning for sports facilities involves reserving land for open space with built facilities and consideration of how such amenities will be develop (Food and Agriculture Organization of the UN, 2016). Nowadays, sports as a multiple-sided and continually changing activity has coalesced in the modern lifestyle of urban society. Since the 1950's, there is a constant growth in sports participation in many European countries. In some countries, growth has stabilized (Van Bottenburg et al., 2005). This affects urban planning by the construction of various sports facilities and open (sports) parks in many cities.

According to Chapin (2002), sports facilities have an extensive variety of favorable and adverse impacts on their neighboring areas and cities on a broader scale. Their impacts would be considered as social, physical, safety and even political, economic, legal and environmental issues. Because a simple facility with the capacity of a few hundred people with sports facilities design the social fabric part together with the town hall and buildings of religions and serve to a small local community. The categories of sports facilities in his study are comprised of several outdoor recreational areas, courses to the indoor arena, dome, and single or multipurpose amenities (Chapin, 2002).

European Commission (2007) states within the last two decades, land-use, globalization and rapid growth of urban area in undeveloped and developing countries underline the significance of sports and sports amenities. Government and social institutions highlight the positive effects of sports on health, as well as the importance of social compliance. In contemporary political discourse, sports are investigated not only regarding its economic effect but also concerning its potential for struggling with poverty, unemployment, crime, and discrimination (Collins, 2014). Besides, Campbell and Harrison (1999) declare that sports would contribute to life quality of both individuals and communities, improve health, boost social unity, encounter anti-sociality, and promote individual self-regard and self-assurance.

Sports have become necessary to prevent health problems and to maintain a healthy life. So, it is recommended to all citizens by all relevant institutions and relevant authorities. UN has seen sports as a tool for "development" and "peace." So, they support a task force to enhance the society and sports connection and in 2005 report this mission was denoted as the relation between sports and health, education, sustainable development, peace, communication, partnerships (UN Inter Agency, 2005). As in the world, the number of people doing sports in Turkey is increasing day by day. Especially the metropolitan municipalities have built many sports facilities in order to meet the demand of the people in cities. In these mega cities, sports facilities are seen as a place of socialization as well as for sports.

There are different approaches to the sports facilities within the urban areas. That is why a comprehensive literature review from the regulations of sports areas within the spatial planning codes and blueprints that have been developed by different city planning organizations embedded in the study. The codes and regulations are based on the suitability of the minimum values of the formulas or urbanization conditions. However, the critical case is to observe the consequences of the formulas and conditions on how they contribute to public

demand.

Volunteered Geographic Information (VGI) is a way to understand public demands which are primarily and terminologically depends on Public Participation (PP) with Geographic Information Systems (Gulnerman and Karaman, 2015; Sieber, 2006). VGI is a newer terminology than the PP- Geographic Information Systems (PPGIS). In addition to the severity of empowering NGO, populist groups and rest of the organizations are based on communities, to increase the contribution of the public in defining policies is the use cases of GIS which are implied by PPGIS (Sieber, 2006). The idea behind it explained by Anderson (Anderson, 1995) with one of the urban planning approach consulted by Public Participants. Public participation has evolved in time with the technology like the invention of web 2.0 and GNSS within smartphones (Goodchild, 2007). The terminology of this participation also has evolved by this technology. Citizen science, neo-geographers, and volunteers are some of these participators [Ball, 2002; Goodchild, 2009; Tulloch, 2008].

In this study, the demand for sports facilities is tested with social media, and Twitter users' spatial data related to sports contents used as demand dataset. Social media data which become highly available can be used to make predictive models for sports events (Ristea, 2018). Twitter has been chosen for this study due to the reason that this social media platform exceeds 28 million active users in Turkey which is one-quarter of the total population of the country (Statista, 2016). As a consequence of the number of users (participators), platforms provide the excessive data source for participation projects which is supported by unconscious volunteers (Gulnerman et.al, 2016; Shekhar, 2015).

2. MATERIALS AND METHODS

2.1 Metric Entropy Method and Its Relation about Sports Facility and Implementation

Entropy, briefly defined as the measure of the indefiniteness of a system, is also the second law of thermodynamics. This measurement is explicitly connected to information content and in association with the quantification of information transfer attempts within a communication system (Fairbairn, 2006).

Maps are giving us a picture of the environment, and since the early ages, they have been used as the abstraction of the real world for thousands of years. The description of cartographic representations can be defined with the term "complexity," considering the general nature. There have been many attempts with practical testing to measure the complexity of the literature. These studies date the back the too late 1940s by Shannon (1948) and Shannon et al. (1951) which is named as information theory and was carried out to communication theory.

The first study adopting entropy to cartographic communication for quantitative measurement of map information has been done by Sukhov (1967; 1970). Statistics of the different types of symbols used on the map taken into account. Numbers of each type of symbols are taken into consideration. Information is modeled as a probabilistic process in these studies. Entropy is computed as follows Eq. (1), assuming X, the random message variable, $P_1, P_2, \ldots P_i, \ldots P_n$ are the probabilities of different message choices;

$$H(X) = H(P_1, P_2, \ldots, P_n) = -\sum_{i=1}^{n} P_i * \ln(P_i) \qquad (1)$$

A new method for calculating the topological information of the map is suggested by Neumann (1994). The method is two-staged, classifying the vertices due to their neighboring relations and forming a dual graph, then computing the entropy. The entropy of the map is calculated as follows Eq. (2), assuming N: the total number of the symbols, M: number of symbol types and Ki: number of symbols for an ith type. Then and the probability for each type of symbols is: where P_i is the probability of ith symbol type, i =1, 2, …. M.

$$H(X) = H(P_1, P_2, \ldots, P_M) = -\sum_{i=1}^{M} P_i * \ln(P_i) \qquad (2)$$

Later on, Bjørke (1996) questioned the usefulness of such topological information and compared maps in different scale and design, in order to evaluate the information on maps quantitatively. Metrical entropy method is introduced considering the variation of the distances between the map objects. n is the number of objects, S is the whole area tessellated by S_i where S_i is the Voronoi regions of each sports facility (i=1, 2, ... n^{th}), P_i is the probability ($P_i = \frac{S_i}{S}$) and the entropy H(M) was defined as Eq. (3) given below:

$$H(M) = H(P_1, P_2, \ldots, P_n) = -\sum_{i=1}^{n} \frac{S_i}{S} * (lnS_i - lnS) \quad (3)$$

The concept of occupied space by objects in the map is related to the metric information. As the space occupied by the objects are approximately equal on the map, the information contained on the map will increase. Otherwise, the amount of information will decrease. So, the probability can be significant for the determination of entropy by using the ratio between the Voronoi region of the map and designated part of the area (Li and Huang, 2002).

Forming the mosaics on the map will be the most suitable solution to determine the occupied spaces by the objects and these regions will contain all of the objects in the map. The most appropriate method for this solution is the Voronoi diagrams (Lee et.al, 2000).

2.2 Voronoi Diagrams

The earliest documented knowledge about Voronoi diagrams is dated back to two scientists who lived in the Renaissance period: Johannes Kepler (1571-1630) and Ren´e Descartes (1596-1650). Descartes used the Voronoi diagrams to confirm that the distribution of matter in the universe, forms vortices centered at fixed stars. Moreover, Voronoi and Delaunay tessellations generated by integer lattices had been introduced by Kepler. Mathematician Johann Peter Gustav Lejeune Dirichlet (1850), created some of his seminal work on quadratic forms. Following earlier ideas by Kepler and Carl Friedrich Gauss, he considered Voronoi partitions of space are caused by integer grid points as sites (Liebling, 2012). Voronoi diagrams are also called Dirichlet tessellations or Wigner-Seithz (Watson, 1994; Sukumar et.al, 2001). The Voronoi diagrams investigation is extended to a higher dimension by Voronoi's studies

(Voronoi, 1908; 1909). A Voronoi diagram is a 2-D plane divided into the polygonal regions. Each of these regions is associated with a specific map object. The associated region with this characteristic is the locus of points closer to that object than to any other map objects (Li and Huang, 2002).

3. CASE STUDY

The study aims to test the sports facility supply in the urban area. For this purpose, the authors assessed the distribution of sports facilities by social media data. Metric entropy method is used as a norm for the quantitative measure of spatial information on maps. This paper also evaluated the location of the sports facilities by using such a quantitative norm. This method experimented with a case study, studied in Istanbul for defining the spatial distribution of the sports facilities. First of all, the existing sports facilities were overlaid by districts of the city of Istanbul. Then, Voronoi diagrams were created for the sport facility locations and metric entropy calculations were carried out.

The third step of the case study was to determine the sport facility users' demands by using the geo-referenced social media data. As a result, the demands of the users were measured by selecting the sports facility locations in relation with the district. These measures represent the consistency between the selected locations in districts and user needs in a scientific manner.

In order to determine the public need for sports facilities, Twitter tweets with location information were used. The tweets in May 2016 in the bounding box of Istanbul is filtered through Twitter Streaming API using Java-based Geo Tweets Downloader tool and stored into PostGIS database (Gengeç, 2015).

Social media data has been accepted as the demand of society. In this study, citizens who tweeted about a kind of sports, having texts such as "football," "basketball," "fitness," "swimming," "tennis" etc. are filtered and used in the spatial analysis. Such tweets meant a relation with sports and assumed that there is demand for it. There were more than 870.475 of tweets (maximum 40.507 tweets on 15.05.2016 and minimum 22.633 tweets on 27.05.2016) during the identified time interval, and 6710 of them were determined to be related to sports. Social media data used, "number of total tweets by day" and "number of sports tweets by day" can be seen in Table 1 and Figure 1(a) and 1(b). The number of total tweets and number of the sports facility in the districts of Istanbul city are shown in Table 2.

Table 1   Number of total tweets and number of sports tweets by day.

Date	Tweet	Date	Sports Tweets
01.05.2016	31161	01.05.2016	740
02.05.2016	26602	02.05.2016	184
03.05.2016	25953	03.05.2016	153
04.05.2016	26844	04.05.2016	231
05.05.2016	27090	05.05.2016	174
06.05.2016	29717	06.05.2016	158
07.05.2016	35742	07.05.2016	206
08.05.2016	35658	08.05.2016	122
09.05.2016	27119	09.05.2016	164
10.05.2016	25940	10.05.2016	170
11.05.2016	26862	11.05.2016	156
12.05.2016	27136	12.05.2016	149
13.05.2016	29869	13.05.2016	159
14.05.2016	35182	14.05.2016	160
15.05.2016	40507	15.05.2016	640
16.05.2016	28575	16.05.2016	152
17.05.2016	25682	17.05.2016	159
18.05.2016	27752	18.05.2016	294
19.05.2016	34798	19.05.2016	457
20.05.2016	28735	20.05.2016	148
21.05.2016	27475	21.05.2016	109
22.05.2016	25588	22.05.2016	110
23.05.2016	23775	23.05.2016	140
24.05.2016	23875	24.05.2016	144
25.05.2016	23664	25.05.2016	364
26.05.2016	23109	26.05.2016	128
27.05.2016	22633	27.05.2016	371
28.05.2016	28578	28.05.2016	94
29.05.2016	28373	29.05.2016	92
30.05.2016	23473	30.05.2016	105
31.05.2016	23008	31.05.2016	125
Total	**870475**		**6558**
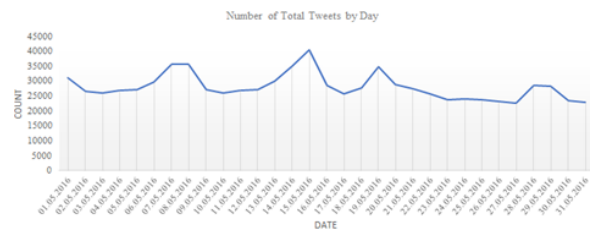
(a)
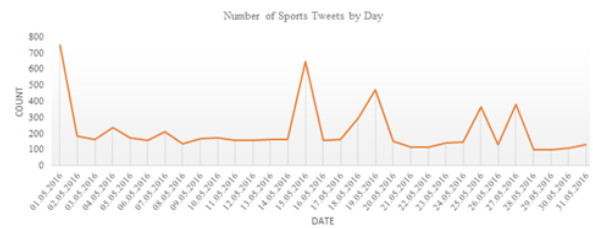
(b)

Figure 1(a) Number of total tweets and the number of sports tweets 1(b) number of sports tweets by day

144

Table 2 Number of total tweets and number of sports tweets by the districts.

Districts	Tweet	Tweet Entropy	Sports Facility	S. Facility Entropy
Adalar	10	0.7729	8	0.9388
Arnavutkoy	8	0.5873	6	0.3166
Atasehir	1062	0.8966	7	0.3151
Avcilar	91	0.8921	5	0.4709
Bagcilar	88	0.6601	5	0.9040
Bahcelievler	105	0.5072	11	0.6510
Bakirkoy	267	0.6389	11	0.8044
Basaksehir	176	0.8652	5	0.5822
Bayrampasa	66	0.6490	9	0.3872
Besiktas	720	0.9381	7	0.7828
Beykoz	136	0.7703	10	0.7967
Beylikduzu	40	1.0000	2	0.8265
Beyoglu	118	0.8932	10	0.4042
Buyukcekmece	46	0.7287	9	0.7736
Catalca	6	0.2629	6	0.0000
Cekmekoy	49	0.6554	5	0.7186
Esenler	45	0.7218	3	0.7603
Esenyurt	97	0.8237	6	0.4387
Eyup	134	0.6453	16	0.4595
Fatih	200	0.7846	11	0.5401
Gaziosmanpasa	33	0.5636	10	0.5019
Gungoren	76	0.4978	5	0.8404
Kadikoy	1139	0.9417	9	0.7751
Kagithane	99	0.9602	5	0.9178
Kartal	63	0.7021	10	0.7800
Kucukcekmece	102	0.5552	12	0.5769
Maltepe	172	0.9024	4	0.4453
Pendik	89	0.6122	17	0.8184
Sancaktepe	23	0.5623	8	0.4511
Sariyer	195	0.7900	18	0.7694
Sile	6	0.6687	2	0.3810
Silivri	19	0.5107	8	0.5449
Sisli	604	0.8402	6	1.0000
Sultanbeyli	15	0.5168	5	0.6901
Sultangazi	32	0.6218	6	0.9552
Tuzla	37	0.7204	3	0.8713
Umraniye	155	0.6241	9	0.8806
Uskudar	188	0.7741	12	0.8298
Zeytinburnu	47	0.7561	8	0.2319

Istanbul Metropolitan area has 309 units for sports facilities allocated to 39 districts of Istanbul city. All the sports facilities within the districts were presented in dot map format in Figure 2 and shown in a clustered column chart in Figure 3. Every dot represents one sports facility in Figure 2. Districts that have the most supply for sports facilities are Eyup, Sariyer, and Pendik. The districts which have the second highest supply class are Bahcelievler, Bakirkoy, Fatih, Kucukcekmece, and Uskudar.
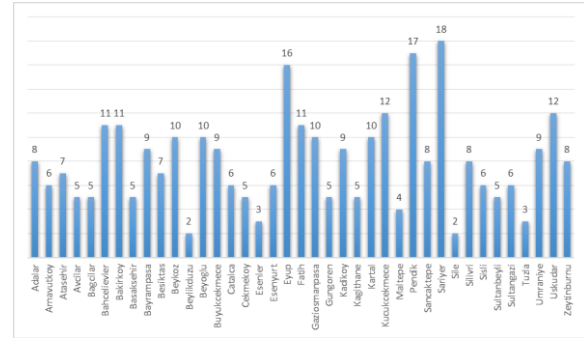

Figure 2 Distribution of sports facilities

Figure 3 Number of Sports Facilities by Districts

The tweets having texts such as "football", "basketball", "fitness", "swimming," "tennis" etc. were presented in a dot map format in Figure 4 and shown in clustered column chart in Figure 5. Every dot represents a single tweet in Figure 4. The most sports-related tweets are determined within the boundaries of Atasehir, Besiktas, Kadikoy and Sisli districts.
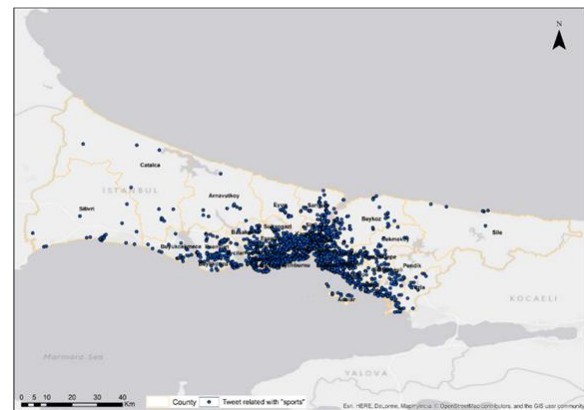

Figure 4 Distribution of tweets.

Figure 5 Number of sports related tweets by the districts

Distribution of both sports facilities and people's tweets on sports respectively as supply and demand have been mapped above according to their counts in related districts. However, there is no consideration for the location of the sports facilities and tweets if those are not involved in the same district's boundary even though, those have more capability to supply due to proximity.

Metric entropy method is useful for considering the impact areas of each sports facilities. The results of entropy within the districts have been spatially joined, then mapped as five natural break classes and presented in choropleth map format with the light to dark tones of red color in Figure 6.

Except for spatial distribution of the tweet demands for the sports facilities, the entropy of the demands for sports determined. This method helped to visualize, which districts require more supply as sports facilities. By considering this, each tweet has its Voronoi area and entropy value without district boundary, the value of total entropy has been calculated for total Voronoi areas including each district and shown in Table 2. Entropy values of tweets related to sports were classified and presented in choropleth map and shown in Figure 7 with light to dark tones of blue color.

Accordingly, in Figure 7, the districts with highest needs to sports facilities are expressed in blue color, which are Atasehir, Avcilar, Besiktas, Beylikduzu, Beyoglu, Basaksehir, Kadikoy, Kagithane, and Maltepe.
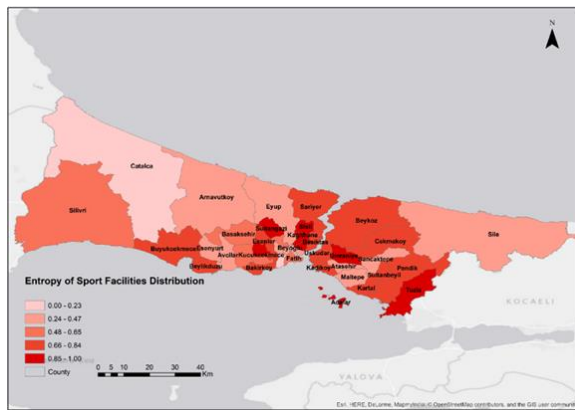

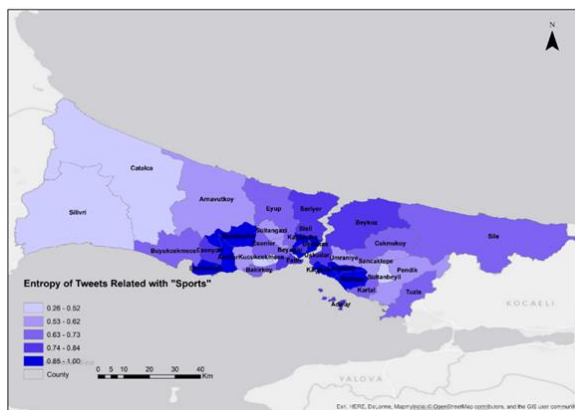Figure 6 Entropy of sports facilities respect to districts

Figure 7 Entropy of tweets related to sports respect to districts of Istanbul.

The results in Figure 6 and Figure 7 show the unbalanced distribution of sports facilities based on demand and supply. In addition to that, Figure 8 shows both entropy values and differences between tweet entropy and sport facility values. Evaluation of all these results is mentioned in "Conclusion and Outlook" section.
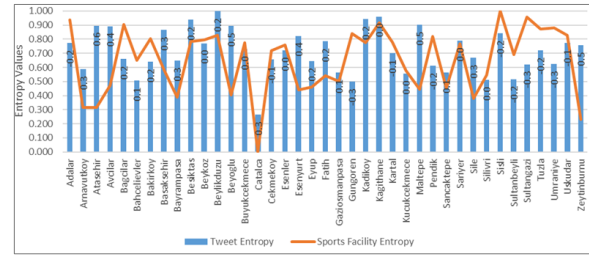

Figure 8 Differences between tweet entropy and sports facility entropy values

4. RESULTS AND DISCUSSION

Sports facility distribution in the urban design as an affecting manner of the daily routine may stimulate and change the lifestyle of the related society. Therefore, the design should contribute to and increase the demand for sports in society. As stated in the earlier sections, sports facilities in the urban environment play a significant role in the health of society, as much as on individual health. Sports facility distribution in the urban area has various essential effects to the region like the economy. The example of the UK in 2015 provides an essential outcome for the effects of a sports facility on the country's economy. Inactivity of British society has adverse effects on the economy where low activity has cost National Health Service around £7.4 billion annually (Sport, 2015).

As illustrated in Figure 8, a new result was obtained by calculating the difference between tweet entropy and sports facility entropy values. Thus, tweet entropy columns and sports facility columns overlaid. According to the results of this analysis, it can be interpreted whether the sports facilities are sufficient and whether they are located in significant locations. If a district has a low entropy value of sports facility, existing sports facilities are homogeneously located in that district. Similarly, low tweet entropy values indicate that the tweets for sports facility are homogeneously distributed to the district. When a district has both same grade sports facility and tweet entropy values, sports facilities in the district meet the demands and facilities located on significant locations. On the other hand, if the difference value is negative, locations of tweets are homogeneously distributed in the district meaning the sports facilities demanded from the homogeneously distributed people in the district, but the locations of sports facilities are not distributed homogeneously. So, these sports facilities are located in a narrow part of the district, which is not related to tweet locations, and they are away from the people tweeting.

On the contrary, when the difference value is positive, even if sports facilities are homogeneously distributed, it can be understood that there are not enough people searching for sports facilities in near of these sports facilities. In such a case, locations of the sports facilities are not suitable/significant for the people demands. In summary, it can also be understood that the locations of sports facilities cannot be successfully be determined when the difference is positive or negative. Moreover, increasing the absolute value of the difference is the indication of the disunity between locations of demands and sports facilities.

5. CONCLUSION

In this paper, the importance of sports facilities in an urban area and the needs of an active society have been evaluated and analyzed. The current distribution of sports facilities in Istanbul was evaluated by combining four scientific approaches of urban design, entropy, social media, and geographic information. Moreover, urban design principles and regulations for the sports facilities have been studied and summarized as an element of social infrastructure areas based on spatial planning code of Turkey. Metric entropy method was used as a criterion to compare the location of the sports facilities. This method can be an essential component in estimating the success of a project or site plan including the location of sports facilities in the district. Thus, existing or planned sports facilities can be evaluated by the method, and significant results could be obtained and discussed.

Based on the findings of this study, a different approach for the determination of the locations of sports facilities regarding of the community demands has been introduced. These findings will provide a useful basis for further researches. Metric entropy method can contribute to planning activities for future investment on sports facilities. Additionally, it may lay a foundation for the other metropole cities, where living millions of people are living and maybe an essential criterion for sports activities that will affect thousands of people.

REFERENCES

Adams, T. (1935). Outline of town and city planning: A review of past efforts and modern aims. Russell Sage Foundation.

Agriculture Organization of the United Nations Interdepartmental Working Group on Land Use Planning. Guidelines for land-use planning. (1993). Food and Agriculture Organization of the United Nations.

Anderson, L.T. (1995). Guidelines for preparing urban plans. Planners Press, American Planning Association

Bale, J. (2002). Sports geography. ISBN 0419252304, Routledge, Taylor & Francis Group, NY-USA.

Ball, M. (2002). Cultural explanation of regional property markets: A critique. Urban Studies, 39, 1453-1469.

Bjørke, J.T. (1996). Framework for entropy-based map evaluation. Cartography and Geographic Information Systems, 23, 78-95.

Campbell, J., (1999). Harrison S. Professional sports and urban development: A brief review of issues and studies, 21.

Coates, D., & Humphreys, B. R. (2003). Professional sports facilities, franchises and urban economic development. Public Finance and Management, 3(3), 335-357.

Collins, M. (2014). Sport and social exclusion. ISBN 978-0-415-56881-4, Routledge, Taylor & Francis Group, NY-USA.

Chapin, T. (1999). The political economy of sports facility location: An end-of-the-century review and assessment Marquette Sports Law Review, 10.

Chapin, T.S. (2002). Identifying the real costs and benefits of sports facilities. Citeseer.

Chapin, T.S. (2004). Sports facilities as urban redevelopment catalysts: Baltimore's camden yards and cleveland's gateway. Journal of the American Planning Association, 70, 193-209.

Davies, L.E. (2008). Sport and the local economy: The effects of stadia development on the commercial property market. Local Economy, 23, 31-46.

De Wrachien, D. (2003). Land use planning: a key to sustainable agriculture. In Conservation Agriculture (pp. 471-483). Springer, Dordrecht.

European Commission. (2007). White paper on sport.

Fairbairn, D. (2006). Measuring map complexity. Cartographic Journal 43, 224-238.

Gengec, N. (2015). Geotweet downloader.

Goodchild, M.F. (2007). Citizens as sensors: The world of volunteered geography. GeoJournal, 69, 211-221.

Goodchild, M. (2009). Neogeography and the nature of geographic expertise. Journal of location based services, 3, 82-96.

Gulnerman, A.G.; Karaman, H. (2015). In PPGIS case studies comparison and future questioning, Computational Science and its Applications (ICCSA), 15th International Conference on, IEEE: pp 104-107.

Gulnerman, A.; Gengec, N.; Karaman, H. (2016). Review of public tweets over Turkey within a pre-determined time. ISPRS Annals of the Photogrammetry, Remote Sensing and Spatial Information Sciences, 4, 153.

Iscan F, Ilgaz, A. (2017). Analysis of geographic/urban information system web presentations of local governments in Turkey, International Journal of Engineering and Geosciences, 2 (3), 75-83.

Kozma, G. (2014). The spatial development of sports facilities within the cities: A central European case study. Geosport for Society, Editura universităţii din Oradea, 1, 19-28.

Kozma, G.; Pénzes, J.; Molnár, E. (2016). Spatial development of sports facilities in Hungarian cities of county rank. In Bulletin of Geography. Socio-economic Series, Vol. 31, p 37.

Kuşçu Ş.Ç., Türk, T., Ödül, H. and Çelik, M.N. (2018). Detection of paragliding fields by GIS, International Journal of Engineering and Geosciences, 3 (3), 119-125.

Lee, Y.; Li, Z.; Li, Y. (2000). Taxonomy of space tessellation. ISPRS Journal of Photogrammetry and Remote Sensing, 55, 139-149.

Li, Z.; Huang, P. (2002). Quantitative measures for spatial information of maps. International Journal of Geographical Information Science, 16, 699-709.

Liebling, T.M.; Pournin, L. (2012). Voronoi diagrams and delaunay triangulations: Ubiquitous siamese twins. Documenta Mathematics, ISMP, 419-431.

Mumford, L. (1938). The culture of cities by Lewis Mumford. Harcourt, Brace and company: New York.

Neumann, J. (1994). The topological information content of a map/an attempt at a rehabilitation of information theory in cartography. Cartographica: The International Journal for Geographic Information and Geovisualization, 31, 26-34.

Ristea, A.; Kurland, J.; Resch, B.; Leitner, M.; Langford, C. (2018). Estimating the spatial distribution of crime events around a football stadium from georeferenced tweets. ISPRS International Journal of Geo-Information, 7, 43.

Sieber, R. (2006). Public participation Geographic Information Systems: A literature review and framework. Annals of the Association of American Geographers, 96, 491-507.

Sukhov, V. (1967). Information capacity of a map entropy. Geodesy and Aerophotography, 10, 212-215.

Sukhov, V. (1970). Application of information theory in generalization of map contents. International Yearbook of Cartography, 10, 41-47.

Sukumar, N., Moran, B., Yu Semenov, A., & Belikov, V. V. (2001). Natural neighbour Galerkin methods. International journal for numerical methods in engineering, 50(1), 1-27.

Schilling, J.; Linton, L.S. (2005). The public health roots of zoning: In search of active living's legal genealogy. American journal of preventive medicine, 28, 96-104.

Shannon, C.E. (1948). A mathematical theory of communication. Bell System Technical Journal, 27, 623-656.

Shannon, C.E.; Weaver, W.; Burks, A.W. (1951). The mathematical theory of communication (review). Philosophical Review, 60.

Shekhar, S. (2015). From GPS and Google Maps to spatial computing.

Sport England. (2015). Active design: Planning for health and wellbeing through sport and physical activity. Public Health England.

Statista. (2016). Number of monthly active Twitter users worldwide from 1st quarter 2010 to 3rd quarter 2015 (in millions).

Tulloch, D.L. (2008). Is VGI participation? From vernal pools to video games. GeoJournal, 72, 161-171.

Thornley, A. (2002). Urban regeneration and sports stadia. European Planning Studies, 10, 813-818.

UN Inter-Agency Task Force on Sport for Development and Peace. (2005). Sport as a tool for development and peace: Towards achieving the United Nations millennium development goals.

United Nations. (2016). The world's cities in 2016: Data booklet.

Van Bottenburg, M.; Rijnen, B.; W.J.H. Mulier Instituut, C.v.S.-W.S.; Sterkenburg, J.C. (2005). Sports participation in the European Union: Trends and differences. Arko Sports Media.

Voronoi, G. (1908). Nouvelles applications des paramètres continus à la théorie des formes quadratiques. Deuxième mémoire. Recherches sur les parallélloèdres primitifs. Journal für die reine und angewandte Mathematik (Crelles Journal), 198-287.

Voronoi, G. (1909). Nouvelles applications des paramètres continus à théorie des formes quadratiques. Journal für die reine und angewandte Mathematik, 67-182.

Watson, D.F.; Philip, G.M. (1984). Triangle based interpolation. Journal of the International Association for Mathematical Geology, 16, 779-795.

LAND SURFACE TEMPERATURE ANOMALIES IN RESPONSE TO CHANGES IN FOREST COVER

Behnam Khorrami [1*], Orhan Gunduz [2], Nilanchal Patel [3], Souad Ghouzlane [4], Mohamed Najar [5]

[1,4,5] Dokuz Eylul University, The Graduate School of Natural and Applied Sciences, Department of GIS, Izmir, Turkey
(Behnam.Khorrami/Mohamed.Najar@ogr.deu.edu.tr,); **ORCID 0000-0003-3265-372X, 0000-0002-9107-961X.**
(souad.ghouzlane@gmail.com), **ORCID 0000-0001-5781-5874**

[2] Dokuz Eylul University, Faculty of Engineering, Department of Environmental Engineering Izmir, Turkey
(orhan.gunduz@deu.edu.tr); **ORCID 0000-0001-6302-0277**

[3] Birla Institute of Technology Mesra, Department of Remote Sensing, Ranchi, India
(npatel@bitmesra.ac.in); **ORCID 0000-0003-1011-8419**

ABSTRACT: Land cover/use changes specially the forest cover changes affect the local surface temperature (LST) of the earth. In this study, a combination of remote sensing and GIS techniques was used to scrutinize the interactions between LST anomalies and deforestation in Sardasht County, NW Iran. The land cover/use change layers of the study area were extracted from Landsat satellite imagery based on Binary Encoding classification and change detection technique. The radiometric correction analysis were done for each Landsat image to derive LST map layers. According to the results, a descending trend in forest cover with a total 2560 ha decline in area and an ascending trend of about 4 degrees rise in surface temperature values on both forest and non-forest areas were detected in the study area from 1984 to 2017. The temporal and spatial analysis yielded high rates of reverse temporal correlation (-0.81) between forest areas and LST anomalies while the correlation value of 0.76 was found for non-forest areas and LST. The regression analysis of the values confirmed the correlation results to be trustable at 99 percent. It was also found that the deforested areas of the study area correlate with the LST rise spatially with a very high correlation (0.98) from which a tangible interaction of the parameters can be inferred.

1. Introduction

Land Surface Temperature (LST) is an important environmental parameter having valuable applications in different disciplines especially environmental sciences. Earth and environmental scientists take its benefit to monitor the interactions between surface temperature and climate conditions as there is a direct relation between climate change and LST variations. The variations in surface temperatures can also affect other important environmental phenomena like ice melting, drought, evapotranspiration, deforestation etc. Similar to human body temperature, the earth's surface temperature can be used as a diagnostic tool to detect and monitor arising challenges relating to rising surface temperatures. As LST changes impact soil moisture trends, some of the researchers have used this parameter to monitor and detect drought events in recent years (Karnieli et al ,2010; Son et al ,2012; Sruthi and Aslam ,2015; Arslan et al ,2016; Zhang et al ,2017; Gidy et al ,2018). Similarly, many researchers have recently focused on interactions between LST and landcover/landuse (LCLU) changes and confirmed that there is a clear correlation between surface temperature and land cover changes. For instance, Bakar et al (2016), applied three different indices to study the impacts of LCLU changes on LST and suggested that the NDVI, NDBI and MNDWI indices can be applied to monitoring land cover impacts on LST. Ding and Shi (2013), suggested that the development rate of Beijing Metropolis in China have led to the surface temperature increase of the city due to massive fast changes of land use. Amiri et al (2009) applied the Temperature Vegetation Index (TVI) to assess the interactions of LST and heat island of Tabriz city and recommended to use multi-temporal imageries to obtain better and more useful results. Xiao and Weng (2006) found that there is a strong agreement between surface temperature increases and built-up expansions. The direct implications of desertification and greenness loss on LST increase was confirmed by Entezari et al (2016). Manoharan et al (2009) analysed the deforestation rate and its impacts on regional temperatures and soil moisture and found very high correlation between NDVI, LST and soil moisture.

Sardasht is one of the green counties of Iran covered with Oak Forests which play a key role in social, economic and environmental sustainability of the western parts of the country. The combination of human interference in the nature of the region due to population growth in one hand and the widespread climate change impacts on the other hand, have put the health and existence of these resources in peril in recent decades. Since no study has been done in Iran West Forests regarding LST changes, the current study was designed to assess the status of land cover/use and surface temperature to see the now and then status of forest cover and LST values as well as the possible linkage between LST and deforestation/afforestation processes.

2. Materials and Methods
2.1. Study Area

Sardasht is one of the wooded counties of the country located between geographic coordinates of 45°13′48′′ to 45°42′00′′ E and 35°57′36′′ to 36°28′12′′ N in SW of West Azerbaijan province, NW of Iran (Figure1). It is a mountainous region with an average height of 1521m above sea level and is located on the green belt of oak forests in west of the country known as 'West Oak Forests' which sprawls from south to north. A moderate mountain climate dominates the local hydrometeorology of the area with an average precipitation of 724 mm/y and annual temperature of 13.3°C (Beygi Heidarlou et al., 2018). A concise information about the datasets are shown in Table 1. Remotely sensed images of different Landsat missions of NASA were downloaded from its online database (https://landsat.gsfc.nasa.gov/data/).
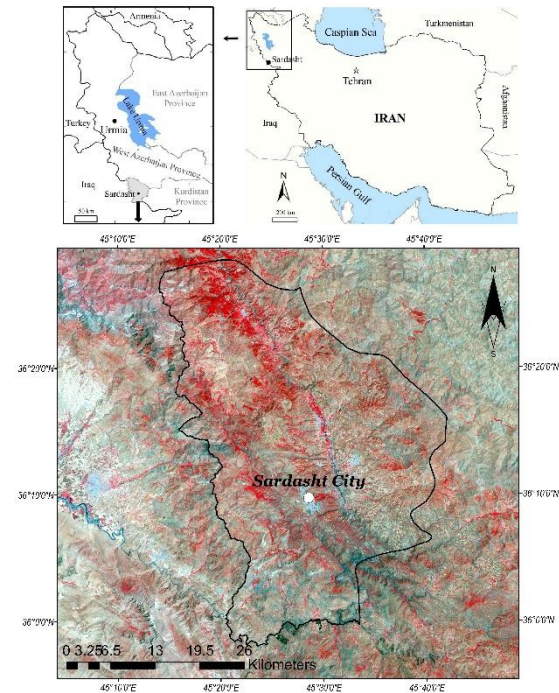

Figure 1. Geographic position of the study area (Landsat 8, 2016).

2.2. Digital Image Processing
2.2.1. Atmospheric Corrections

Satellite remote sensors are negatively influenced from atmospheric conditions (aerosols, clouds etc.) which lower the contrast of image features and harden the interpreter's task to detect real world features correctly. Since Landsat level-1 imageries are not corrected atmospherically, the images are first corrected for disturbing atmospheric conditions to pave the way for the commence of image classification procedure. In the current study, the Dark Object Subtraction (DOS) method was implemented for all the used imageries. DOS is an image-based method (Gilmore et al, 2015) which is used widely in remote sensing practices to eliminate the additive scattering (Cavez and Pet, 1988) impacts of the atmosphere from remote sensing data.

Table 1. Characteristics of the selected Multitemporal Landsat imageries for Sardasht county (path/row: 168/35).

Landsat Mission	5	5	5	5	7	5	5	7	8
Sensor	TM	TM	TM	TM	ETM+	TM	TM	ETM+	OLI
Acquisition Year	1984	1986	1993	1998	2002	2006	2010	2013	2017
Acquisition Date	27-Aug	02-Sep	19-Jul	19-Sep	06-Sep	09-Sep	19-Aug	17-Sep	23-Sep

2.2.2. Image Classification with Binary Encoding

As most raw data forms of satellite imagery restrict their scientific applications, image processing methods need to be implemented in order to extract useful information. Image classification is a well-known and routine step in any image processing procedure, in which each pixel or object is allocated to a real world feature on earth depending on the nature of the classification method (Pixel based or Object based). Its overall goal is to assign image pixels to land cover classes automatically (Kumar and Singh, 2013). Land cover/land use classification practices can be done by different strategies and algorithms provided by digital image processing tools (Cetin et al, 2004). The supervised classification method of Binary Encoding was applied in this study to do image classification.

The Binary Encoding (BE) is a standard classification technique for satellite imageries (Xie and

Xiaohua (2012), in which the spectral data of images are put into 0s and 1s. The classification process in this approach is done based on a mean spectral threshold in a way that the pixels which fall below and above the threshold are classified as 0 and 1 respectively (ENVI Tutorials, 2012). Since it is mostly applied when there are just two target classes, in the present study the BE technique was used to derive two required land cover classes (Forest and Non Forest). To remove the annoying shadow effects on the imageries, the ratio transformation was implied for digitizing the training shapefile for classification. The results obtained from BE algorithm were enhanced using the appropriate NDVI values for each imagery. Eventually, the abnormal pixel values were removed by applying a Majority filter. This filter replaces the abnormal values by the most common value surrounding the cells.

Table 2. The accuracy assessment results of the classification for the study period

Year		Land Use / Land Cover ID										
		0	1	0	1	0	1	0	1		
		Producer's %		User's %		Commission Error		Omission Error		Overall Accuracy %	Kappa Coef
1984		100	100	100	100	0	0	0	0	100	1
1986		100	100	100	100	0	0	0	0	100	1
1993		90.17	92.77	92.87	90.07	9.83	7.23	7.13	9.93	91.45	0.82
1998		88.5	77.5	73.21	90.63	11.5	22.5	26.79	9.37	82	0.64
2002		97.22	90.57	92.11	96.64	7.89	3.36	2.78	9.43	94.10	0.88
2006		97.70	96.97	97.14	97.56	2.86	2.44	2.30	3.03	97.35	0.95
2010		95.03	97.47	97.73	94.48	2.27	5.52	4.97	2.53	96.17	0.92
2013		96.35	97.96	98.40	95.36	1.60	4.64	3.65	2.04	97.05	0.94
2017		97.81	96.15	96.76	97.40	3.24	2.60	2.19	3.85	97.05	0.94
	LCLU ID: Forest (1), Non Forest (0)										

2.3. Accuracy Assessment

The final step in any image classification approach is to check the accuracy of the classification to guarantee the trustworthiness of the results. The classification error matrix is one of the mostly used approaches in accuracy assessment practices in which the classified images are compared with ground truth points (Kumar and Singh, 2013). In this study the accuracy of the extracted LCLU map layers was assessed by applying ground-truth control points obtained from high-accuracy classification results of the previous studies and visual interpretation of remotely sensed imageries in order to achieve the highest possible precision. Overall accuracy, Kappa coefficient, user's and producer's accuracy values and commission and omission errors (Foody, 2002; Lu et al., 2004; Shooshtari and Gholamalifard, 2015) were computed (Table 2). The results of the assessment indicated that the classification accuracy has been satisfactory leading to the overall accuracy of more than 90% throughout the study period.

2.4. Retrieving Land Surface Temperature

Land surface temperature (LST) is a remotely sensed product demonstrating surface temperature of the earth where 'the received energy (heat and radiation) of the sun is absorbed, reflected or dispersed' (Anandababu et al, 2018). While some satellite sensors offer ready-to-use LST maps (at large scales), the usual and more applicable method for LST retrieval is to use thermal bands (TIR) of remotely sensed Landsat imageries. The mentioned steps below are the general approach of LST retrieval process which were followed in the current study to derive LST layers out of Landsat images for the study area. The specific parameters of thermal bands of different sensors used in the current study were received from metadata files offered with each sensor products by Landsat mission.

2.4.1. DN to Radiance Conversion

Digital numbers of thermal bands can be converted to the spectral radiances using the following equation (1). It depicts the outgoing energy radiated by the earth's surface sensed by each band at top of the atmosphere (Waters et al, 2002).

$$L_\lambda = \left(\frac{L_{Max} - L_{Min}}{(QCAL_{Max} - QCAL_{Min})} \right) \times (DN - QCAL_{Min}) + L_{Min} \quad (1)$$

Where DN is the digital number of each pixel, LMAX and LMIN are calibration constants, QCALMAX and QCALMIN are the highest and lowest range of values for rescaled radiance in DN. The units for $L\lambda$ are W/m2/sr/μm.

2.4.2. Radiance to Reflectance

Reflectance is defined as the ratio of incoming radiation to the outgoing radiation of the surface (Waters et al, 2002). It can be computed using the equation 2.

$$\rho_p = \frac{\pi \times L_\lambda \times d^2}{ESUN_\lambda \times \cos \theta_s} \quad (2)$$

Where ρ_p is reflectance (Unitless), L_λ is spectral radiance, d is Earth-Sun distance in astronomical units, $ESUN_\lambda$ is Mean solar exoatmospheric irradiances, and θ_s is solar zenith angle in degrees.

2.4.3. Reflectance to At-Satellite Temperature

The following equation is used to convert the radiance to temperature.

$$T = \frac{K_2}{\ln(\frac{K_1}{L_\lambda} + 1)} \quad (3)$$

Where T is effective at-satellite temperature (Kelvin), K1 and K2 are constants for Landsat images (Markham and Barker, 1987).

2.4.4. At-Satellite Temperature to Surface Temperature

At the final step, desired LST can be calculated using the following equation (Artis and Carnahan, 1982).

$$LST = \frac{BT}{1 + (\lambda \times \frac{BT}{P}) \ln(e)} \quad (4)$$

Where BT is at satellite brightness temperature, λ is the wavelength of emitted radiance, P=h×c/s (1.438×10-2mk) P=14380, h= Planck's constant (6.626×10-34 Js), s=Boltzmann Constant (1.38×10-23 J/K), c= Velocity of light (2.998x10-8 m/s).
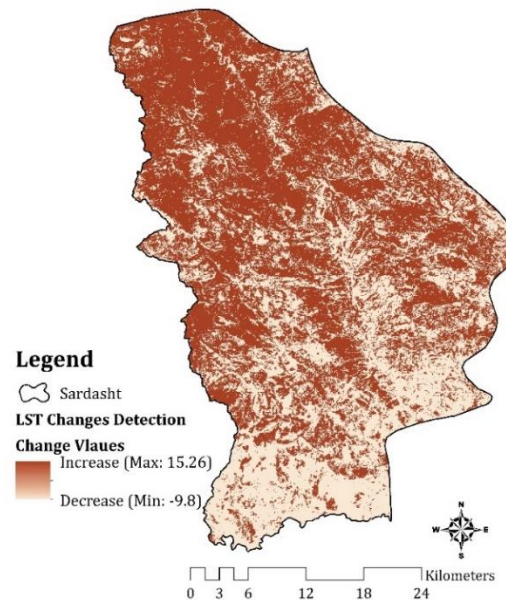

Figure 2. The visual fluctuations of LST values in the study area.

3. Results and Discussion

3.1. LST Anomalies

Calculating the required LST maps, the temporal variations of the environment temperature on each land cover class of the study area were extracted (Table 3). The results shows that while a slight wax and wane is seen in the values, the total trend of LST measures is ascending for both the land covers with an almost the same changes

(4.0 degrees in non-forest and 3.9 degrees in forest class) through the study period.

The change detection map of LST also illustrates the spatial spread of the LST changes throughout the area. Figure 2, shows the total LST variations from 1984 to 2017 for the study area. While the max and min variations

are 15 and -9.8 degrees respectively, the mean values correspond the temporal trends as mentioned before.

Table 3. The areal-mean LST variations regarding each LCLU category

Land Cover	LST								
	1984	1986	1993	1998	2002	2006	2010	2013	2017
Non Forest	37.99	37.22	36.37	34.71	37.09	40.86	41.65	39.62	41.90
Forest	33.71	33.27	32.18	30.29	33.68	36.33	37.67	35.45	37.60

3.2. Land Cover/Use Changes

The statistics derived from LCLU map layers (Table 4) shows the temporal changes in Forest and Non-Forest areas during time. As expected, the trends are ascending for non-forest and descending for forest areas (Figure 4) with a high correlation value (about 98.5% for each land cover). These changes have been pictured for better understanding in figure 3. The results indicate about 7700 hectares decline in forest area in the last three decades, which corresponds to 5.6% of the total area of the region. On the other hand the destructed forest has been transformed into the other land uses, which was seen from increased non-forest area.

To examine the spatial changes occurred in forest cover of the region, the change detection map was derived (Figure 3). The figure represents the total status of deforestation and afforestation process in the region during the last three decades. According to the change detection information obtained for the period 1984-2017, about 9700 ha forest cover change was detected from which 7700 ha was defined as forest loss and 2000 ha as forest gain. About 128000 ha of the study area was detected to suffer no change during the same period.
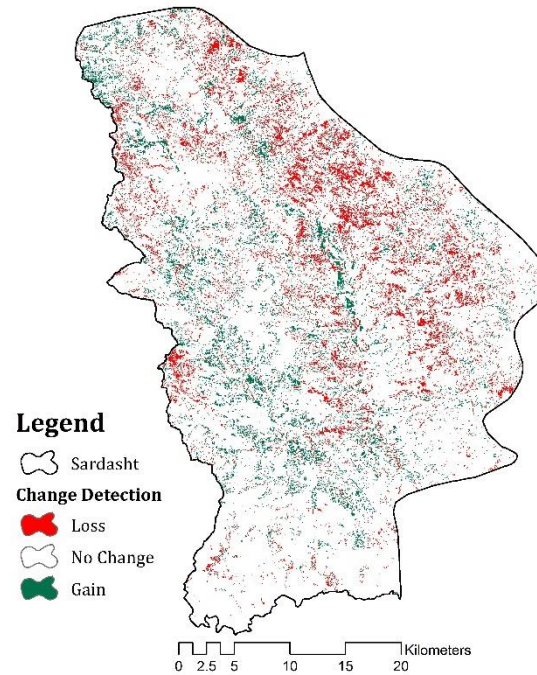

Figure 3. The spatial illustration of forest cover changes during the study period.

Table 4. The LCLU changes for each category from 1984 to 2017.

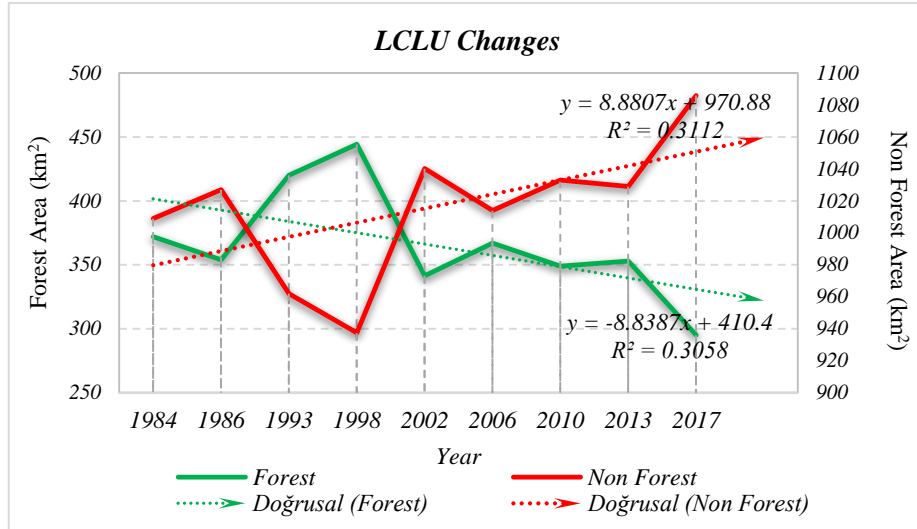| Land Cover	Area (km²)								
	1984	1986	1993	1998	2002	2006	2010	2013	2017
Non Forest	1009	1027	962	809	1024	1014	1033	1029	1086
Forest	372	354	420	573	358	367	349	353	295

Figure 4. The temporal changes of land cover/use values

3.3. Forest/Non-Forest Cover Changes Impacts on LST Variations

The wooded areas have a great potentiality to alleviate the harsh climatic conditions interacting with the sun radiations thus providing shadow to lower the temperatures. Theoretically, the forest degradation would have reverse impact on temperature values (either air or surface temperature) so that the more deforestation occurs, the more the temperature rises up. To study this relation in Sardasht County, the calculated measures were compared in a statistical manner. Comparing the two change detection maps (LST and LCLU) a very high spatial correlation coefficient of 0.98 was detected between forest loss and LST increase areas which confirms the found relation spatially. On the other hand the high correlation (98.2%) was detected for forest gain areas with LST changes.

To reveal the LST feedbacks to the current forest and non-forest cover change information, the temporal trend lines were drawn as shown in Figures 5 and 6 respectively. Accordingly, though the trend lines of forest change mimic each other in some short periods (1984 and 2006), the relation between deforestation and LST variations seems logical for the remaining periods with a total temporal correlation of   -0.81 which is meaningful at 0.01 significance level where the destructed forest leads to increasing temperatures through time. On the other hand the trends in non-forest areas follows the LST trends through the study period indicating the positive relation between changing non-forested areas and LST values with an estimated correction of 0.71. Table 5 shows the correlation statistics of forest/non-forest temporal changes and LST variations during the study period.
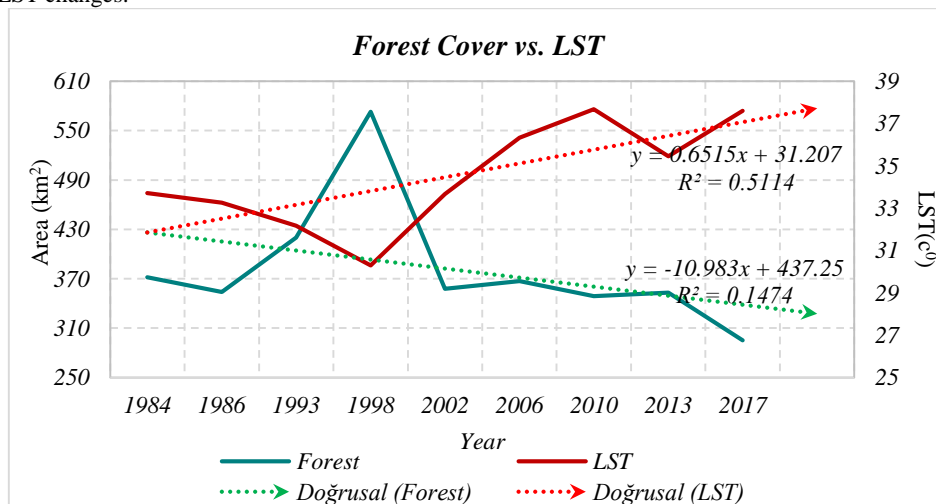

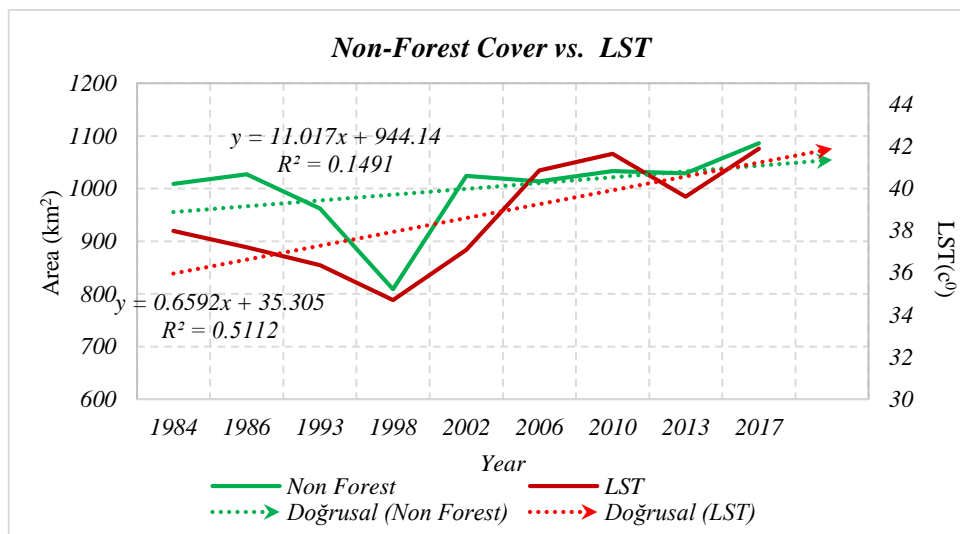Figure 5. The temporal interactions of forest and LST changes

Figure 6. The temporal interactions of non-forest and LST changes.

Table 5. The correlation rate and linear regression function of LCLU and LST changes

	Regression Function	R	Significance level
Forest/ LST	Y= 44.26 - 0.0256×X	-0.81	0.01
Non Forest/ LST	Y= 14.15 + 0.0245×X	0.76	0.01

Overall, the results indicated that the study area has suffered severe degradation process from 1984 to 2017 loosing 2560 ha of its forest coverage. The temporal results suggested that a rational trend obtains between deteriorating process of LCLU changes and LST fluctuations in both forest and non-forest classes. The decreasing forest cover was associated with increasing LST in cleared out areas with a mean value of 3.8^0C. On the other hand, 4^0C of mean LST increase was found in the increasing non-forest areas. The spatial comparison of the changes also revealed that the total changes in forest cover (deforestation and afforestation) and LST trends go hand in hand closely with a 98.5% and 98.2% of correlation for forest loss and forest gain points with LST changes respectively which proves the direct negative contribution of forest change to increasing surface temperatures.

4. Conclusion

The main goal of the current study was to analyze the impacts of deforestation on land surface temperature variations. Since some of the important environmental phenomena can be inferred from temperature anomalies of the earth's surface, monitoring LST changes seems to have a pivotal role in any environmental conservation policy. In this study the temporal as well as spatial changes of land cover/use and surface temperatures were analyzed to incorporate the results in assessment of the possible expected impacts of the changing LCLU on LST variations. As a concluding results for this study it can be said that deforestation process as an outcome of human interferences in the nature have had the most tangible implications for the changing temperature values of the environment of Sardasht. The LST anomalies appeared to have a close relation with deforestation and afforestation processes so it is suggested that LST monitoring can be used as a diagnostic mean to study the health and status of wooded areas to make the decision makers much more able to guard these natural resources.

References

Amiri R., Weng Q., Alimohammadi A. and Alavipanah S.K (2009). Spatial–temporal dynamics of land surface temperature in relation to fractional vegetation cover and land use/cover in the Tabriz urban area, Iran. Remote sensing of environment, 113(12), pp.2606-2617.

Anandababu D., Purushothaman BM. and Babu SS (2018). Estimation of Land Surface Temperature using LANDSAT 8 Data. International Journal of Advance Research, Ideas and Innovations in Technology. 4(2):177-86.

Arslan M., Zahid R.and Ghauri B (2016). Assessing the occurrence of drought based on NDVI, LST and rainfall pattern during 2010–2014. Geoscience and Remote Sensing Symposium (IGARSS), 2016 IEEE International (pp. 4233-4236). IEEE.

Artis D.A. and Carnahan W.H (1982). Survey of emissivity variability in thermography of urban areas. Remote Sensing of Environment, 12(4), pp.313-329.

Bakar S.B.A., Pradhan B., Lay U.S. and Abdullahi S (2016). Spatial assessment of land surface temperature and land use/land cover in Langkawi Island. In IOP Conference Series: Earth and Environmental Science.Vol. 37, No. 1, p. 012064.

Beygi Heidarlou H., Banj Shafiei A., Erfanian M., Tayyebi. and Alijanpour A (2015). Detection of land cover changes in Sardasht during time period of 1993 to 2016. The International Conference on Natural Resources

Management in Developing Countries, Iran, Tehran, 25 Feb. 2015.

Cetin M., Kavzoglu T. and Musaoglu N (2004). Classification of multi-spectral, multi-temporal and multi-sensor images using principal components analysis and artificial neural networks: Beykoz case. In Proceedings XXth International Society for Photogrammetry and Remote Sensing-Congress, pp. 12-23.

Chavez Jr. and Pat S (1988). An improved dark-object subtraction technique for atmospheric scattering correction of multispectral data. Remote sensing of environment 24, no. 3: 459-479.

Ding H. and Shi W (2013). Land-use/land-cover change and its influence on surface temperature: a case study in Beijing City. International Journal of Remote Sensing, 34(15), pp.5503-5517.

Entezari A., Ahmadi A., Aliabadi K., Khosravian M. and Ebrahimi M (2016). Monitoring Land Surface Temperature and Evaluating Change Detection Land Use (Case Study:Parishan Lake Basin), Hydrogeomorphology, v2[8],113-139.

Foody GM. (2002). Status of land cover classification accuracy assessment Remote Sensing of Environment 80:185-201 doi:10.1016/S0034-4257(01)00295-4.

Gidey E., Dikinya O., Sebego R., Segosebe E. and Zenebe A (2018). Analysis of the long-term agricultural drought onset, cessation, duration, frequency, severity and spatial extent using Vegetation Health Index (VHI) in Raya and its environs, Northern Ethiopia. Environmental Systems Research, 7(1), p.13.

Gilmore S., Saleem A. and Dewan A. (2015). Effectiveness of DOS (Dark-Object Subtraction) method and water index techniques to map wetlands in a rapidly urbanising megacity with Landsat 8 data. Research@ Locate'15, pp.100-108.

Karnieli A., Agam N., Pinker R.T., Anderson M., Imhoff M.L., Gutman G.G., Panov N. and Goldberg A. (2010). Use of NDVI and land surface temperature for drought assessment: Merits and limitations. Journal of climate, 23(3), pp.618-633.

Kumar M. and Singh R.K. (2013). Digital Image Processing of Remotely Sensed Satellite Images for Information Extraction. In Conference on Advances in Communication and Control Systems (CAC2S).

Lu D., Mausel P., Brondizio E. and Moran E. (2004). Change detection techniques. International journal of remote sensing. 1; 25(12):2365-401.

Manoharan V.S., Welch R.M. and Lawton R.O. (2009). Impact of deforestation on regional surface temperatures and moisture in the Maya lowlands of Guatemala. Geophysical Research Letters, 36(21).

Markham B.L. and Barker J.L. (1987). Thematic Mapper bandpass solar exoatmospheric irradiances. International Journal of remote sensing 8, no. 3 517-523.

Research Systems, Inc. ENVI tutorials. Research Systems, September, 2001 Edition. gers.uprm.edu/geol6225/pdfs/envy_tutorial.pdf (Accessed 05.09.2018).

Shooshtari SJ. and Gholamalifard M. (2015). Scenario-based land cover change modeling and its implications for landscape pattern analysis in the Neka Watershed, Iran Remote Sensing Applications: Society and Environment 1:1-19

Son N.T., Chen C.F., Chen C.R., Chang L.Y. and Minh V.Q (2012). Monitoring agricultural drought in the Lower Mekong Basin using MODIS NDVI and land surface temperature data. International Journal of Applied Earth Observation and Geoinformation, 18, pp.417-427.

Sruthi S. and Aslam M.M. (2015). Agricultural drought analysis using the NDVI and land surface temperature data; a case study of Raichur district. Aquatic Procedia, 4, pp.1258-1264.

Waters R., Allen R., Bastiaanssen W., Tasumi M. and Trezza R. (2002). Surface energy balance algorithms for land, Idaho implementation, advanced training and user's manual. NASA, USA.

Xiao H. and Weng Q. (2007). The impact of land use and land cover changes on land surface temperature in a karst area of China. Journal of environmental management, 85(1), pp.245-257.

Xie H. and Xiaohua T. (2012). An inproved binary encoding algorithm for classification of hyperspectral images. In Hyperspectral Image and Signal Processing (WHISPERS), 2012 4th Workshop on, pp. 1-4. IEEE.

Zhang X., Yamaguchi Y., Li F., He B. and Chen Y. (2017). Assessing the impacts of the 2009/2010 drought on vegetation indices, normalized difference water index, and land surface temperature in Southwestern China. Advances in Meteorology. Volume 2017, Article ID 6837493, 9 pages.